

Dissertation  
submitted to the  
Combined Faculties for the Natural Sciences and for Mathematics  
of the Ruperto-Carola University of Heidelberg, Germany  
for the degree of  
Doctor of Natural Sciences

Presented by

**Alexander Feuerborn, Dipl.-Biol.**

Born in: Gütersloh, Germany

Oral-examination: tba

2010

# **The Forkhead factor FoxQ1 influences epithelial plasticity and modulates TGF- $\beta$ 1 signalling**

## **Referees:**

**Prof. Dr. rer. nat. Peter Angel**

**Prof. Dr. med. Hermann-Josef Gröne**



<b>LIST OF FIGURES</b>	<b><i>i</i></b>
<b>LIST OF TABLES</b>	<b><i>ii</i></b>
<b>SUMMARY</b>	<b><i>iii</i></b>
<b>ZUSAMMENFASSUNG</b>	<b><i>v</i></b>
<b>1. INTRODUCTION</b>	<b>7</b>
<b>1.1 Signal transduction</b>	<b>7</b>
<b>1.2 The TGF-<math>\beta</math> family of cytokines</b>	<b>8</b>
1.2.1 TGF- $\beta$ signalling – the canonical TGF- $\beta$ -Smad pathway	10
1.2.2 TGF- $\beta$ Smad-independent signalling cascade	14
<b>1.3 Epithelial to mesenchymal transition (EMT) – a remarkable example of cellular plasticity</b>	<b>16</b>
1.3.1 EMT-markers	17
1.3.2 Crucial transcriptional regulators for EMT and epithelial plasticity	18
<b>1.4 Types of EMT</b>	<b>20</b>
1.4.1 Type 1 – EMT in embryogenesis and organ development	20
1.4.2 Type 2 – EMT during tissue regeneration and organ fibrosis	21
1.4.3 Type 3 – EMT during cancer progression and metastasis	22
<b>2. HYPOTHESIS AND OBJECTIVES</b>	<b>24</b>
<b>3. MATERIAL AND METHODS</b>	<b>25</b>
<b>3.1 Material</b>	<b>25</b>
3.1.1 Chemicals	25
3.1.2 Buffers and solutions	25
3.1.3 Media	26
3.1.4 Antibodies	27
3.1.5 Plasmids	28
3.1.6 Primers	28
3.1.7 small interfering RNAs (siRNAs)	28
3.1.8 DNA and protein ladder	29
3.1.9 Multi-component systems ('Kits')	29
3.1.10 Equipment	30
3.1.11 Cell lines and bacteria	30
<b>3.2 Methods</b>	<b>31</b>
3.2.1 Molecular biological methods	31
3.2.1.1 Isolation of plasmids from bacteria – 'Mini-prep'	31
3.2.1.2 Isolation of plasmids from bacteria on a large scale – 'Maxi-prep'	31
3.2.1.3 Measurement of nucleic acid concentration (DNA/RNA)	32
3.2.1.4 Digestion of DNA via endonucleases (restriction digest)	32
3.2.1.5 Electrophoretic separation of DNA	32
3.2.1.6 Extraction of DNA from agarose gels	32
3.2.1.7 Ligation of DNA fragments	33
3.2.1.8 Transformation of <i>E.coli</i> -DH5 $\alpha$ with plasmid DNA	33
3.2.1.9 Isolation of total RNA from eukaryotic cells using Trizol®	34
3.2.1.10 Isolation of total RNA from eukaryotic cells for microarray analyses	34
3.2.1.11 Selective enrichment of thio-uridine (4sU) labelled and newly-transcribed RNA	34
3.2.1.12 Measurement of RNA quality and quantity	36
3.2.1.13 Synthesis of cDNA - Reverse transcription	36
3.2.1.14 Quantitative Real-time PCR (qRT-PCR)	37

3.2.1.15 Gene expression profiling	38
3.2.2 Cell biological methods	39
3.2.2.1 Culture of eukaryotic cells	39
3.2.2.2 Freezing of eukaryotic cells	39
3.2.2.3 Thawing of eukaryotic cells	39
3.2.2.4 Transfection of small interfering RNAs	39
3.2.2.5 Generation of stably transfected NM18 cells	40
3.2.2.6 TGF- $\beta$ 1 treatment of NMuMG cells and subclones	40
3.2.2.7 Migration assay	41
3.2.2.8 MTT-assay	41
3.2.2.9 Cell cycle analyses	41
3.2.2.10 Transmission-electron microscopy	42
3.2.3 Protein-biochemical methods	42
3.2.3.1 Preparation of total protein cellular lysates	42
3.2.3.2 Determination of protein concentration – Bradford assay	42
3.2.3.3 SDS-polyacrylamide gel electrophoresis (SDS-PAGE)	43
3.2.3.4 Western Blot – Transfer of proteins onto nitrocellulose membranes	43
3.2.3.5 Confocal microscopy	44
3.2.4 Biostatistical methods	44
3.2.4.1 Analyses of gene expression profiling	44
3.2.4.2 Categorization of differentially expressed genes using selected GO-terms in Cytoscape/Bingo	45
3.2.4.3 Student’s t-test	46
3.2.4.4 Transcription Factor Matrix-Scan (TFM-Scan)	46
<b>4. RESULTS</b>	<b>47</b>
<b>4.1 Identification of differentially expressed transcription factors during TGF-<math>\beta</math>1 signalling</b>	<b>47</b>
4.1.1 TGF- $\beta$ 1-induced EMT in NMuMG cells	47
4.1.2 Applicability of NMuMG cells for NIAC-NTR-based gene expression profiling	49
4.1.3 NIAC-NTR-based gene expression profiling of TGF- $\beta$ 1-induced NMuMG cells	51
4.1.4 Several transcription factors of the Forkhead-family are transcriptionally regulated during early TGF- $\beta$ 1 signalling	52
<b>4.2 FoxQ1 regulates various cellular features in mammary epithelial cells as dissected by RNAi-mediated repression of FoxQ1</b>	<b>54</b>
4.2.1 FoxQ1 controls epithelial cell morphology and cell size of NM18 cells	54
4.2.2 Repression of FoxQ1 induces the accumulation of F-actin in circular structures (‘actin rings’) and results in a different localisation of the cytoskeleton-associated protein Tmod3	56
4.2.3 FoxQ1 suppression enhances the migratory capacity of NM18 cells	58
4.2.4 Cellular proliferation and G1/S-cell cycle transition is impaired upon FoxQ1 repression – FoxQ1 suppression affects the expression of Cyclin-dependent kinases (CDKs)	60
4.2.5 FoxQ1 repression results in the establishment of pronounced cell-cell contacts	62
4.2.6 FoxQ1 repression alters the outcome of TGF- $\beta$ 1-induced EMT-like progression and affects EMT-associated marker expression	63
<b>4.3 Functional analyses of NM18 cells overexpressing FoxQ1</b>	<b>65</b>
4.3.1 Establishment of FoxQ1 overexpressing NM18 cells	65
4.3.2 Enhanced expression of FoxQ1 does not induce proliferation and only modestly alters cell sheet organisation	67
4.3.3 Overexpression of FoxQ1 modulates TGF- $\beta$ 1 induced alterations in epithelial morphology and results in a modified ECM	68

<b>4.4 A role of FoxQ1 in TGF-<math>\beta</math>1-dependent gene expression changes associated with EMT-like progression</b>	<b>72</b>
4.4.1 FoxQ1 repression alters the expression of transcription factors and genes encoding junction proteins which are associated with TGF- $\beta$ 1-dependent EMT-like progression	72
<b>4.5 Regulatory aspects of FoxQ1</b>	<b>75</b>
4.5.1 FoxQ1 is induced independently of TGF- $\beta$ 1-induced Smad4 signalling and is a downstream target of Zeb1	75
<b>5. DISCUSSION</b>	<b>77</b>
<b>5.1 Several Forkhead transcription factors are regulated during TGF-<math>\beta</math>1 signalling</b>	<b>78</b>
<b>5.2 Functional analyses of FoxQ1 in mammary epithelial cells</b>	<b>80</b>
5.2.1 FoxQ1 regulates cell size/morphology, cytoskeletal arrangements, cell migration and intercellular adherence	80
5.2.2 FoxQ1 regulates cell cycle G1/S-transition in NM18 cells by regulating the expression of CDKs	82
5.2.3 Overexpression of FoxQ1 modulates TGF- $\beta$ 1-mediated formation of cell protrusions/morphology and results in a modified ECM	83
5.2.4 TGF- $\beta$ 1-dependent increase in FoxQ1 expression is independent of Smad4	85
5.2.5 Suppression of FoxQ1 affects the expression of genes associated with TGF- $\beta$ 1-induced EMT-like processes	86
<b>6. SUPPLEMENTS</b>	<b>89</b>
<b>7. LITERATURE</b>	<b>95</b>
<b>ABBREVIATIONS</b>	<b>103</b>
<b>ACKNOWLEDGEMENTS</b>	<b>106</b>

## LIST OF FIGURES

Fig. 1. Principles of signal transduction.	8
Fig. 2. Synthesis and post-translational modification scheme of TGF- $\beta$ superfamily members	9
Fig. 3. Schematic representation of TGF- $\beta$ receptors Type I and Type II.	11
Fig. 4. Principal features of Smad-proteins.	12
Fig. 5. The canonical TGF- $\beta$ -Smad pathway.	14
Fig. 6. TGF- $\beta$ 1-induced EMT in NMuMG cells.	48
Fig. 7. NMuMG cells can be used for NIAC-NTR-based gene expression profiling.	50
Fig. 8. NIAC-NTR-based gene expression profiling during early TGF- $\beta$ 1 signalling.	52
Fig. 9. Summary of differentially expressed Forkhead-transcription factors during early TGF- $\beta$ 1 signalling.	53
Fig. 10. siRNA-mediated repression of FoxQ1 results in morphological changes in NM18 cells.	55
Fig. 11. Repression of FoxQ1 results in the formation of 'actin rings' in NM18 cells.	56
Fig. 12. Repression of FoxQ1 expression leads to changes in Tmod3 protein localisation.	58
Fig. 13. FoxQ1 repression enhances the migratory capacity of NM18 cells.	59
Fig. 14. FoxQ1 suppression reduces cell proliferation, potentially via the regulation of G1/S-phase cell cycle transition.	61
Fig. 15. Cell-cell contacts are reorganized upon FoxQ1 knock-down.	62
Fig. 16. Repression of FoxQ1 reduces cell dissociation and repression of E-cadherin during TGF- $\beta$ 1-induced EMT-like progression.	65
Fig. 17. Stable overexpression of FoxQ1 in NM18 cells.	66
Fig. 18. Overexpression of FoxQ1 does not enhance the proliferative capacity of NM18 cells.	67
Fig. 19. Tmod3 and F-actin distribution in FoxQ1-overexpressing cells.	68
Fig. 20. Enhanced expression of FoxQ1 influences the outcome of TGF- $\beta$ 1-induced changes in cell morphology.	69
Fig. 21. The EMT-markers E-cadherin and fibronectin are not differentially expressed between control and FoxQ1-overexpressing cells upon TGF- $\beta$ 1-induced EMT.	70
Fig. 22. Overexpression of FoxQ1 alters extracellular distribution of the ECM component fibronectin.	71
Fig. 23. Summary of differentially expressed genes during TGF- $\beta$ 1 signalling in dependency of FoxQ1 expression.	73
Fig. 24. Western blot analyses of protein expression of intercellular junction proteins and the transcription factor Ets-1 upon FoxQ1 knock-down.	74
Fig. 25. TGF- $\beta$ 1-dependent induction of FoxQ1 is independent of Smad4 signalling in NM18 cells.	75
Fig. 26. RNAi-mediated repression of Zeb1 leads to a decreased expression of FoxQ1.	76
Fig. 27. Control of cellular protrusions takes effect on migratory characteristics of cells.	84
Fig. 28. Hypothetical model of potential cross-talk between FoxQ1, Zeb1, Zeb2 and Ets-1 during TGF- $\beta$ 1 signalling.	87

**LIST OF TABLES**

Tab. 1. Buffers for the enrichment of newly-transcribed RNA _____	26
Tab. 2. Gene name, sequence and annealing temperature of the used primer _____	28
Tab. 3. siRNA name, target sequence and species _____	29
Tab. 4. Name and origin of applied 'kits' _____	29
Tab. 5. Designation and origin of regularly used equipment _____	30
Tab. 6. qRT-PCR cycling conditions _____	37
Tab. 7. Overview of selected GO-terms and their respective definition _____	45

## SUMMARY

Cytokines belonging to the TGF- $\beta$  family ubiquitously participate in several cellular processes and elicit cell-context specific responses in various cell types.

In recent years, attention has been drawn to understand the TGF- $\beta$ 1-dependent signalling cascades which alter the differentiation state of epithelial cells, especially the de-differentiation of an epithelial cell into a mesenchymal-like cell type, also referred to as EMT (epithelial-mesenchymal transition).

EMT-processes, characterized by the loss of E-cadherin expression, loss of cell-cell adhesion, and an enhanced cellular mobility have originally been described as developmental processes, essential for gastrulation and mesoderm development as well as the formation of migratory neural crest cells.

Nowadays, regardless of the original description known from developmental biology, the term 'EMT' is used to describe several changes of epithelial cells into fibroblastoid-like cells. Partially, this is due to the use of equivocal markers that aim to define an EMT-process. Under pathological conditions, EMT-like processes have been proposed to result in organ fibrosis and to participate in cancer progression, though this is still a matter of intense scientific debate.

Nevertheless, *in-vitro* as well as *in-vivo* studies of cytokine induced EMT-associated processes have critically contributed to the identification and characterization of factors that regulate cell plasticity and to a better understanding of the complex cytokine-induced changes in epithelial differentiation.

In this work, using high-throughput microarray techniques, the Forkhead factor FoxQ1 was identified as transcriptionally induced in a TGF- $\beta$ 1-responsive cell culture model of cytokine-induced EMT-like progression, suggesting a potential impact of FoxQ1 expression in the modulation of epithelial plasticity.

Subsequent RNAi-based functional analyses revealed that FoxQ1 influences epithelial plasticity by affecting the arrangement of cytoskeletal proteins, the formation of cell-cell contacts, and junction protein expression (e.g. E-cadherin and Occludin). In addition, FoxQ1 was found to regulate cell proliferation by affecting the expression of Cyclin-dependent kinases and to modify the migratory capacity of epithelial cells.

In relation to TGF- $\beta$ 1 signalling, this work provides evidence that FoxQ1 is induced in a Smad4-independent manner and is a putative downstream target of the transcription factor Zeb1.

Transient repression as well as stable overexpression of FoxQ1 remodelled TGF- $\beta$ 1-dependent alterations of cell morphology and provided evidence that FoxQ1 is a potent mediator of TGF- $\beta$ 1 signalling.

Microarray-based gene expression analyses of TGF- $\beta$ 1-induced epithelial cells with an impaired FoxQ1 induction indicates that FoxQ1 is a potent mediator of TGF- $\beta$ 1-dependent gene expression changes, including the differential expression of transcription factors that have previously been linked to the regulation of epithelial plasticity and EMT-like progression.

## ZUSAMMENFASSUNG

Zytokine der TGF- $\beta$  Familie sind wichtige Vermittler zahlreicher zellulärer Prozesse und agieren zelltyp-spezifisch.

In den letzten Jahren wurde vor allem Gewicht auf das Verständnis von TGF- $\beta$ 1 abhängigen Signalkaskaden gelegt, die die Differenzierung von Epithelzellen beeinflussen, insbesondere die De-differenzierung einer Epithelzelle in eine mesenchymal-ähnliche Zelle, ein Vorgang der auch als EMT (epithelial-mesenchymale Transdifferenzierung) bezeichnet wird.

EMT-Prozesse, die durch den Verlust der Expression von E-cadherin, den Verlust von Zelladhäsion und einer erhöhten zellulären Mobilität gekennzeichnet sind, wurden ursprünglich als entwicklungsbiologische Prozesse beschrieben, die unerlässlich für die Gastrulation und die Mesoderm-Entwicklung, als auch für die Ausbildung migrierender Zellen der Neuralleiste sind.

Heute wird der Begriff ‚EMT‘ vielfach verwendet, um verschiedenste Übergänge von Epithelzellen zu Fibroblasten-ähnlichen Zellen zu beschreiben. Dies ist teilweise auf die Verwendung von mehrdeutigen Markern zurückzuführen, die einen ‚EMT‘-Prozess definieren sollen. Unter pathologischen Bedingungen sollen EMT-ähnliche Prozesse darüber hinaus an fibrotischen Veränderungen von Organen und dem Fortschreiten von Krebserkrankungen beteiligt sein. Dies ist wissenschaftlich nicht abschließend geklärt.

Dennoch, *in-vitro* als auch *in-vivo* Studien über Zytokin-induzierte EMT-ähnliche Prozesse haben entscheidend zur Identifizierung und Charakterisierung von Faktoren beigetragen, die die Plastizität einer Zelle regulieren. Darüber hinaus haben jene Studien zu einem verbesserten Verständnis der komplizierten Zytokin-induzierten Vorgänge geführt, die die Differenzierung einer Epithelzelle beeinflussen.

In dieser Arbeit wurde in einem TGF- $\beta$ 1 sensitivem *in-vitro* EMT-Zellkultur-Modell mittels Hochdurchsatz-Mikroarray Technik der Forkhead-Faktor FoxQ1 als transkriptionell induziert identifiziert.

Anschließende RNAi-basierte funktionelle Analysen ergaben, dass FoxQ1 die Plastizität von Epithelzellen beeinflusst und sowohl zu einer veränderten Anordnung zytoskeletaler Proteine, vermehrten Zell-Zell-Kontakten als auch einer verstärkten Expression von epithelialen ‚Junction‘-Proteinen führt (z.B. E-cadherin und Occludin).

Außerdem beeinflusst FoxQ1 sowohl die Zellproliferation, vermutlich über die Regulation Zyklin-abhängiger Kinasen, als auch die Migration epithelialer Zellen.

In Bezug auf TGF- $\beta$ 1 abhängige Signalkaskaden zeigt diese Arbeit, dass FoxQ1 unabhängig von Smad4 induziert wird und in seiner Expression vom Transkriptionsfaktor Zeb1 moduliert werden kann.

Die transiente Repression, als auch die stabile Überexpression von FoxQ1 führten zu einer veränderten TGF- $\beta$ 1-abhängigen Zellmorphologie und legt nahe, dass FoxQ1 ein bedeutender Vermittler der TGF- $\beta$ 1 Signalkaskade ist.

Mikroarray-basierte Analysen der Genexpression von TGF- $\beta$ 1 induzierten Epithelzellen mit veränderter FoxQ1-Induktion zeigten, dass FoxQ1 die Expression von TGF- $\beta$ 1 Zielgenen wesentlich beeinflusst. Dazu zählen unter anderem Transkriptionsfaktoren, die bereits mit der Regulation epithelialer Plastizität, als auch EMT-ähnlichen Prozessen in Verbindung gebracht wurden.

# 1. INTRODUCTION

## 1.1 Signal transduction

Living cells constantly sense and process information from their exterior.

An appropriate extracellular signal evokes an intracellular response and often leads to changes in gene expression and the cells phenotype.

The ability of a cell to react accordingly to a signal is achieved through transducing an external signal within the cell to finally adapt to the new environment.

The process of signal transduction involves ordered sequences of biochemical reactions within the cell and, in case of extracellular signals, usually starts with the cell sensing the incoming signal through specialized proteins, the receptors.

The receptors, either transmembrane or being located in the cytosol of a cell, are activated by the signal and forward it via downstream signalling cascades, which eventually leads to a physiological response of the cell. This physiological response often includes specific changes in gene expression (Fig. 1).

There are many different classes of receptors and respective signals that lead to context-specific adaptations of a cell in a given environment.

The following section introduces the TGF- $\beta$  superfamily, a class of cytokines that is involved in various cell-physiological processes.

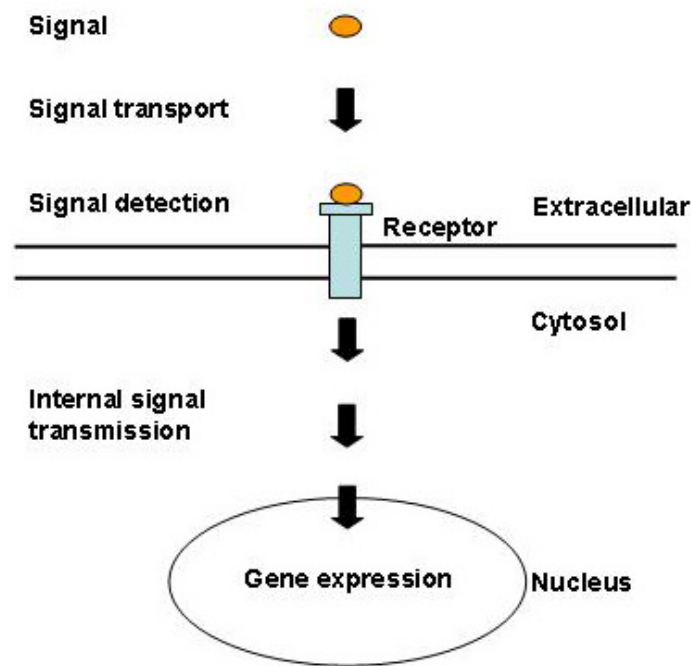


**Fig. 1. Principles of signal transduction.**

An extracellular signal is detected by specific receptors. Intracellular signalling molecules transduce the original signal into cellular behaviour.

## 1.2 The TGF- $\beta$ family of cytokines

The TGF- $\beta$  family of cytokines consists of two subfamilies – the TGF- $\beta$ /Activin/Nodal and the BMP/GDF/MIS subfamily. The classification of the family members is based on sequence similarities as well as on the specific signalling pathways they target (Shi and Massague, 2003).

The TGF- $\beta$  superfamily consists of more than 40 cytokine members. Despite their diversity, all are structurally related and share a common scheme of synthesis.

TGF- $\beta$  related proteins are synthesized as large pre-pro-proteins, consisting of a hydrophobic signal peptide, an N-terminal pro-domain and a C-terminal, biologically active, peptide (Herpin et al., 2004) (Fig. 2).

The C-terminal fragment is derived through the subsequent cleavage of the hydrophobic signal peptide and the N-terminal fragment from the intermediate pro-protein. Proteolytic cleavage of the N-terminal fragment usually occurs at a consensus site through furin-type pro-protein convertase. However, alternative usage of proteolytic sites may result in the generation of mature peptides with extended N-termini and potentially discrete biological functions (Cui et al., 1998; Herpin et al., 2004; Ozkaynak et al., 1992).

TGF- $\beta$ -related proteins are usually secreted from cells as mature peptides forming homo- and heterodimers. However, in the case of the vertebrate TGF- $\beta$  isoforms, TGF- $\beta$ 1, TGF- $\beta$ 2 and TGF- $\beta$ 3, the pro-domain remains associated with the mature peptide, yielding complexes that need to be activated before exerting their biological function (Khalil, 1999; Sinha et al., 1998). The associated dimerized pro-protein derived from the N-terminal region is also referred to as LAP (*'latency associated peptide'*), whereas the dimer protein derived from the C-terminal region is called the mature TGF- $\beta$  (Khalil, 1999).

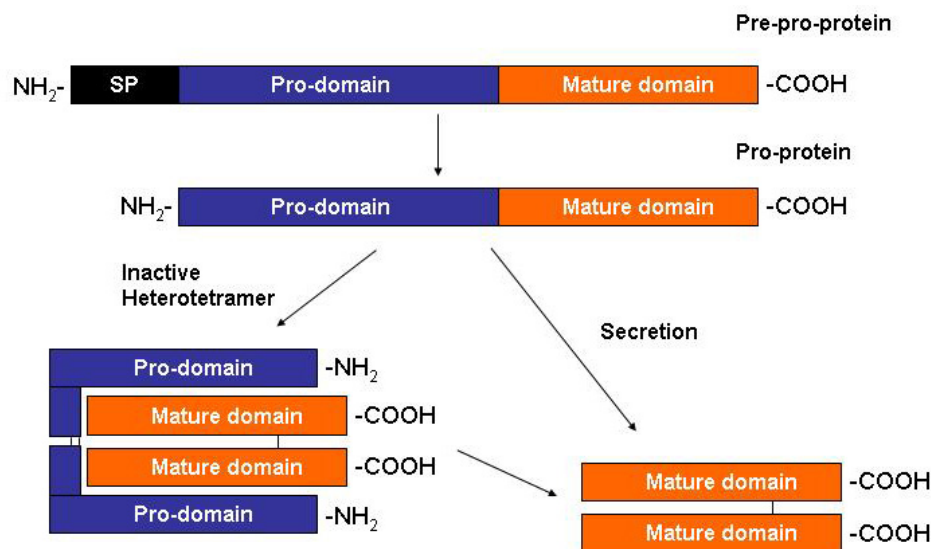


**Fig. 2. Synthesis and post-translational modification scheme of TGF- $\beta$  superfamily members** TGF- $\beta$  ligands are translated as 'pre-pro-proteins'. After proteolytic cleavage of the signal peptide (SP) and the N-terminal pro-domain, a dimeric C-terminal peptide is either released free or as an inactive form, which remains associated non-covalently with the N-terminal pro-domain (LAP- complex). Modified from (Herpin et al., 2004).

The release and therefore activation of TGF- $\beta$  from the LAP-TGF- $\beta$  complex occurs by various mechanisms and include the proteolytic cleavage of the LAP by proteases like plasmin (Lyons et al., 1988) and the interaction of the LAP with LAP-binding proteins, like thrombospondin-1 (Crawford et al., 1998).

Since TGF- $\beta$  cytokines and their respective receptors are ubiquitous proteins and involved in the regulation of a plethora of diverse cellular functions, the proper control of TGF- $\beta$  activity is critical for the maintenance of normal physiology.

The following section highlights signalling cascades of the TGF- $\beta$  subfamily of cytokines.

### 1.2.1 TGF- $\beta$ signalling – the canonical TGF- $\beta$ -Smad pathway

TGF- $\beta$  signalling regulates a diverse set of cellular processes in various species, in developing as well as mature tissues. This includes the regulation of cell proliferation, apoptosis and differentiation (Bierie and Moses, 2006; Massague et al., 2000; Patterson and Padgett, 2000; Shi and Massague, 2003; Ten Dijke et al., 2002).

The three TGF- $\beta$  isoforms signal through Type I (T $\beta$ RI), Type II (T $\beta$ RII) and Type III (betaglycan or endoglin) TGF- $\beta$  receptors to elicit cell context-specific intracellular signalling cascades.

T $\beta$ RI and T $\beta$ RII are structurally related serine/threonine kinases. The human genome comprises 7 T $\beta$ RI (ALK1, ALK2, ALK3/BMPRI1A, ALK4/ActR1B, ALK5/T $\beta$ RI, ALK6/BMPRI1B and ALK7) and 5 T $\beta$ RII (ActR-IIA, ActR-IIB, T $\beta$ RII, BMPRII and MIS/AMHR-II) serine/threonine kinases dedicated to TGF- $\beta$  signalling. Both receptor types are organized into an N-terminal extracellular ligand binding domain, a transmembrane domain and an intracellular C-terminal domain, which harbours the serine/threonine kinase activity (Shi and Massague, 2003).

The TGF- $\beta$ s have a high affinity for the Type II receptors but do not interact significantly with isolated Type I receptors (Massague, 1998). In the absence of a ligand, the Type I and Type II receptors remain homodimeric in the membrane. Binding of a dimeric ligand to the Type II receptors initiates the formation of a heterotetrameric receptor complex. Each receptor binds one monomer of the ligand (Massague, 1998; Shi and Massague, 2003).

The Type I receptors contain a typical serine- and glycine-rich sequence motif of ~30 amino acid residues directly N-terminal to their kinase domain. This so called 'GS-domain' becomes phosphorylated after the formation of the heterotetrameric receptor complex by the constitutive kinase activity of the Type II receptors (Fig. 3).

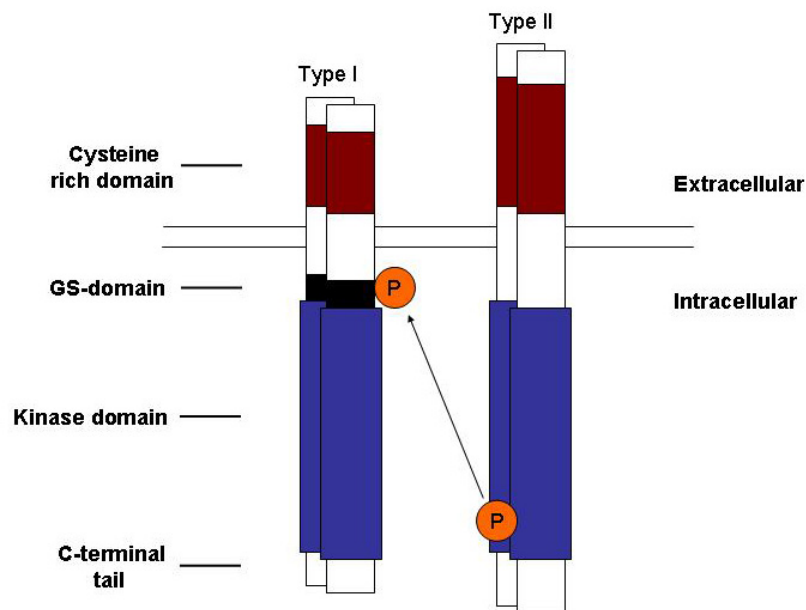


**Fig. 3. Schematic representation of TGF- $\beta$  receptors Type I and Type II.**

Binding of a ligand to the Type II receptors leads to the formation of a heterotetrameric complex, consisting of dimeric Type I and Type II receptors. Constitutively active Type II receptors subsequently phosphorylate (orange) Type I receptors on specific serine and threonine residues in the 'GS-domain' (black) which allows the propagation of the signal via downstream mediators. Modified from (Derynck and Feng, 1997; ten Dijke and Hill, 2004).

The phosphorylation of the GS-domain activates the Type I receptors and allows the propagation of the signal to further downstream mediators – the Smad proteins (Wrana et al., 1994)

The Smad-protein family consists of eight members and can be divided into three classes: R-Smads (*receptor-regulated* Smads: Smad1, Smad2, Smad3, Smad 5 and Smad8), Co-Smads (*common-mediator* Smads: Smad4) and the I-Smads (*inhibitory* Smads: Smad 6 and Smad7).

R-Smads are the only class of Smads that can directly be phosphorylated by TGF- $\beta$  receptors (Kretschmar et al., 1997; Macias-Silva 1996).

The activated Type I receptors ALK4, ALK5 and ALK7 phosphorylate the R-Smads Smad2 and Smad3, whereas the remaining Type I receptors phosphorylate the R-Smads Smad1, Smad5 and Smad8. This phosphorylation occurs at two C-terminal serine residues present in the SxS motif (Fig. 4). The R-Smads Smad2 and Smad3 respond to signalling by the TGF- $\beta$  subfamily, whereas Smad1,-5- and 8 respond mostly to signalling by the BMP subfamily of cytokines.

The R-Smads and the Co-Smad Smad4 consist of an N-terminal MH1- (*Mad homology 1*) and a C-terminal MH2- (*Mad homology 2*) domain. These conserved domains are connected by a less conserved linker domain of variable length. In contrast, the I-Smads lack the MH1 domain (Fig. 4). Moreover, the Co-Smad Smad4 and the R-Smads, with the exception of the most common splice variant of Smad2, show sequence-specific DNA binding capacity, though the affinity for DNA is rather low. The intrinsic DNA-binding capacity is encoded in the MH1 domain, which harbours an 11-residue  $\beta$ -hairpin structure that contacts the DNA at a 5'-AGAC-3' sequence, also known as the SBE (*Smad binding element*). The MH1 domain further contains an NLS sequence (*nuclear localisation signal*) which facilitates the nuclear translocation. Smad3 and Smad4 can interact with  $\alpha$ -importin (Smad4) and  $\beta$ -importin (Smad3) via their NLS sequence (Xiao et al., 2000a; Xiao et al., 2000b).

In addition, Smad4 harbours an NES (*nuclear export signal*) that specifically interacts with exportin-1 (Pierreux et al., 2000; Watanabe et al., 2000).

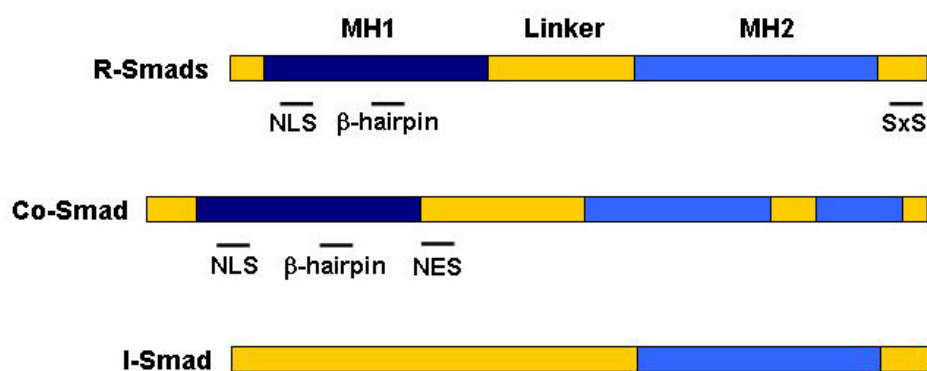


**Fig. 4. Principal features of Smad-proteins.**

The MH1 (purple) and MH2 (blue) domains are conserved domains in R-Smads and the Co-Smad Smad4. The MH1 is not present in the I-Smads. The MH1 domain contains an NLS sequence (*nuclear localisation signal*) and a  $\beta$ -hairpin structure. The Co-Smad Smad4 further contains a NES sequence (*nuclear export signal*). Modified from (ten Dijke and Hill, 2004).

Access of the activated Type I receptors to the R-Smads is facilitated by additional proteins. For example, the R-Smads Smad2 and Smad3 can be immobilized near the cell surface through the scaffolding protein SARA (*Smad anchor for receptor activation*) (Tsukazaki et al., 1998). Other adaptor proteins that may facilitate TGF- $\beta$  signalling by providing access of the Type I receptors to Smad2 and Smad3 include Disabled-2, Axin and  $\beta$ -spectrin (Furuhashi et al., 2001; Hocevar et al., 2001; Tang et al., 2003).

The MH1- and MH2-domains of the R-Smads and Smad4 inhibit each other by direct interaction. The inhibition is relieved upon phosphorylation of the R-Smads by Type I receptors, enabling the Smad proteins to form complexes and to accumulate in the nucleus (ten Dijke and Hill, 2004) (Fig. 5).

Furthermore, the phosphorylation of R-Smads leads to the destabilization of the interaction with SARA and increases the overall affinity to the Co-Smad Smad4 (Xu et al., 2000).

Smad proteins cooperate with further numerous transcription factors in order to tightly bind to respective target promoters (e.g. FoxH1 and E2F4). The Smad-interacting transcription factors therefore define the precise response of a cell to a ligand. Furthermore, Smad-interacting transcription factors may be cell-type specific and are themselves regulated by other signalling pathways. Activated Smad-protein complexes additionally interact with co-repressors (e.g. SnoN) and co-activators (e.g. p300) that further define signalling specificity (Massague et al., 2005).

In contrast to the R-Smads, the I-Smads antagonize TGF- $\beta$  signalling. This is achieved by different mechanisms. I-Smads have been shown to compete with R-Smads for binding to activated Type I receptors. I-Smads are further capable of recruiting Smurf1 and Smurf2 (*Smad ubiquitination regulatory factor*), E3-ubiquitin ligases, to activated Type I receptors which leads to the degradation of the receptors and the termination of the signal (Shi and Massague, 2003) (Fig. 5).

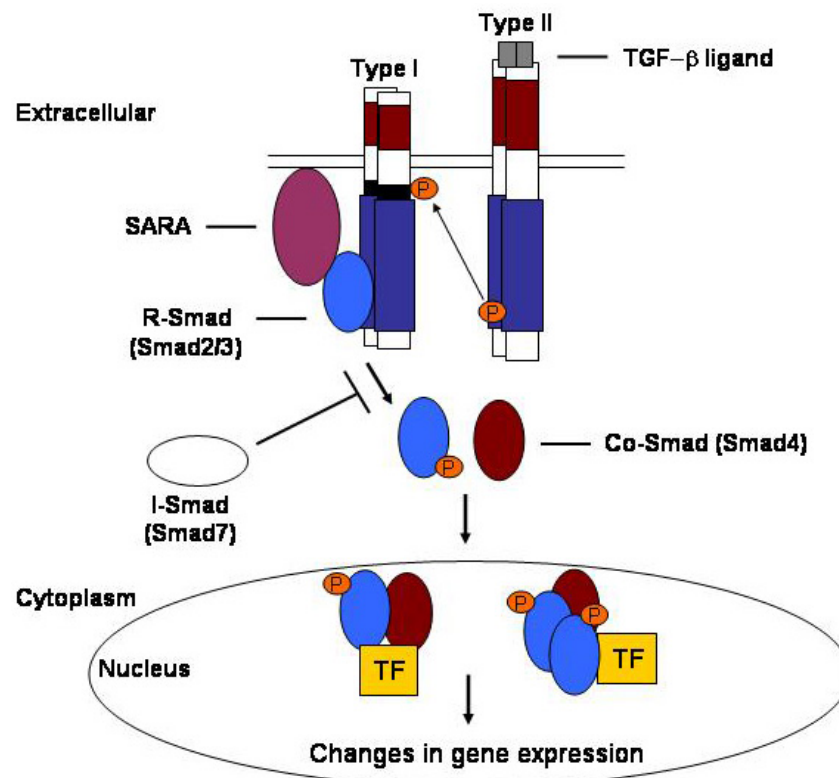


**Fig. 5. The canonical TGF- $\beta$ -Smad pathway.**

Upon ligand binding the constitutive active Type II receptor phosphorylates the Type I receptor in the GS-domain. The signal is further propagated by the direct phosphorylation of Smad2/3 in their C-terminal SxS domain. Smad2 and Smad3 form heterotrimeric or dimeric complexes with Smad4, translocate to the nucleus and causes changes in gene expression in combination with further transcription factors (TF). Smad7 antagonizes TGF- $\beta$  signalling by competing for phosphorylation with Smad2/3. In complex with Smurf1/2, Smad7 can also polyubiquitinate the activated Type I receptor, leading to the degradation of the receptor and the termination of the signal (not shown). TF – Transcription factor. Modified from (Derynck and Zhang, 2003).

### 1.2.2 TGF- $\beta$ Smad-independent signalling cascade

Beside the canonical TGF- $\beta$ -Smad pathway, TGF- $\beta$  further activates Smad-independent signalling cascades.

Some of these cascades reveal extensive crosstalk with the canonical Smad-pathway, whereas others might induce TGF- $\beta$ -dependent processes, independent of transcriptional responses.

TGF- $\beta$  signalling activates MAPK-pathways (*mitogen-activated protein kinase*) as well as Rho-like GTPases, including RhoA, Rac and Cdc42 (Derynck and Zhang, 2003).

In multicellular organisms there are three major subfamilies of MAPKs – ERK (*extracellular signal regulated kinases*), JNK (*c-jun NH<sub>2</sub> terminal kinases*) and the four p38 enzymes (*p38 $\alpha$ - $\delta$* ).

MAPKs are components of a cellular phosphorelay system, consisting of sequentially activated kinases. Upstream acting kinases, the MKKKs (MAPK kinase kinases) and the MKKs (MAPK kinases) sequentially pass on the phosphorylation, which finally leads to the activation of the MAPKs.

MAPKs have a great impact on cellular physiology which is also reflected on the diversity of their own substrates. These substrates include other protein kinases, transcription factors, phospholipases and cytoskeletal proteins (Johnson and Lapadat, 2002).

MAPK-pathways have been shown to affect gene expression not only on the level of transcription (e.g. via activating or inactivating further transcription factors), but also post-transcriptionally on the level of mRNA stability.

The regulation of mRNA stability is an important mechanism in the control of gene expression and allows a rapid tuning of mRNA levels in cells (Khabar, 2005).

RNA stability is principally regulated by *cis*-acting sequences as well as *trans*-acting factors that can bind to the *cis*-acting elements, which results in the stabilization or destabilization of a respective RNA. The most common *cis*-acting elements recognized to control RNA stability are AU-rich elements (AREs). The AREs are short interspersed nucleotide stretches found in the 3'-UTR of labile RNAs with the minimal ARE sequence being a nonamer (UUAUUUAUU) (Chen and Shyu, 1995; Lagnado et al., 1994). The AREs are divided into three categories. Class I and class II AREs mainly differ in the number of the pentameric AUUUA-stretches, whereas Class III AREs lack the AUUUA-motif but contain U-rich regions (Dean et al., 2004).

Several dozen ARE-containing RNAs have already been identified to be post-transcriptionally regulated by the p38 MAPK-kinase pathway, including mRNAs encoding chemokines, cytokines and transcription factors (Brook et al., 2000; Frevel et al., 2003).

*In-vitro* analyses have revealed that the RNA-destabilizing protein TTP (tristetraprolin) can be phosphorylated by p38 or MK2 (also known as MAPKAPK2), a downstream kinase of p38 itself, thus modifying its effects on RNA stability (Carballo et al., 2001; Mahtani et al., 2001).

However, it is also apparent that not all ARE-harboring RNAs are regulated on the level of stability, nor exclusively by the p38 MAPK-kinase pathway. In fact, UV-induced stabilization of ARE-containing transcripts is independent of the p38 MAPK-pathway (Bollig et al., 2002).

TGF- $\beta$  further activates Rho-like GTPases. Members of this protein family, especially Rho, Rac and Cdc42 are involved in the regulation of intracellular actin dynamics and affect the cytoskeletal organization (Bishop and Hall, 2000).

The ability of TGF- $\beta$  to affect multiple, potentially cross-talking pathways simultaneously, renders TGF- $\beta$  a highly complex signalling system. Specificity and the cell response upon TGF- $\beta$  activation further depends on context-specific expression of respective TGF- $\beta$  effector molecules.

TGF- $\beta$ -induced Smad-dependent as well as Smad-independent signalling mechanisms have been shown to strongly influence the plasticity of epithelial cells and TGF- $\beta$  induced epithelial-mesenchymal transition (EMT) (Nawshad et al., 2005).

The next section introduces the EMT phenomenon in more detail.

### **1.3 Epithelial to mesenchymal transition (EMT) – a remarkable example of cellular plasticity**

Epithelial and mesenchymal cells are the two main cell types of metazoans (Acloque et al., 2009).

Epithelial cells are typically characterized by intercellular adhesion complexes in their lateral membranes which enable them to be closely attached to each other and to form cell layers. They display an apico-basal polarity, defined by the expression of different proteins at the apical- or basal side respectively, and are separated by the basement membrane from other tissues in the body.

In contrast to epithelial cells, mesenchymal cells are capable of moving individually through the extracellular matrix since they lack intercellular junctions and do not display an apico-basal polarity (Thiery and Sleeman, 2006).

A transition of primitive epithelial cells into mesenchymal cells, referred to as EMT, was first described as a process in the primitive streak of chicken embryos (Hay, 1995).

The transition of early epithelial cells into mesenchymal cells has been studied and confirmed in additional embryonic cell systems, including embryonic lens epithelium (Greenburg and Hay, 1986).

Whereas the conversion of an epithelial cell into a mesenchymal cell is referred to as EMT, the reverse of such a process is known as mesenchymal-epithelial transition (MET).

The EMT-process is a remarkable example of epithelial cellular plasticity, since the morphological changes during EMT include the loss of apical-basal polarity, dissolution of junctional protein complexes and the reorganization of the cytoskeleton. Furthermore, cells undergoing EMT reveal alterations in their migratory capacity and responses to external signals (Gotzmann et al., 2004; Lee et al., 2006).

The phenomenon of epithelial plasticity and especially EMT is not restricted to developmental biology but in fact has found its place in stem cell- and cancer-related research (Thiery et al., 2009).

However, the term 'EMT' itself is used in a rather loose manner nowadays and covers diverse changes of epithelial cells towards a fibroblastoid appearing cell-type.

The term 'EMT' has been adopted to contexts that deviate from the original description of a true EMT-process, which actually describes a cell-lineage switch from primitive epithelial cells to mesenchymal cells (Nawshad et al., 2005).

Confusion about the term 'EMT' further stems from the different approaches that have been used to study the process, including the usage of a non-standardized and sometimes controversial set of different markers, leaving the term 'EMT' in different contexts not well defined.

### **1.3.1 EMT-markers**

Epithelial cells in culture undergoing an EMT-like process usually show an obvious change in cellular morphology. Epithelial cells lose their typical 'cobblestone'-sheet structure, separate from each other and acquire an elongated cell shape. These morphological changes are paralleled by the differential expression of certain cell markers that are used to define an EMT-like process.

A prototypical feature of epithelial cells undergoing an EMT-process, is the reduced and finally lost expression of the epithelial marker E-cadherin, a member of the adherens junction protein family (Hay and Zuk, 1995).

The reduced expression of E-cadherin is often accompanied by an increased expression of N-cadherin, a type of cadherin expressed in mesenchymal cells, fibroblasts and neural tissue. This change in cadherin expression is also referred to as 'cadherin-switch' (Zeisberg and Neilson, 2009).

A more controversial marker for assessing an EMT is the intermediate filament protein vimentin, that is expressed in various cells, including glial and endothelial cells (Franke et al., 1978) but transiently or permanently also in some epithelial cells (Grone et al., 1987).

The ECM (*extracellular matrix*) glycoprotein fibronectin is another marker, whose increased expression is of potential use to follow up an EMT-process. Fibronectin exists in at least 20 splice forms in humans and binds to other components of the ECM and to the heterodimeric cell-surface integrin receptors which link the ECM with the cytoskeleton (White et al., 2008). Integrin receptors consist of various non-covalent combinations of 18  $\alpha$ - and 8  $\beta$ -subunits, giving rise to 24 distinct integrin receptors (van der Flier and Sonnenberg, 2001). Integrin-mediated signalling is highly complex, partially due to redundancy of ligand binding and therefore functional outcome of distinct integrin receptors. Fibronectin itself binds to different integrins, including  $\alpha_4\beta_1$ ,  $\alpha_4\beta_7$ ,  $\alpha_5\beta_1$ ,  $\alpha_v\beta_1$  and  $\alpha_9\beta_1$  (van der Flier and Sonnenberg, 2001).

Thus, fibronectin is important for cell adhesion, migration, cell growth and differentiation (Geiger et al., 2001; Pankov and Yamada, 2002). Since fibronectin is produced by various cell types, including fibroblasts and epithelial cells, its use as a marker of EMT is limited.

Additional markers, whose cellular localisation or expression changes during EMT, include cytoskeletal proteins (e.g.  $\alpha$ -SMA,  $\beta$ -catenin), ECM proteins (e.g. collagens, laminin), transcription factors and microRNAs (Kalluri and Weinberg, 2009; Lee et al., 2006; Zeisberg and Neilson, 2009).

Especially the identification and further characterization of certain transcription factors has contributed significantly to an improved understanding of the molecular mechanisms underlying EMT-like processes and epithelial cell plasticity (Prindull and Zipori, 2004).

The next section will highlight some of these recently identified transcription factors.

### **1.3.2 Crucial transcriptional regulators for EMT and epithelial plasticity**

Several transcription factors are involved in regulating cellular plasticity and EMT. These include the Snail transcription factor family members Snail1 and Snail2 (formerly Slug). Snail family members participate in the development of the mesoderm and in the specification and migration of the neural crest (Nieto, 2002).

Snail1 is widely recognized as a direct inhibitor of E-cadherin transcription but also affects other cellular features, including the expression of mesenchymal cell markers, cell

proliferation and apoptosis (Batlle et al., 2000; Cano et al., 2000; Hajra et al., 2002; Zeisberg and Neilson, 2009).

Moreover, transcription factors belonging to the ZEB family of zinc-finger transcription factors have crucial roles in the EMT-process. Vertebrates have two homologous ZEB proteins known as Zeb1 ( $\delta$ EF1, Areb6, Zfhx1a) and Zeb2 (Sip1, Zfhxb1). Each of them consist of two separate Zinc-finger cluster and each cluster is capable of binding to specific sequences (5'-CACCT(G)-3') within the regulatory regions of target genes (Remacle et al., 1999). Zeb1 and Zeb2 have been shown to directly repress the transcription of E-cadherin as well as genes responsible for the establishment of epithelial cell polarity and junctional complexes (e.g. Pkp2, Pkp3, Crb3 and Cx26) (Aigner et al., 2007a; Aigner et al., 2007b; Shirakihara et al., 2007; Vandewalle et al., 2005).

Furthermore, the transcription factor FoxC2 (formerly known as MFH-1 – *mesenchyme forkhead 1*) has recently been shown to be induced in cells which undergo an EMT-process. FoxC2 promotes mesenchymal differentiation during EMT and is induced by multiple signals, including TGF- $\beta$  signalling. In contrast to the aforementioned transcription factors, FoxC2 does not seem to repress the transcription of E-cadherin, but is involved in redirecting membranous E-cadherin to the cytoplasm (Mani et al., 2007).

FoxA1 and FoxA2 are transcription factors that have been shown to repress an EMT-process by the positive regulation of E-cadherin expression (Song et al.). FoxA2 further influences epithelial polarity and epithelialisation in the endoderm germ layer of mouse embryos (Burtscher and Lickert, 2009)

FoxA1, FoxA2 and FoxC2 belong to a family of evolutionarily conserved transcription factors, which are defined by the common DNA-binding domain, referred to as forkhead box or winged helix domain.

This domain mainly consists of three  $\alpha$ -helices, three  $\beta$ -helices and two wings which form a helix-loop-helix like motif (Clark et al., 1993).

The Forkhead factors (Fox-factors) are classified into subfamilies. In humans 17 subfamilies (FoxA-R), harbouring at least 41 family members, have been identified. The function and regulation between the subfamilies vary significantly. Fox-factors control a wide variety of biological processes including proliferation, invasion, differentiation and apoptosis (Brunet et al., 1999; Lee et al., 2005; Wang et al., 2005). Though the knowledge about the Fox-proteins is still scarce, the deregulation of members of some subfamilies (FoxF, FoxO, FoxM, FoxC,

FoxA, FoxP and recently also FoxQ) have been functionally implicated in certain types of cancer, including breast cancer, hepatocellular cancer and colorectal cancer (Kaneda et al., ; Mani et al., 2007; Nilsson et al.).

Other transcription factors that have been shown to be critically involved in promoting EMT-processes include Twist, KLF6 (*Krüppel like factor*), Goosecoid, Ets-1 and the CBF-A/KAP-1 complex (Hartwell et al., 2006; Holian et al., 2008; Shirakihara et al., 2007; Venkov et al., 2007; Yang et al., 2007).

The activation and expression of the various EMT-promoting transcription factors is strongly dependent on cell-context and intracellular signalling cascades, including MAPK-, Smad- and Akt-signalling.

However, even though some markers are considered a hallmark for EMT, others are more variable in their specificity and validity.

In an effort to standardize the analysed markers, it has been proposed that EMT can be classified into three general subtypes, based on the physiological context in which the process occurs (Kalluri and Weinberg, 2009; Zavadil and Bottinger, 2005; Zeisberg and Neilson, 2009).

- 1) Type 1 - EMT during embryogenesis and organ development
- 2) Type 2 - EMT during tissue regeneration and organ fibrosis
- 3) Type 3 - EMT during cancer progression and metastasis

## **1.4 Types of EMT**

### **1.4.1 Type 1 – EMT in embryogenesis and organ development**

Two well studied EMTs during embryogenesis and organ development are represented by the process of gastrulation and the formation of migratory neural crest cells.

The term 'gastrulation' essentially describes the formation of the three germ layers ectoderm, endoderm and mesoderm and occurs in all metazoans.

The first sign of gastrulation is the formation of the primitive streak (Hay, 1990). The primitive streak itself is established through the ingression of epiblast cells which subsequently give rise to the mesendoderm. The mesendoderm further separates into the mesoderm and the endoderm via an EMT-process (Hay, 1995).

The EMT-process associated with gastrulation is largely dependent on canonical Wnt signalling since embryos deficient of Wnt3 fail to undergo the EMT-process associated with gastrulation (Liu et al., 1999).

The formation of migratory neural crest cells is a further example of an EMT-process during embryogenesis. These cells derive from the neuroectoderm, dissociate from the neural folds via an EMT-process and spread throughout various parts of the embryo, where they finally differentiate into other cell types (e.g. peripheral and enteric neurons and pigment cells) (Huang and Saint-Jeannet, 2004).

#### **1.4.2 Type 2 – EMT during tissue regeneration and organ fibrosis**

Fibrosis might occur in a variety of organs which are mainly composed of epithelial cells, such as kidney, lung and the liver (Willis and Borok, 2007). Inflammatory signals derived from proliferating interstitial fibroblasts and inflammatory cells lead to an organ-destructive accumulation of *extracellular matrix* (ECM) called fibrosis.

Some observations suggest that EMT-like processes contribute to fibrosis in animal models of diseased kidneys. The analyses of diseased human kidney biopsies, revealed co-expression of epithelial and mesenchymal markers in epithelial cells (Rastaldi et al., 2002; Vongwiwatana et al., 2005). Furthermore, genetically tagged proximal tubular epithelial cells contributed to the generation of myofibroblasts via EMT in an *in-vivo* model of acute renal injury (Iwano et al., 2002). In addition, it has been shown that the activation of the EMT-promoting transcription factor Snail1 is sufficient to induce kidney fibrosis in adult transgenic mice (Boutet et al., 2006).

However, considerable doubts have been raised against the contribution of EMT towards kidney fibrosis *in-vivo*. Genetically labelled tubular epithelial cells did not show any signs of mesenchymal marker expression upon injury induced kidney fibrosis, whereas the same cells were shown to express EMT-associated markers in a TGF- $\beta$ -dependent manner *in-vitro* (Humphreys et al.).

Thus, the extent to which an EMT-process contributes to organ fibrosis *in-vivo* remains to be further resolved and needs careful re-evaluation. In contrast, there is evidence *in-vitro* that EMT phenotypes occur in different non-malignant epithelial cells of different origin. This includes renal, hepatic and pulmonary cells in which a process associated with the

expression of mesenchymal marker proteins can be induced by different stimuli (Willis and Borok, 2007).

### **1.4.3 Type 3 – EMT during cancer progression and metastasis**

Throughout cancer progression, cancerous cells often acquire the capability to disseminate from the primary tumour site and to localise and group in distant organs, a process called metastasis.

The dissemination of cancer cells from the primary tumour site requires the cancer cells to leave the epithelial sheet structure and to invade through the underlying basement membrane.

The observation that epithelial cancer cells may gain mesenchymal characteristics, associated with the expression of putative mesenchymal markers (e.g.  $\alpha$ -SMA and vimentin), has been proposed to contribute to the acquisition of the malignant phenotype (Yang and Weinberg, 2008). Furthermore, cancer cells expressing mesenchymal markers are often found at the invasive front of the primary tumour and are therefore thought to resemble cells which will finally establish metastatic sites.

For several carcinomas, the tumour-associated stroma is thought to be the source for EMT-inducing signals, e.g. HGF and TGF- $\beta$ 1, which stimulate the expression or activate the EMT-promoting transcription factors, including Snail1, Snail2, Zeb1 and Twist among others (Medici et al., 2008; Shirakihara et al., 2007). The full repertoire of EMT-inducing agents during cancer progression as well as the implemented transcription factors involved in orchestrating the EMT program remains elusive.

Additionally, in order to initiate secondary tumour formation in distant organs, EMT-derived migratory cancer cells might undergo a MET process to revert back to an epithelial phenotype. Even though such a mechanistic model might explain the phenotypic similarity of primary cancer cells and the cancer cells found at secondary sites, its validity is far from being proven *in-vivo* (Kalluri and Weinberg, 2009).

In fact, though several studies have indicated the potential impact of an EMT-process for the progression of cancer cells, it still remains a matter of intense debate among the scientific community if an EMT-process actually occurs *in vivo* during cancer progression (Giannelli, 2009; Tarin et al., 2005; Thompson et al., 2005).

Though in some human tumours one can find histological cellular features that resemble the description of an EMT-process, for example loss of polarity, loss of cell-lineage-specific cytological features and dedifferentiation of cells, these descriptions might be the outcome of an extreme plasticity change of cancer cells, rather than a true lineage switch of epithelial cancer cells into another differentiated (mesenchymal) cell type (Tarin et al., 2005).

## 2. HYPOTHESIS AND OBJECTIVES

The multifunctional cytokine TGF- $\beta$ 1 profoundly affects epithelial plasticity and is a major inducer of EMT-processes.

Though studies on TGF- $\beta$ 1 signalling have led to the identification of several transcription factors differentially expressed during TGF- $\beta$ 1 signalling, only a few of them have actually been shown to be involved in the regulation of epithelial morphogenesis, differentiation and TGF- $\beta$ 1-induced EMT-like processes.

We hypothesized that additional transcription factors are involved in mediating changes in epithelial plasticity and TGF- $\beta$ 1-dependent EMT, which have not been described yet.

Therefore, the present work utilizes a TGF- $\beta$ 1-responsive cell culture model to identify differentially expressed transcription factors during TGF- $\beta$ 1 signalling that might mediate changes in epithelial plasticity and might thus be functionally relevant for TGF- $\beta$ 1-induced EMT-progression.

In the second part of this work, a newly identified transcription of the Fox-family of proteins interacting with TGF- $\beta$ 1 signalling is further characterized with regards to:

- 1) cellular functions - with emphasis on epithelial differentiation
- 2) potential modulation of TGF- $\beta$ 1 signalling, including downstream target genes with a focus on EMT-progression *in-vitro*
- 3) the regulation of its expression

### 3. MATERIAL AND METHODS

#### 3.1 Material

##### 3.1.1 Chemicals

All used chemicals were obtained from the companies Sigma, Merck, Roche, Roth and J.T. Baker.

##### 3.1.2 Buffers and solutions

10 x PBS buffer	1.37 M NaCl · 26.8 mM KCl · 100 mM Na <sub>2</sub> HPO <sub>4</sub> · 17.6 mM KH <sub>2</sub> PO <sub>4</sub> · pH 7.4
PBS-T	0.1% (v/v) TWEEN® 20 in 1 x PBS
Tris-buffer	100 mM Tris Base · adjust pH with 1 M HCl to pH 7.4
RIPA buffer	50 mM Tris HCl pH7.4, 150 mM NaCl, 2 mM EDTA, 1% (v/v) NP-40 (Nonidet)
Cell-lysis buffer	RIPA Buffer · 1 mM PMSF · 1 x Complete-EDTA-free-Protease Inhibitor Cocktail
4x Separation gel buffer	150 mM Tris base · pH 8.8 adjusted with HCl · 0.1% (w/v) SDS
4x Stacking gel buffer	0.5 M Tris base · pH 6.8 adjusted with HCl · 0.1% (w/v) SDS
10x Running buffer	250 mM Tris Base · 1.92 M Glycine · 1% (w/v) SDS
10x Transfer buffer	250 mM Tris base · 1.92 M Glycine
1x Transfer buffer	25 mM Tris Base · 192 mM Glycine · 15% (v/v) Methanol
Blocking buffer	5% milk powder (w/v) in PBS-T
Hybridization buffer	3% milk powder (w/v) in PBS-T
Ponceau Red Stain	0.5% (w/v) Ponceau Red; 1% (v/v) Acetic Acid in H <sub>2</sub> O
5 x TBE	450 mM Tris-borate · 10 mM EDTA
Rotiphorese® 30 (37.5:1)	30% (w/v) acrylamide/bisacrylamide, mixing ratio 37.5:1 (Roth, Germany)
TEMED	N,N,N',N'-Tetramethylethylenediamin (Sigma, Germany)

**Tab. 1. Buffers for the enrichment of newly-transcribed RNA**

Abbreviation	Composition
Buffer A	50 mM Sodium acetate, pH 5.3 0.2 M Sodium chloride 0.1% (w/v) SDS 4 mM EDTA
Wash buffer WA	50 mM Sodium acetate, pH 5.3 0.5 M Sodium chloride 0.1% (w/v) SDS 4 mM EDTA
Wash buffer WB	25 mM Sodium acetate, pH 5.3 10 mM Sodium chloride 0.1% (w/v) SDS 4 mM EDTA
Wash buffer WC	50 mM Sodium acetate, pH 5.3 0.5 M Sodium chloride 0.1 (w/v) SDS 4 mM EDTA 25% (v/v) deionized formamide
Elution buffer	50 mM Sodium acetate, pH 5.3 0.2 M Sodium chloride 0.1% (w/v) SDS 4 mM EDTA 20 mM $\beta$ -mercaptoethanol

### 3.1.3 Media

DMEM	Dulbecco's Modified Eagles Medium (LGC Standards GmbH, Germany) · 10% (v/v) FBS · 10 ng/ml bovine insulin (Sigma, Germany)
PBS for cell culture	Dulbeccos's Phosphate Buffered Saline (Sigma, Germany)
Trypsin-EDTA	10 x Trypsin-EDTA solution (Sigma, Germany) diluted in cell culture grade PBS
FBS	Fetal bovine serum (Gibco® Invitrogen, Germany)
Lysogeny Broth (LB-media)	5g/l yeast extract · 10g/l tryptone · 10g/l sodium chloride
LB plates	Lysogeny Broth media · 15g/l agar

### 3.1.4 Antibodies

<u>Primary antibodies (Clone)</u>	<u>Company</u>
mouse-anti-E-cadherin (36)	BD Biosciences, Germany
mouse-anti-N-cadherin (32)	BD Biosciences, Germany
mouse-anti-CDK6 (DCS83)	Cell Signalling, Germany
rabbit-anti-Fibronectin (A0245)	DAKO, Germany
mouse-anti-Occludin (OC 3F10)	Invitrogen, Germany
rabbit-anti-MarvelD2	Invitrogen, Germany
mouse-anti-DDK (4C5)	Origene, USA
mouse-anti-Jup (PG 5.1, supernatant)	Progen, Germany
mouse-anti-CDK4 (C-22)	Santa Cruz Biotechnology, Germany
mouse-anti-Smad4 (B-8)	Santa Cruz Biotechnology, Germany
goat-anti-Tmod3 (M-16)	Santa Cruz Biotechnology, Germany
mouse-anti-Ets-1 (C-4)	Santa Cruz Biotechnology, Germany
rabbit-anti-Cyclin D1 (SP4)	Thermo Scientific, Germany
mouse-anti- $\alpha$ -tubulin (B-5-1-2)	Zymed Laboratories, Invitrogen, Germany
<u>Secondary antibodies</u>	<u>Company</u>
HRP-conjugated Swine-anti-rabbit	DAKO, Germany
HRP-conjugated Goat-anti-mouse IgG+IgM	Jackson Immuno Research Laboratories, USA
HRP-conjugated Goat-anti-mouse IgG	Santa Cruz, Germany
HRP-conjugated Donkey-anti-goat IgG	Santa Cruz, Germany
Alexa fluor 488 nm conjugated Goat-anti-mouse IgG	Molecular Probes, Invitrogen, Germany
Alexa fluor 488 nm conjugated Donkey-anti-rabbit IgG	Molecular Probes, Invitrogen, Germany
Alexa fluor 546 nm conjugated Donkey-anti-goat IgG	Molecular Probes, Invitrogen, Germany

### 3.1.5 Plasmids

<u>Plasmid name</u>	<u>Company</u>
pCMV6 Entry (Myc-/DDK tagged) Mouse cDNA clone FoxQ1 Accession No. NM_008239.3 Catalog No. MR206286	OriGene Technologies, USA
pIRESpuro3	ClonTech Laboratories, Germany

### 3.1.6 Primers

Primers were designed by the software *Primer 3* and obtained from Biospring (Germany).

The lyophilized pellets were dissolved to a 100 or 200  $\mu$ M stock solution.

Primer sequences are provided in Tab. 2.

**Tab. 2. Gene name, sequence and annealing temperature of the used primer**

<b>Gene name</b>	<b>Sequence (forward and reverse)</b>	<b>Annealing Temp. [°C]</b>
Gapdh	5'-actccactcttcaccttc, 5'-gggccagggtttcttactcc	60
Wisp1	5'-gggtgtgtggctcagggtaaa, 5'-tcaaacaggaacagaaactg	63
Vanin1	5'-ccctgaagtgttgctgagtg, 5'-ctcccaaagagcccgatg	60
bHLHB2	5'-gctaaaaaggggtccatctcc, 5'-tttcaacacaagcagagtg	59
Stk17b	5'-gccactcacaaaagtaagca, 5'-cgaaggggaacacacaaact	61
FoxA2	5'-cccgagggtactcttcc, 5'-agcgccacataggatgac	61
FoxQ1	5'-agcgaaggaacacttttggga, 5'-ggaagacaagcgaggaatga	59
Zeb1	5'-aagcagccagagaagagctg, 5'-ccacatcaacactggctgctc	64

### 3.1.7 small interfering RNAs (siRNAs)

All siRNAs were predesigned and obtained from Qiagen (Hilden, Germany). Lyophilized pellets were reconstituted in provided dilution buffer to a final concentration of 20  $\mu$ M, heated for 1 min at 90°C and further incubated at 37°C for 1 hour. Afterwards, the siRNAs were stored at -20°C till use. Tab. 3 displays the designation of the siRNAs and their respective target sequences.

**Tab. 3. siRNA name, target sequence and species**

siRNA name	Target sequence	Species
Mm_FoxQ1_1_HP siRNA	5'-ctccatcaaagtgccttaa	mouse
Mm_Zfhx1a_3_HP siRNA	5'-cccagaatttaaagaagaaa	mouse
Negative control siRNA	N/A	N/A
Negative control siRNA alexa-fluor 488 nm	N/A	N/A

N/A – Not Applicable

### 3.1.8 DNA and protein ladder

#### DNA ladders

100 bp DNA ladder (range 100 bp-2072 bp)

1 kb DNA ladder (range 506 bp-12216 bp)

#### Company

Invitrogen, Germany

Invitrogen Germany

#### Protein ladder

Precision Plus Protein All Blue Standards  
#161-0373 (range 10 kDa-250kDa)

#### Company

Bio-Rad Laboratories, Germany

### 3.1.9 Multi-component systems ('Kits')

**Tab. 4. Name and origin of applied 'kits'**

Name	Company
RNeasy® Mini Kit	Qiagen, Germany
RNase free DNase kit	Qiagen, Germany
Plasmid Mini Kit	Qiagen, Germany
QIAquick PCR purification kit	Qiagen, Germany
QIAquick gel extraction kit	Qiagen, Germany
GenElute™ MaxiPrep Kit	Sigma-Aldrich, Germany
SuperScript™ First Strand System for RT-PCR	Invitrogen, Germany
LightCycler® FastStart DNA Master SYBR Green I	Roche, Germany

### 3.1.10 Equipment

Tab. 5 summarizes regularly used equipment. Specifications about less often used equipment is referred to in the respective text passages.

**Tab. 5. Designation and origin of regularly used equipment**

Equipment designation	Company
Agilent Bioanalyzer 2100 System	Agilent Technologies, Germany
Mini Trans-Blot cell	Bio-Rad Laboratories, Germany
Mini-PROTEAN 3 Cell electrophoresis system	Bio-Rad Laboratories, Germany
LightCycler	Roche, Germany
FacsCalibur	BD Biosciences, Germany
Leica TCS-SL and Leica confocal software (v. 2.61)	Leica, Germany
Ultrospec 2000 UV/Visible Spectrophotometer	Pharmacia Biotech, Germany
2301 Macrodrive 1 Power Supply (PCR)	LKB, Germany

### 3.1.11 Cell lines and bacteria

#### Cell line designation and features

NMuMG cells (*Namru mouse mammary gland*)  
- spontaneously transformed epithelial cell line of the mouse mammary gland. This cell line displays cells with heterogeneous morphology.

NM18 cells  
- subclone of the parental NMuMG cell line. This subclone appears homogenous in morphology.

NM18-pRS cells and NM18-pRS-S4kd cells  
- stably transfected NM18 cells.  
NM18-pRS cells stably integrated the pRS plasmid, whereas NM18-pRS-S4kd cells harbour the pRS plasmid encoding a shRNA against mouse Smad4.

#### Bacteria

Subcloning Efficiency™ DH5α™ Competent Cells

#### Supplier

LGCStandards, Germany

P. ten Dijke, Leiden University Medical Center

P. ten Dijke, Leiden University Medical Center

Invitrogen, Germany

## 3.2 Methods

### 3.2.1 Molecular biological methods

#### 3.2.1.1 Isolation of plasmids from bacteria – ‘Mini-prep’

For the isolation of plasmids from bacteria, the Plasmid Mini Kit (Qiagen, Germany) was used according to the manufacturer’s instructions. Briefly, *E.coli DH5 $\alpha$*  bacteria were grown overnight in 2 ml LB-media including 100 $\mu$ g/ml Ampicillin (Roche, Germany) or 30  $\mu$ g/ml Kanamycin (Sigma, Germany). The bacteria were incubated at 37°C and 220 rpm on a rotation-shaker (SM 30 C control, Neolab, Germany).

1.5 ml of the bacteria suspension was subsequently harvested by centrifugation (13.000 rpm, 1 min.). After disposal of the supernatant, the pellet was further processed according to the Plasmid Mini Kit instructions. Finally, plasmids were eluted in 30-50  $\mu$ l Tris-HCl buffer (10 mM Tris-HCl, pH 8.5).

#### 3.2.1.2 Isolation of plasmids from bacteria on a large scale – ‘Maxi-prep’

For the preparation of larger amounts of plasmids the GenElute™ MaxiPrep Kit (Sigma-Aldrich, Germany) was used according to the manufacturer’s instructions.

Briefly, 2 ml of a freshly grown bacterial culture (6 -8 h; 37°C; 220 rpm) were diluted 1:1000 in 150 ml LB-media including 100  $\mu$ g/ml Ampicillin or 30  $\mu$ g/ml Kanamycin and further incubated overnight (37°C; 220 rpm). The culture was harvested by centrifugation (5000 x g, 10 min.) and further processed according to the recommendations.

The isolated plasmids were eluted in 3 ml of provided elution buffer (3000 x g, 5 min.). The plasmid DNA was subsequently precipitated with isopropanol. Therefore, 1/10 volume of sodium acetate (3 M, pH 5.2) and 1 volume of pure isopropanol were added to the eluted plasmid and incubated on ice for 1 h. The DNA was pelletized by centrifugation (12.000 x g, 30 min., 4°C) and subsequently washed with 70% (v/v) ethanol. After an additional centrifugation step (12.000 x g, 5 min., 4°C), the plasmid DNA was redissolved in an appropriate volume of 10 mM Tris-HCl, pH 8.5. Plasmids were usually kept at 4°C and for long-term storage at -20°C.

### **3.2.1.3 Measurement of nucleic acid concentration (DNA/RNA)**

Concentrations of nucleic acids can be determined by measuring the optical density (OD) at a wavelength of 260 nm in a crystal cuvette using a spectrophotometer.

The concentration is determined by the OD, the dilution factor and a specific multiplication-factor specific for DNA or RNA, respectively. In the case of DNA, an OD reading of 1 corresponds to a concentration of 50 µg/ml and in the case of RNA to a concentration of 40 µg/ml. The ratio of OD<sub>260</sub> and OD<sub>280</sub> reveals contamination of the samples with proteins. A ratio of 1.8-2.0 is recommended.

Analysed samples were diluted in deionized H<sub>2</sub>O and measured in an Ultrospec 2000 photometer (Pharmacia Biotech, Germany).

### **3.2.1.4 Digestion of DNA via endonucleases (restriction digest)**

Plasmid DNA was digested using sequence specific endonucleases. 1-5 µg of plasmid DNA were digested in a total volume of 50 µl. One Unit of the appropriate enzyme was used per µg DNA and incubated for one hour at 37°C.

The restriction digests were employed in buffer systems suggested by the supplier of the respective enzymes (3.2.1.7).

### **3.2.1.5 Electrophoretic separation of DNA**

For the electrophoretic separation of DNA, 0.8-1.5% (w/v) agarose gels were prepared using TBE-buffer. To visualize separated DNA, ethidium bromide (final concentration 0.5 µg/ml) was added to the agarose gels. An appropriate volume of DNA was mixed with 6 x Loading Dye Solution (Fermentas, Germany) and subsequently separated on the gels. The DNA was visualized and documented via the GelDoc™ 2000 Gel Documentation System (Bio-Rad Laboratories, Germany).

### **3.2.1.6 Extraction of DNA from agarose gels**

DNA fragments were isolated from agarose gels using the QIAquick gel extraction kit (Qiagen, Germany) according to the manufacturer's recommendations.

Briefly, DNA fragments were separated on agarose gels and excised from the gel using a sterile scalpel. The excised DNA was further processed according to the instructions.

### 3.2.1.7 Ligation of DNA fragments

In order to subclone the Myc/DDK-tagged FoxQ1 coding fragment from pCMV6 Entry into the pIRESpuro3 plasmid, the FoxQ1-coding fragment, including the Myc/DDK-tag, was released from pCMV6 Entry by sequential digestion using *Bam*HI (Roche, Germany) and *Fse*I (New England Biolabs, Germany).

The released FoxQ1-coding DNA fragment was isolated from an agarose gel using the QIAquick Gel extraction kit (see 3.2.1.6). Blunt-ends were generated using *Pfu* polymerase (Fermentas, Germany). Briefly, 43.5 µl of the eluted DNA fragment were incubated (72°C, 20 min.) with 1.25 U of *Pfu* polymerase and 200 µM dNTPs (Invitrogen, Germany) in a final volume of 50 µl.

The DNA fragment was purified using the QIAquick PCR purification kit (Qiagen, Germany) according to the manufacturer's recommendations and phosphorylated using T4 polynucleotide kinase (New England Biolabs, Germany) following the supplier's protocol for phosphorylating DNA 5'-ends.

The phosphorylated DNA fragment was subsequently ligated into *Eco*RV digested and dephosphorylated (Shrimp Alkaline Phosphatase, Promega, Germany) pIRESpuro3, using T4 ligase (Fermentas, Germany). Different molar ratios (1:3 and 1:10) of pIRESpuro3 and the DNA insert were incubated with 1 U T4 ligase in a total volume of 20 µl (overnight, 16°C).

The sequence of the Myc/DDK-tagged version of FoxQ1 was verified via sequencing. DNA sequencing was performed in the core sequencing facility of the DKFZ.

### 3.2.1.8 Transformation of *E.coli*-DH5α with plasmid DNA

In order to transform *E.coli* DH5α, 30-50 µl aliquots of bacteria were briefly thawed on ice. Usually, 50-100 ng of plasmid DNA were added to the bacteria suspension and further incubated on ice for 30 min.

The bacteria were heat-shocked for 45 sec. at 42°C and cooled down on ice before adding 500 µl of LB media and subsequent incubation at 37°C (220 rpm, 1h).

Varying dilutions of the bacterial culture were plated on selective LB-agar plates and incubated overnight at 37°C.

### 3.2.1.9 Isolation of total RNA from eukaryotic cells using Trizol®

The Trizol method to isolate RNA is based on the protocol of Chomczynski and Sacchi (Chomczynski and Sacchi, 1987).

Briefly, 1 ml of Trizol reagent was added per 10 cm<sup>2</sup> culture-vessel surface. To complete cell lysis, cultured cells were incubated for 5 min. at RT. Subsequently, 1/5 volume of chloroform was added and thoroughly mixed by inverting the tubes. After incubating the samples for 2-3 min. at RT, the phenol and aqueous phases were separated by centrifugation (12.000 x g, 15 min., 4°C). The aqueous phase was subsequently mixed with 1/2 volume of isopropanol (referring to the initially used amount of Trizol) and incubated at RT for 10 min. Precipitated RNA was pelletized via centrifugation (12.000 x g, 10 min., 4°C), washed with 75% ethanol (8500 x g, 5 min., 4°C) and finally dissolved in RNase-free H<sub>2</sub>O.

RNA samples were incubated with DNaseI (Ambion®, Germany) to reduce DNA contaminations, which may potentially interfere with subsequent reactions. DNaseI digestion was performed according to the manufacturer's recommendations.

### 3.2.1.10 Isolation of total RNA from eukaryotic cells for microarray analyses

RNA that was used for gene expression profiling was isolated using the RNeasy Mini Kit (Qiagen, Germany) including the optional on-column DNase digestion.

Briefly, cultured cells were harvested and lysed using RLT buffer. The cells were homogenized using 0.9 mm needles connected to 2 ml syringes.

The homogenized cells were further processed according to the manufacturer's recommendations.

RNA was eluted from the provided columns with 50 µl of RNase-free H<sub>2</sub>O.

### 3.2.1.11 Selective enrichment of thio-uridine (4sU) labelled and newly-transcribed RNA

The selective enrichment of newly-transcribed RNA was done according to the protocol of Kenzelmann et al. (Kenzelmann et al., 2007).

Briefly, newly-transcribed RNA was labelled by incubating cultured cells with 200 µM 4sU (Sigma, Germany) and 1 µCi H<sup>3</sup>-cytidine (20 Ci/mmol, Biotrend, Germany) for 2 hrs under standard cell culture conditions.

Total RNA was isolated as described in 3.2.1.10.

The thiolated RNA is enriched via a custom-made, agarose-based and mercury-containing matrix (Bio-Rad Affi-Gel 10-modified p-aminophenylmercuryacetate-agarose with a mercury content of 10  $\mu\text{mol/ml}$ ; Squarix Biotechnology, Germany).

100  $\mu\text{g}$  of total RNA were mixed with 600  $\mu\text{l}$  buffer A (see Tab. 1) in a siliconized tube (Eppendorf, Germany), heated to 70°C for 5 min. and cooled on ice.

Subsequently, 500  $\mu\text{l}$  of the mercury-containing matrix were transferred to a reaction tube containing a *small spin column* inlay (Qiagen, Germany) and centrifuged at <1000 rpm (minimum speed) for 30 sec. The packed matrix should have a volume of ~150  $\mu\text{l}$  and should not dry out.

The matrix was subsequently washed with DEPC-H<sub>2</sub>O and buffer A (5 x 400  $\mu\text{l}$  each) and finally mixed with the RNA.

The mixture was incubated in the dark for 4 hrs at 4°C under constant rotation using program F1 and 8 rpm (Intelli Mixer-2, ITF, Germany).

After this incubation period, the matrix was washed with various buffers that differ in their pH, salt content and temperature. The following protocol was used (all centrifugation steps were performed for 30 sec. using 400  $\mu\text{l}$  of the respective buffer at the minimal speed; < 1000 rpm).

- 4 x buffer A at RT
- 3 x buffer WA at RT
- 3 x buffer WA at 50°C
- 3 x buffer WB at 50°C
- 3 x buffer WC at 50°C
- 3 x buffer WA at 50°C
- 3 x buffer WB at RT
- 3 x buffer WC at RT
- 6 x buffer WA at RT
- 3 x buffer A at RT

The thiolated RNA was eluted from the matrix using the Elution buffer in the following order:

- 3 x Elution buffer at RT
- 2 x Elution buffer at 50°C
- 1 x Elution buffer at RT using 200  $\mu\text{l}$  and 2 min. centrifugation

The eluted RNA was individually precipitated from the six elution fractions using Pellet Paint® co-precipitant (Merck, Novagen®, Germany) according to the manufacturer's instructions.

Finally, the RNA was dissolved in DEPC-H<sub>2</sub>O in a total volume of 10 µl. 1 µl of the eluate was used for the analysis of RNA amount and quality (3.2.1.12). In addition, 1 µl was mixed with 10 ml of Rotiszint 22 (Carl Roth, Germany) in order to measure scintillation using a LS6500 Liquid Scintillation Counter (Beckmann Coulter, Germany). 10 ml of Rotiszint 22 were used as reference value. The incorporation of radioactive nucleotides into RNA was determined as *specific activity* by calculating the cpm-value (*counts per minute*) per µg of enriched RNA.

Total (non-enriched) and enriched RNA were used for comparative gene expression profiling (3.2.1.15 – NIAC-NTR-based *gene expression profiling*).

### **3.2.1.12 Measurement of RNA quality and quantity**

The quality and quantity of RNA that was used for gene expression profiling was analysed using the 2100 Agilent Bioanalyzer System (Agilent Biotechnologies, Germany) according to the suppliers protocol (program - *RNA 6000 nano assay, eukaryotic total RNA*).

Quality of the analysed RNA is determined by the automatic assignment of a RIN (RNA integrity number) and the ratio between the abundantly present 28S and 18S rRNA species.

RNA with a RIN of ~10 and a ratio of 28S/18S rRNA of ~2 is considered highest RNA quality.

### **3.2.1.13 Synthesis of cDNA - Reverse transcription**

Isolated total RNA was reverse transcribed to obtain cDNA using the SuperScript™ First Strand System (Invitrogen, Germany). Briefly, 150 ng-1 µg of total RNA were mixed with 1 µl dNTPs (10 mM) and 1 µl oligo-dT<sub>12-18</sub> primer (500 µg/ml) in a total volume of 8 µl. The samples were incubated at 65°C for 5 min. and subsequently chilled on ice. Per reaction 2 µl of 10 x RT-buffer, 4 µl of MgCl<sub>2</sub> (25 mM), 2 µl DTT (Dithiothreitol 0.1 M) and 1 µl of RNaseOUT™ (40 U/µl) were added and further incubated for 2 min. at 42°C. Samples were chilled again on ice, supplemented with 50 U of SuperScript™ II reverse transcriptase and incubated for 50 min. at 42°C.

The reaction was terminated at 70°C for 15 min. and generated cDNA stored at -20°C.

A no-Reverse-Transcriptase control was included every time cDNA was synthesized.

### 3.2.1.14 Quantitative Real-time PCR (qRT-PCR)

Synthesized cDNA (3.2.1.13) was diluted 1:10 in RNase-free H<sub>2</sub>O.

The qRT-PCR was performed using the LightCycler® FastStart DNA Master SYBR Green I System (Roche, Germany) according to the supplier's protocol.

Briefly, qRT-PCR reactions were performed in a total volume of 20 µl in glass LightCycler capillaries (Roche, Germany). Usually, 2 µl of diluted cDNA were mixed with 2 µl of the respective primer mix (final concentration of each primer 0.5 µM), 2.4 µl of MgCl<sub>2</sub> (final concentration 4 mM), 2 µl of SYBR-Green mix and filled up with 11.6 µl H<sub>2</sub>O. Zeb1 expression was analysed in cDNA samples with a final MgCl<sub>2</sub> concentration of 2 mM.

All primers and their annealing conditions can be found in Tab. 2.

Each LightCycler run contained a no-Reverse-Transcriptase control to assure that detected signals stemmed from the cDNA and not from contaminating DNA.

The expression of target genes were normalized to the expression of Gapdh and relative fold changes were calculated using the  $\Delta\Delta C_t$  method according to Livak and Schmittgen (Livak and Schmittgen, 2001).

**Tab. 6. qRT-PCR cycling conditions**

Number of Cycles	Temperature [°C]	Duration	Step
1 x	95	10 min.	Denaturation
	95	5 sec.	Denaturation
40-45 x	x <sup>#</sup>	10 sec.	Annealing
	72	5-10 sec.	Elongation
1x	72	5 min.	Termination
1 x	65-99	0.1 °C/sec.	Melting curve

<sup>#</sup>- annealing temperatures for specific primers are summarized in Tab. 2

### 3.2.1.15 Gene expression profiling

#### *NIAC-NTR-based gene expression profiling*

The enriched RNA (3.2.1.11) and respective total RNA were linearly amplified using the GeneChip® Two-Cycle Synthesis Kit (Affymetrix, Germany) according to the supplier's instructions.

Briefly, RNA was reverse transcribed into double-stranded cDNA (ds-cDNA). The ds-cDNA was subsequently *in-vitro* transcribed overnight using the MegaScript® kit (Ambion, Germany). The resulting cRNA was purified using IVT cRNA Cleanup Spin Columns and used for a second round of ds-cDNA synthesis. After clean-up of the ds-cDNA via cDNA Cleanup Spin Columns™, the second round ds-cDNA was used to generate biotin-labelled antisense cRNA using the GeneChip™ IVT labelling kit.

5 µg of biotinylated cRNA were purified, fragmented and hybridized onto 430\_2.0 mouse arrays according to manufacturer's instructions. The microarray chips were scanned using a GeneChip™ scanner 3000.

#### *Gene expression profiling of FoxQ1 knock-down cells treated with TGF-β1*

Gene expression profiling of FoxQ1 knock-down cells were performed on GeneChip® Mouse Genome 430A\_2.0 Arrays (Affymetrix, Germany).

Briefly, cells were reverse-transfected with non-silencing (ns-siRNA) or FoxQ1 siRNA (3.2.2.4).

Eight hours after transfection, cells were treated with 5 ng/ml TGF-β1 or respective solvent for an additional 40 hrs.

100 ng total RNA were used to synthesize first-strand cDNA and subsequent second-strand cDNA. The resulting ds-cDNA was further used for *in vitro* transcription and labelling of the resulting cRNA with biotin. Synthesis of cDNA and generation of cRNA was done with the GeneChip® 3' IVT Express Kit (Affymetrix, Germany) according to the supplier's protocol.

6.5 µg cRNA were purified, fragmented and hybridized onto GeneChip® Mouse Genome 430A\_2.0 Arrays according to the manufacturer's instructions. The microarray chips were scanned with a GeneChip™ scanner 3000.

All microarray experiments were conducted in collaboration with the Microarray-Core facility of the 'Zentrum für medizinische Forschung' (ZMF, University Clinics Mannheim, Germany).

### 3.2.2 Cell biological methods

#### 3.2.2.1 Culture of eukaryotic cells

The mammary epithelial cell line NMuMG (*Namru mouse mammary gland*) was obtained from the American Tissue Cell Collection (ATCC/LGC Standards, Germany) and cultured in L-glutamine containing DMEM media with a reduced bi-carbonate content (cat. 30-2002, ATCC/LGC Standards, Germany) including 10% (v/v) FBS and 10 ng/ml insulin at 37°C in a 5% CO<sub>2</sub> humidified atmosphere.

Cells were sub-cultured by trypsinization and subsequent dilution.

The NMuMG subclones NM18, NM18-pRS and NM18-pRS-S4kd were cultured as the parental NMuMG cells. Media for NM18-pRS and NM18-pRS-S4kd cells contained 5 µg/ml puromycin (Sigma, Germany) which was removed 24 hrs prior to experiments.

#### 3.2.2.2 Freezing of eukaryotic cells

Cells were frozen in cryotubes (Nunc, Germany) in regular growth media containing 5% (v/v) DMSO (Genaxxon BioSciences, Germany).

Briefly, cells were detached from the culture vessels via Trypsin-EDTA and growth media, harvested via centrifugation (1000 × g, 5 min., 4°C), redissolved in the DMSO-containing growth media and transferred to cryotubes.

Cells were stored at -80°C and for long term storage in liquid nitrogen.

#### 3.2.2.3 Thawing of eukaryotic cells

Cells were thawed at 37°C and transferred to pre-warmed media. The media was changed 24 hrs after thawing.

In the case of NM18-pRS and NM18-pRS-S4kd cells, 5 µg/ml of puromycin was added 24 hrs after thawing the cells.

#### 3.2.2.4 Transfection of small interfering RNAs

In order to transiently repress the expression of specific genes, cells were reverse-transfected with siRNAs using HiPerFect reagent (Qiagen, Germany) according to the manufacturer's recommendations.

Briefly, the transfection efficiency was tested using a non-silencing and alexa-fluor conjugated 488 nm siRNA and measured by flow-cytometry.

Typically, 17.500 cells/cm<sup>2</sup> were seeded on appropriate culture plates (usually 12-well, or 6-well plates) in the recommended volume. The respective siRNAs and transfection reagent were incubated for 10 min. at RT in serum-free medium and added drop-wise to freshly seeded cells (in suspension). Cells were transfected with 25 nM siRNA (final concentration). Media was changed after 24 hrs unless stated otherwise.

### 3.2.2.5 Generation of stably transfected NM18 cells

In order to constitutively overexpress FoxQ1 in NM18 cells, cells were transfected with 1 µg of pIRESpuro3-FoxQ1-Myc/DDK (3.2.1.7 and Supplementary Fig. 2) or pIRESpuro3 using the Lipofectamine 2000 reagent (Invitrogen, Germany), according to manufacturer's instructions. Briefly, 20.000 cells/cm<sup>2</sup> were seeded in 12-well plates 24 hrs prior to transfection.

Cells were transfected with plasmids or mock-transfected (Lipofectamine 2000 only) for 24 hrs, harvested and plated on 56 cm<sup>2</sup> dishes (Cellstar, Germany) in several dilutions (1:50 – 1:1000).

Cells were selected with 1 µg/ml puromycin for several days until all mock-transfected cells were dead (2-3 days).

Single colonies that survived selection were isolated using cloning cylinders (Millipore, Germany) and further propagated in puromycin-containing media.

Stably-transfected cells were maintained in puromycin-containing media (1 µg/ml) which was removed from the media 24 hrs before experiments.

### 3.2.2.6 TGF-β1 treatment of NMuMG cells and subclones

All cells were treated with 5 ng/ml TGF-β1 (Peprotech, Germany). Briefly, cells were seeded at a density of 17.500 cells/cm<sup>2</sup> culture vessel surface and further cultured for another 24 hrs. Subsequently, the cells were incubated with media containing 5 ng/ml TGF-β1 or respective solvent.

For the *NIAC-NTR*-based gene expression profiling (3.2.1.15), NMuMG cells were incubated with 200 µM 4sU and TGF-β1 or solvent for 2 hrs.

Cells that were reverse-transfected with siRNAs (3.2.2.4) were treated 8 hrs after transfection without changing the media. Instead, media containing TGF-β1/solvent was added to the transfected cells to a final concentration of 5 ng/ml.

### 3.2.2.7 Migration assay

In order to measure the migratory capacity of cells, a wound-healing assay was employed (Rodriguez et al., 2005).

Briefly, 40.000 cells were reverse-transfected with FoxQ1 siRNA or ns-siRNA (3.2.2.4) on ibiTreat  $\mu$ -Slides (Ibidi, Germany). Upon 24 hrs of transfection, the monolayer was scratched using the tip of a 10  $\mu$ l pipette. Cells were washed with media to remove floating cells.

The wounds were further monitored for 48 hrs using a steREO Discovery.V12 microscope (Zeiss, Germany). Two independent chambers per siRNA were monitored, each containing four selected points. Initial wound sizes and final wound sizes were analysed by measuring the area of the wound in  $\mu\text{m}^2$ .

### 3.2.2.8 MTT-assay

The MTT-assay is a colorimetric assay which is based on the reduction of the MTT-reagent (3-(4,5-dimethylthiazol-2-yl)-2,5-diphenyl tetrazolium bromide, Sigma, Germany) to formazan by mitochondrial enzymes.

Briefly, cells were reverse-transfected in 96-well plates and cultured further for 24 hrs. Subsequently, cells were incubated with 0.5 mg/ml MTT-reagent (dissolved as stock solution in Dulbecco's PBS) in a total volume of 200  $\mu$ l cell culture medium. Cells were incubated for an additional 3 hrs under regular growth conditions. After removing the supernatant, the accumulated formazan was resuspended in 200  $\mu$ l DMSO. The optical density was read on a plate-reader at O.D 560 nm (TecanFluor Plus, Tecan, UK).

Reference O.D. reading was recorded for cells that were not treated with MTT.

### 3.2.2.9 Cell cycle analyses

Cells were reverse-transfected for 48 hrs (3.2.2.4) on 6-well plates. Cells were harvested (4°C, 5 min., 1000 x g) and resuspended in 50  $\mu$ l PBS (4°C).

Cells were fixed by adding 500  $\mu$ l of 70% (v/v) ethanol (-20°C) and further incubated on ice for 90 min.

Fixed cells were harvested (4°C, 5 min., 1000 x g) and resuspended in 69  $\mu$ M propidium iodide-PBS solution (Sigma, Germany) including 10  $\mu$ g/ml RNase A. The cells were incubated for 30 min. at 37°C and analysed via flow-cytometry.

### **3.2.2.10 Transmission-electron microscopy**

Cells were cultured on sterile glass cover slips in 12-well plates.

The samples were fixed in Karnovsky's solution (containing cacodylate) and embedded in araldite (Serva, Germany).

Ultra-thin sections (70 nm, UCT Leica, Germany) were contrasted via uracylacetate and lead acetate. Sections were viewed on a Zeiss 900 electron microscope.

### **3.2.3 Protein-biochemical methods**

#### **3.2.3.1 Preparation of total protein cellular lysates**

Total protein extracts were prepared from cells using RIPA buffer.

Briefly, cells were harvested (RT, 5 min., 1000 x g) and resuspended in various amounts of RIPA buffer, including protease inhibitors. Cells were lysed by pipetting and incubated for 45 min. on ice.

The samples were centrifuged for 15 min. at 4°C (13.000 x g) and the supernatant transferred to a fresh tube.

#### **3.2.3.2 Determination of protein concentration – Bradford assay**

To measure the concentration of total protein lysates (3.2.3.1), Bradford reagent (Sigma, Germany) was used.

Briefly, 5 µl of protein lysates were mixed in 995 µl Bradford reagent and incubated at RT for 5 min.

The O.D. was recorded at 595 nm in a spectrophotometer using cuvettes for single use (Greiner-Bio, Germany). 5 µl RIPA-buffer in 995 µl Bradford reagent was used as a blank.

The protein concentration was calculated from a standard curve that was generated with BSA (range 0-5000 µg/ml).

### 3.2.3.3 SDS-polyacrylamide gel electrophoresis (SDS-PAGE)

For the separation of proteins according to their molecular weight, SDS-polyacrylamide gels were used.

Typically, the separation gels had a content of 10% (w/v) polyacrylamide.

Separation Gel (for 1.5 mm thick gels) 10%		Stacking Gel (for 1.5 mm thick gels) 3.45%	
H <sub>2</sub> O	6.15 ml	H <sub>2</sub> O	3.175 ml
4 x Separation Gel buffer	3.75 ml	4 x Stacking Gel buffer	1.25 ml
Rotiphorese® 30 (37.5:1)	5.0 ml	Rotiphorese® 30 (37.5:1)	575 µl
10% (w/v) APS	150 µl	10% (w/v) APS	37.5 µl
TEMED	10 µl	TEMED	10 µl

20-30 µg of total protein lysates were mixed with 4 x Loading buffer (Roth, Germany) and heated to 95°C for 5 min.

The samples were briefly placed on ice before loading onto the gels. The proteins were separated at a current of 35-45 mA.

### 3.2.3.4 Western Blot – Transfer of proteins onto nitrocellulose membranes

Proteins were further transferred to nitrocellulose membranes (0.45 µM; Schleicher & Schüll, Germany) after separation via SDS-PAGE (3.2.3.3).

Membranes were placed on the gels and covered by 2 layers of whatman paper and 1 layer of sponge per side. Prior to this, the membranes, whatman paper and sponges were pre-soaked in methanol-containing transfer buffer.

The proteins were transferred in transfer buffer at 4°C for 4 hrs using a constant voltage of 75 V.

Afterwards, membranes were stained with Ponceau-Red to check transfer-quality and equal protein loading.

The membranes were blocked with 5% (w/v) milk-PBS-T for 1 h at RT and incubated with primary antibodies (3.1.4) in 3% (w/v) milk-PBS-T (overnight, 4°C).

Unbound primary antibody was removed by washing the membranes with PBS-T (3 x 10 min.) at RT and followed by a 1 h incubation of the membrane with a HRP-conjugated secondary antibody in 3% (w/v) milk-PBS-T.

Membranes were washed as described and incubated with ECL reagents according to the supplier's recommendations (*enhanced chemiluminescens*, GE Healthcare, Germany).

Signals were imaged on blue-light sensitive films (GE Healthcare, Germany).

### **3.2.3.5 Confocal microscopy**

For confocal microscopy, cells were cultured on sterile glass cover slips in 12-well plates. Cells were fixed with pre-cooled acetone (-20°C) for 5 min. on ice and air-dried at RT.

The slides were blocked with 3% (w/v) BSA in PBS for 30 min. at RT and incubated with respective primary antibodies (3.1.4) overnight at 4°C.

The slides were washed with PBS-T (3 x 5 min.) and incubated with an alexa-fluor 488 nm or 546 nm conjugated secondary antibody (3.1.4).

Nuclei were stained with DRAQ5 (Axxora, Germany) for 15 min. at RT.

Actin filaments were visualized with phalloidin (488 nm or 546 nm alexa-fluor conjugated phalloidin, 1:160 in PBS, Molecular Probes, Invitrogen, Germany) for 15 min. at RT.

The slides were embedded in Fluoromount G (Biozol, Germany). Images were acquired and analysed using a Leica TCS-SL microscope and Leica Confocal software (version 2.61, Leica).

## **3.2.4 Biostatistical methods**

### **3.2.4.1 Analyses of gene expression profiling**

Microarray CEL files were imported to R statistical package version 2.7.1 using R Affy package version 1.18.2 (Gautier et al., 2004).

For the GeneChip® Mouse Genome 430 2.0 Arrays, probes were annotated by Custom CDF (Chip definition file for ENTREZ genes) Version 11 and for the GeneChip® Mouse Genome 430A\_2.0 Arrays Custom CDF Version 12 (Dai et al., 2005).

The microarray data was subjected to VSN normalization (*variance stabilisation and normalization*) (Huber et al., 2002).

Significance analysis was performed using the bioconductor package SAMR, which implements SAM statistics in R (Tusher et al., 2001).

A cut-off of 5% FDR (false discovery rate) was applied to identify significantly regulated genes.

### 3.2.4.2 Categorization of differentially expressed genes using selected GO-terms in Cytoscape/Bingo

The Gene Ontology (GO) project is based on a three-structured controlled vocabulary ('ontologies').

These ontologies describe a gene product in terms of its associated 'cellular component', 'biological process' and 'molecular function' which represent the three organizing principles of GO (Harris et al., 2004).

The ontologies are updated and available on a monthly basis via <http://www.geneontology.org>.

Differentially expressed genes (3.2.4.1) were categorized into selected GO-terms using the plug-in BINGO (Biological Networks Gene Ontology tool) in Cytoscape (Maere et al., 2005; Shannon et al., 2003) using all three organizing principles of GO.

The selected GO-terms and their respective definition are summarized in Tab. 7.

**Tab. 7. Overview of selected GO-terms and their respective definition**

GO-term	Definition
	<a href="http://www.geneontology.org">http://www.geneontology.org</a>
'Transcription factor activity'	The function of binding to a specific DNA sequence in order to modulate transcription. The transcription factor may or may not also interact selectively with a protein or macromolecular complex.
'Intercellular junction'	A cell junction that forms a connection between two cells; excludes direct cytoplasmic junctions such as ring canals.
'Cytoskeleton organization and biogenesis'	A process that is carried out at the cellular level which results in the assembly, arrangement of constituent parts, or disassembly of cytoskeletal structures.

#### **3.2.4.3 Student's t-test**

All data are expressed as mean  $\pm$  SEM. For qRT-PCR analyses, significance was tested using paired student's t-test.

All other significance values were estimated by using unpaired student's t-test.

#### **3.2.4.4 Transcription Factor Matrix-Scan (TFM-Scan)**

In order to check DNA sequences for transcription factor binding sites, TFM-Scan was used.

The TFM-Scan explores DNA sequences for locally overrepresented transcription factor binding sites using JASPAR (Defrance and Touzet, 2006)

TFM-Scan is publicly available at <http://bioinfo.lifl.fr/TFM/TFMscan/>.

## 4. RESULTS

### 4.1 Identification of differentially expressed transcription factors during TGF- $\beta$ 1 signalling

#### 4.1.1 TGF- $\beta$ 1-induced EMT in NMuMG cells

NMuMG cells constitute a well-established cell culture model to study TGF- $\beta$ 1-induced EMT-like processes and have previously been used in various studies to analyse underlying molecular mechanisms (Miettinen et al., 1994; Piek et al., 1999; Shirakihara et al., 2007; Xie et al., 2004).

As summarized in Fig. 6, TGF- $\beta$ 1 treatment of NMuMG cells resulted in a switch in cadherin expression, with a reduced expression of E-cadherin and an increased expression of N-cadherin. In addition, the expression of the ECM protein fibronectin was increased (Fig. 6a).

Furthermore, cells treated with TGF- $\beta$ 1 displayed profound changes in their cellular morphology towards a fibroblast-like phenotype. In comparison to respective control cells, treatment with TGF- $\beta$ 1 resulted in the acquisition of an elongated cell shape and the loss of the epithelial-typical 'cobblestone' sheet structure (Fig. 6b). This was paralleled by the acquisition of stress fibres in TGF- $\beta$ 1 treated cells (Fig. 6c).

Together, these data confirm that NMuMG cells undergo a TGF- $\beta$ 1-induced EMT-like process *in-vitro*.

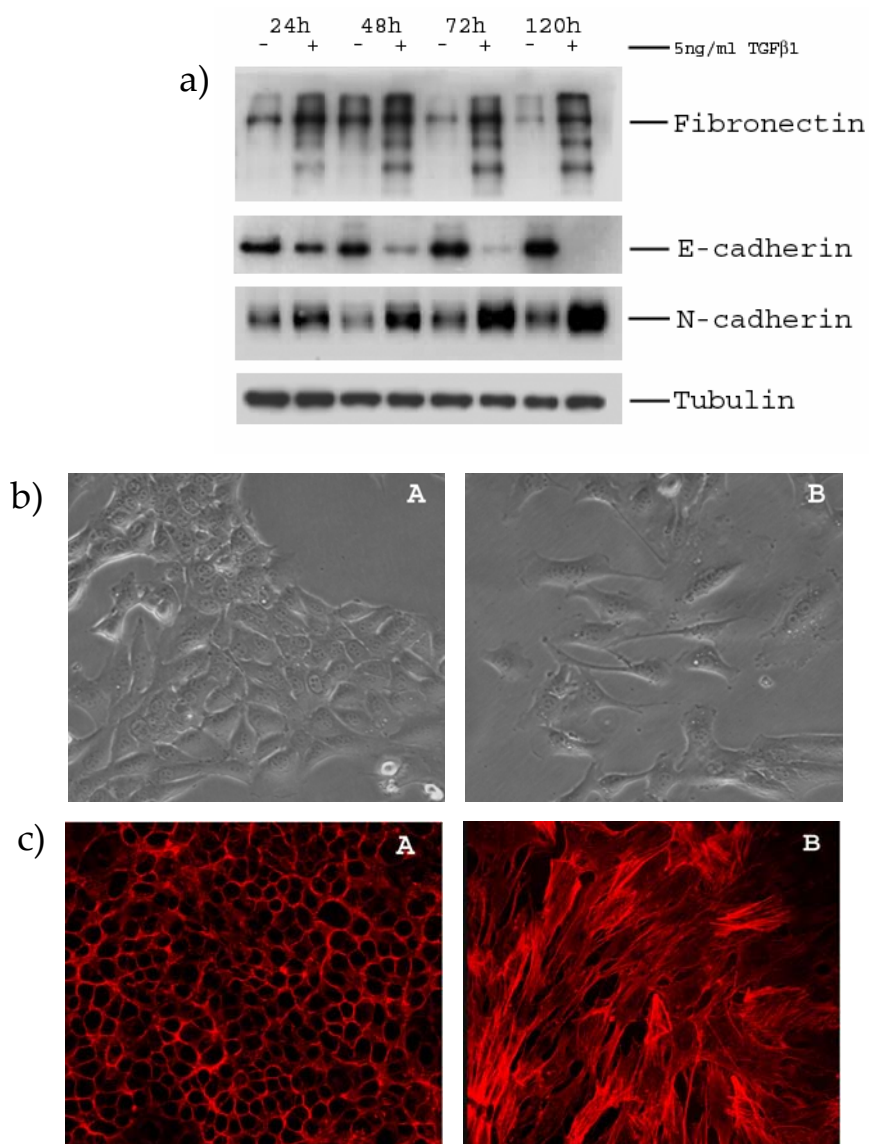


**Fig. 6. TGF- $\beta$ 1-induced EMT in NMuMG cells.**

NMuMG cells were treated with 5 ng/ml TGF- $\beta$ 1 and analysed for EMT-markers. Treatment with TGF- $\beta$ 1 led to a decrease in E-cadherin expression, accompanied by an increase in N-cadherin and fibronectin expression as revealed by Western blot analyses (**a**)

Upon TGF- $\beta$ 1 treatment, NMuMG cells lost their 'cobblestone' sheet structure, lost cell-cell contact and revealed an elongated, fibroblastoid cell morphology (A – control cells 48 hrs, B – cells treated with TGF- $\beta$ 1 for 48 hrs) (**b**).

TGF- $\beta$ 1-treated cells further lost the typical cuboidal actin-staining and acquired actin stress fibres (A – control cells 48 hrs, B – cells treated with TGF- $\beta$ 1 for 48 hrs) (**c**).

#### 4.1.2 Applicability of NMuMG cells for NIAC-NTR-based gene expression profiling

NIAC-NTR (Non-invasive application of captured-newly transcribed RNA) is a recently developed method that allows for high-throughput analysis of transcriptionally regulated gene expression changes.

The method is based on the incorporation of exogenously supplied 4sU (Fig. 7a) into nascent RNA and makes use of the cellular 'pyrimidine salvage pathway'. Thiolated RNA can be isolated via mercury-based chromatography and is compatible with fluorescent-based microarray technology. In combination with the analysis of changes in steady-state RNA, this method is able to assess relative contributions of mRNA synthesis and degradation or stabilization (Kenzelmann et al., 2007). It further enables the detection of differentially-expressed transcripts which are low in abundance.

In order to test if NMuMG cells possess a 'pyrimidine salvage pathway', the cells were incubated with 4sU and <sup>3</sup>H-cytidine for 2 hrs under regular growth conditions.

Thiolated RNA was isolated and analysed via scintillation measurement.

In contrast to RNA of control cells, which were only incubated with <sup>3</sup>H-cytidine (Fig. 7b; lanes 1 and 3), the treatment of cells with 4sU resulted in a significant enrichment in the specific activity of enriched RNA (Fig. 7b, columns 2 and 4).

Additionally, the integrity and overall quality of thiolated and enriched RNA was confirmed on an Agilent Bioanalyzer (Fig. 7c).

Together, these data show that NMuMG cells can be used for NIAC-NTR-based gene expression profiling as they possess an active 'pyrimidine salvage pathway'.

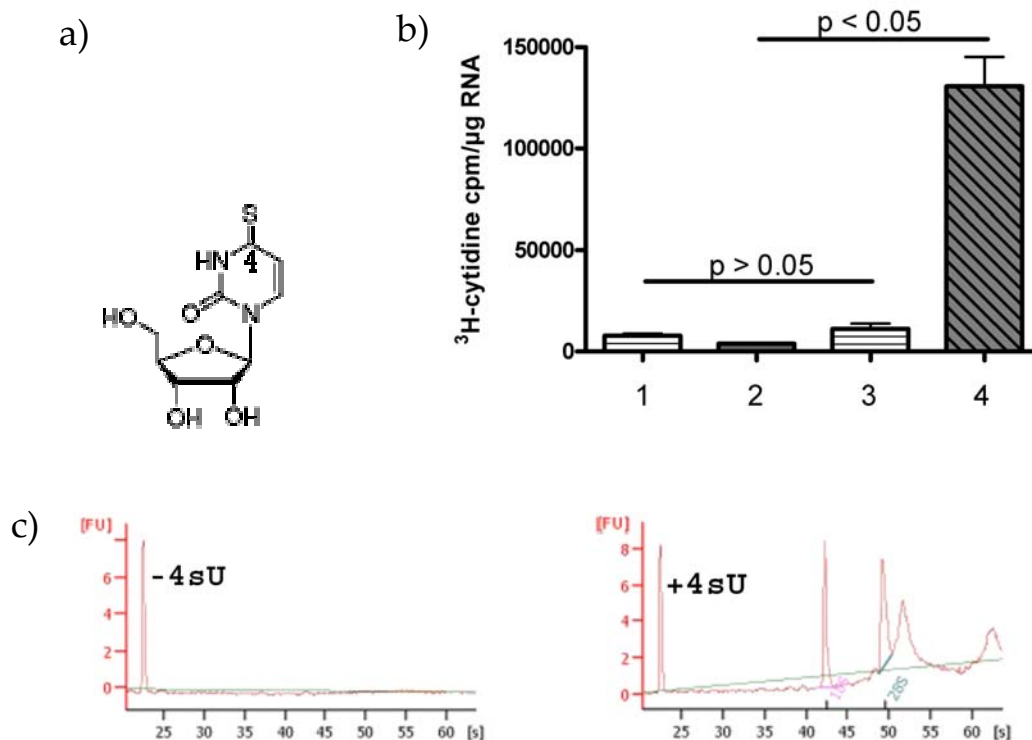


**Fig. 7. NMuMG cells can be used for NIAC-NTR-based gene expression profiling.**

NIAC-NTR is based on the incorporation of 4-thiouridine (4sU) into nascent RNA. 4sU contains sulphur- instead of an oxygen-group at position 4 of the pyrimidine-ring (a).

NMuMG cells were seeded 24 hrs prior to the treatment with 200  $\mu\text{M}$  4sU and 1  $\mu\text{Ci}$   $^3\text{H}$ -cytidine for 2 hrs. Total RNA was isolated and further enriched as described. Specific activity of radioactively labelled RNA was determined by scintillation analysis and expressed as cpm/ $\mu\text{g}$  RNA (1 – total RNA labelled with  $^3\text{H}$ -cytidine, 2 – total RNA labelled with  $^3\text{H}$ -cytidine and 4sU, 3 – enriched RNA labelled with  $^3\text{H}$ -cytidine, 4 – enriched RNA labelled with  $^3\text{H}$ -cytidine and 4sU). The result shows the outcome of three independent experiments. Significance analysis was performed using student's t-test (unpaired, two-tailed) (b).

1  $\mu\text{l}$  of 4sU-labelled (+4sU) and unlabelled RNA (-4sU) of columns 3 and 4 in (b) were analysed on an Agilent Bioanalyzer (c).

### 4.1.3 NIAC-NTR-based gene expression profiling of TGF- $\beta$ 1-induced NMuMG cells

For the NIAC-NTR based gene expression profiling, NMuMG cells were incubated with TGF- $\beta$ 1 or solvent for 2 hrs. In addition, 200  $\mu$ M 4sU were applied to the cells during TGF- $\beta$ 1 incubation. This time point was chosen since several transcription factors have previously been shown to be regulated within the first two hours of TGF- $\beta$ 1 signalling in NMuMG cells (Ishikawa et al., 2008; Shirakihara et al., 2007).

Total and thiolated RNA were isolated, further processed for NIAC-NTR-based gene expression profiling as described and hybridized onto 430\_2.0 mouse arrays. The experiment was performed as independent biological triplicate.

Differentially expressed genes were identified with a FDR < 0.05.

After 2 hrs of TGF- $\beta$ 1 treatment, a total of 1635 differentially expressed genes were identified. The comparison of differentially expressed genes that were either found through the analysis of steady-state-RNA (total RNA) or newly-transcribed RNA (enriched RNA) revealed, that 747 genes were only detected through the analysis of newly-transcribed RNA, whereas 299 genes could only be found as differentially expressed in the steady-state RNA fraction (Fig. 8a).

589 genes were found to be differentially expressed by the analysis of steady-state and newly-transcribed RNA and revealed the same direction in expression change in both fractions.

As previously shown by Kenzelmann et al., genes that are exclusively found in the steady-state RNA pool are regulated by post-transcriptional mechanisms, including mRNA stability and changes in mRNA turnover, whereas transcripts solely detected in the enriched RNA fraction are primarily regulated on the transcriptional level (Kenzelmann et al., 2007).

The differential expression of selected genes was corroborated by LightCycler analysis and was in agreement with the microarray data (Fig. 8b).

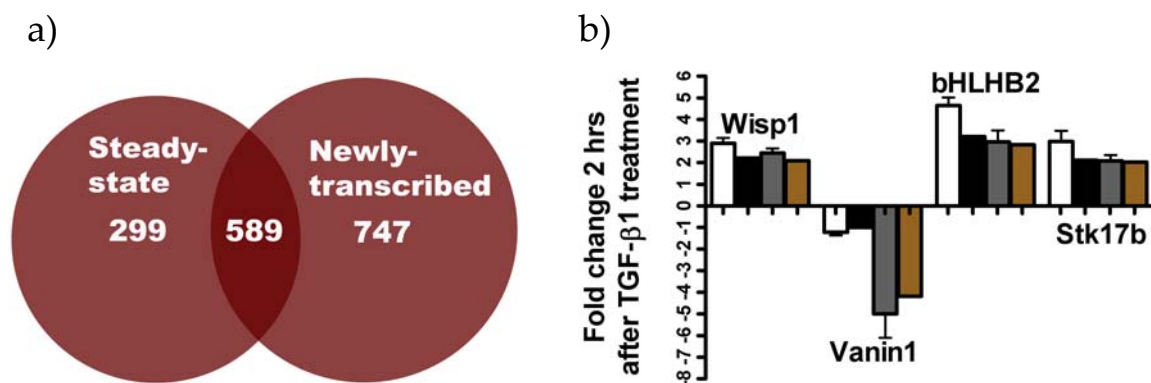


**Fig. 8. NIAC-NTR-based gene expression profiling during early TGF- $\beta$ 1 signalling.**

Treatment of NMuMG cells with 5 ng/ml TGF- $\beta$ 1 for 2 hrs led to the differential expression of 1635 genes (FDR < 0.05). 299 genes were exclusively detected by the analysis of steady-state RNA, whereas 747 genes could only be detected by employing the NIAC-NTR technique (Newly-transcribed). 589 genes were found to be differentially expressed in steady-state as well as newly-transcribed RNA (a).

The expression of randomly selected genes were confirmed by LightCycler analysis (white bar – LightCycler analysis of steady-state RNA; black bar – microarray analysis of steady-state RNA; grey bar - LightCycler analysis of newly-transcribed RNA; brown bar - microarray analysis of newly-transcribed RNA) (b).

#### 4.1.4 Several transcription factors of the Forkhead-family are transcriptionally regulated during early TGF- $\beta$ 1 signalling

In order to identify differentially expressed transcription factors during early TGF- $\beta$ 1 signalling, differentially expressed genes after 2 hrs of TGF- $\beta$ 1 treatment were filtered for the GO term 'Transcription factor activity' using Cytoscape/BINGO.

This resulted in the identification of a total of 116 differentially expressed transcription factors, which were further separated into 'post-transcriptionally regulated' (only differentially expressed in steady-state RNA) and 'transcriptionally regulated' (found in the newly-transcribed RNA fraction) (Supplementary Tab. 1a and 1b).

As summarized in Fig. 9, the microarray analysis revealed several transcription factors belonging to the Forkhead-factor family to be transcriptionally regulated during early TGF- $\beta$ 1 signalling.

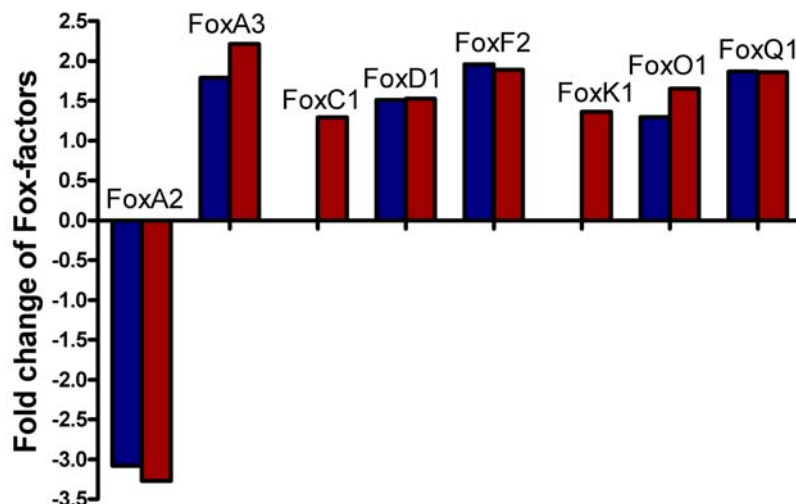


**Fig. 9. Summary of differentially expressed Forkhead-transcription factors during early TGF- $\beta$ 1 signalling.**

Eight members of the Forkhead-factor family were found to be transcriptionally repressed (FoxA2) or induced (FoxA3, FoxC1, FoxD1, FoxF2, FoxK1, FoxO1 and FoxQ1) in a TGF- $\beta$ 1-dependent manner. The figure shows the outcome of the *NIAC-NTR*-based gene expression profiling (blue bar – steady state RNA; red bar – newly-transcribed RNA).

In contrast to the Forkhead-transcription factors, other transcription factors including some of which have previously been associated to an EMT-process (e.g. Hmga2, Smad3 and Zeb1), were found to be regulated post-transcriptionally during early TGF- $\beta$ 1 signalling (Supplementary Tab. 1a and 1b).

The identification of several transcription factors belonging to the Forkhead family was of particular interest since a few Forkhead factors (FoxA2, FoxF1, FoxF2 and FoxC2) have recently been implicated in the regulation of epithelial plasticity and EMT (Burtscher and Lickert, 2009; Mani et al., 2007; Nilsson et al., ; van der Heul-Nieuwenhuijsen et al., 2009). However, it remains unknown if and how additional Forkhead factors influence epithelial plasticity and EMT.

As yet, nothing has been reported on the functional impact of FoxQ1 on epithelial plasticity and TGF- $\beta$ 1-induced EMT. Furthermore, the knowledge about cellular functions of FoxQ1, including the identity of potential target genes is still scarce. Thus, FoxQ1 was chosen for further functional analyses.

## **4.2 FoxQ1 regulates various cellular features in mammary epithelial cells as dissected by RNAi-mediated repression of FoxQ1**

### **4.2.1 FoxQ1 controls epithelial cell morphology and cell size of NM18 cells**

In order to elucidate the functional impact of FoxQ1 on epithelial cell biology, NM18 cells (a morphological homogenous subclone of the parental NMuMG cell line (Deckers et al., 2006)) were transfected with small-interfering RNAs targeting FoxQ1. Transfection efficiency was monitored by transfecting a fluorescently-labelled non-silencing siRNA into NM18 cells and subsequent FACS analysis. The transfection efficiency was >90% (Supplementary Fig. 1).

Due to the low protein expression of FoxQ1 and cross-reactivity of the antibody used, siRNA-mediated repression of FoxQ1 was quantified via qRT-PCR and revealed a reduction in mRNA expression of about ~60-70% 48 hrs after transfection (Fig. 10a).

The knock-down of FoxQ1 resulted in a change of cellular morphology (Fig. 10b; right panel). FoxQ1 siRNA transfected cells appeared elongated and enlarged in their overall size and maintained an epithelial sheet structure. The increase in overall cell size was quantified in phalloidin-stained cells via confocal microscopy and revealed significant differences between FoxQ1-knock-down cells versus respective control cells (Fig. 10c).

These results indicate that FoxQ1 expression is functionally involved in maintaining epithelial cell morphology and cellular size.

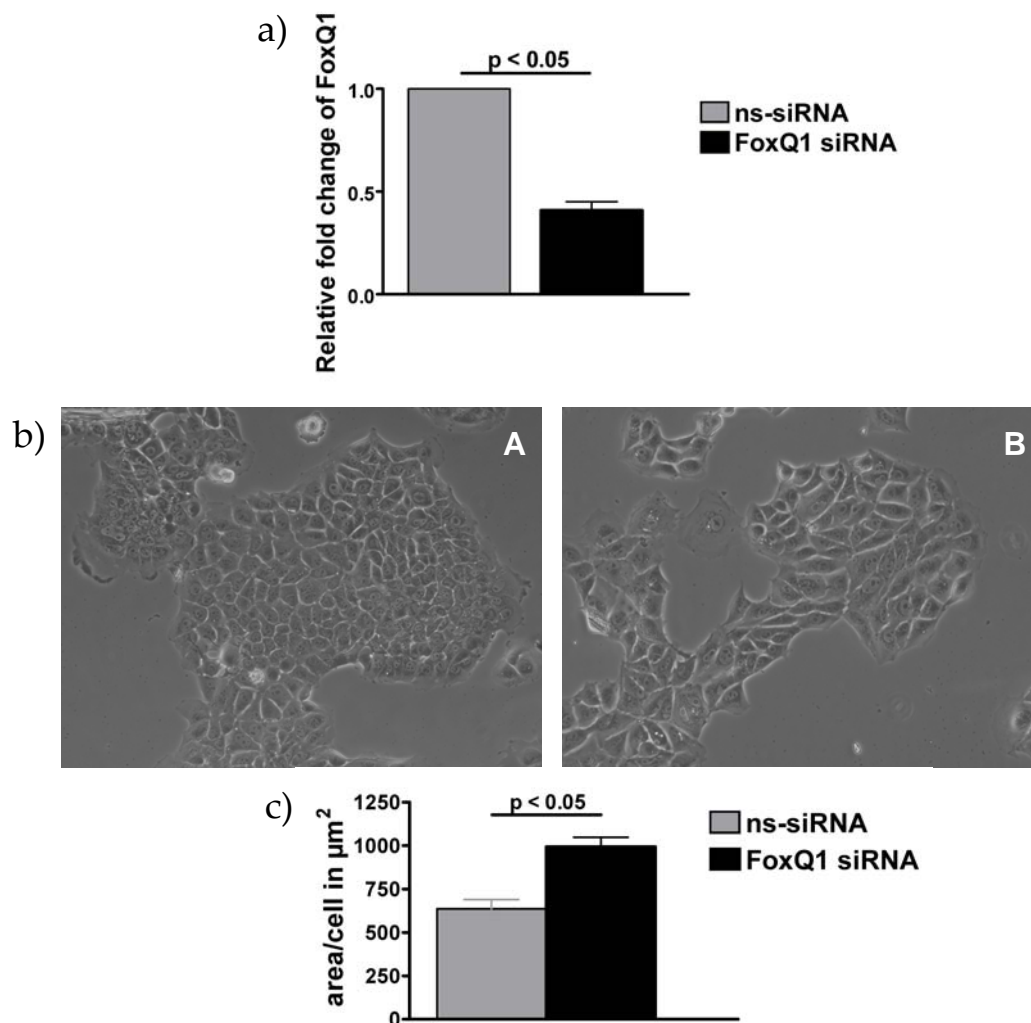


**Fig. 10. siRNA-mediated repression of FoxQ1 results in morphological changes in NM18 cells.**

NM18 cells were reverse-transfected with ns-siRNA or FoxQ1 specific siRNA and analysed for FoxQ1 mRNA expression. FoxQ1 expression was reduced about 60% upon FoxQ1 siRNA transfection (48 hrs). Results show the outcome of three independent experiments. Significance was tested using student's t-test (paired) (a).

FoxQ1 repression resulted in morphological changes in NM18 cells. As compared to control transfected cells (A), FoxQ1 siRNA transfected cells (B) showed an increase in overall cell size, appeared elongated and maintained their epithelial sheet structure (48 hrs) (b).

Quantification of cell size between ns-siRNA and FoxQ1 siRNA transfected cells. Depicted is the outcome of three experiments. Significance was calculated by student's t-test (unpaired) (c).

#### 4.2.2 Repression of FoxQ1 induces the accumulation of F-actin in circular structures ('actin rings') and results in a different localisation of the cytoskeleton-associated protein Tmod3

In order to test if the morphological changes of NM18 cells with a reduced FoxQ1 expression were accompanied by rearrangements in the cytoskeleton, actin fibres in FoxQ1 knock-down cells (48 hrs) were stained with phalloidin.

As shown in Fig. 11, cells with a reduced FoxQ1 expression accumulated F-actin in circular structures, herein referred to as 'actin rings'. These 'ring' structures were not found in control transfected cells.

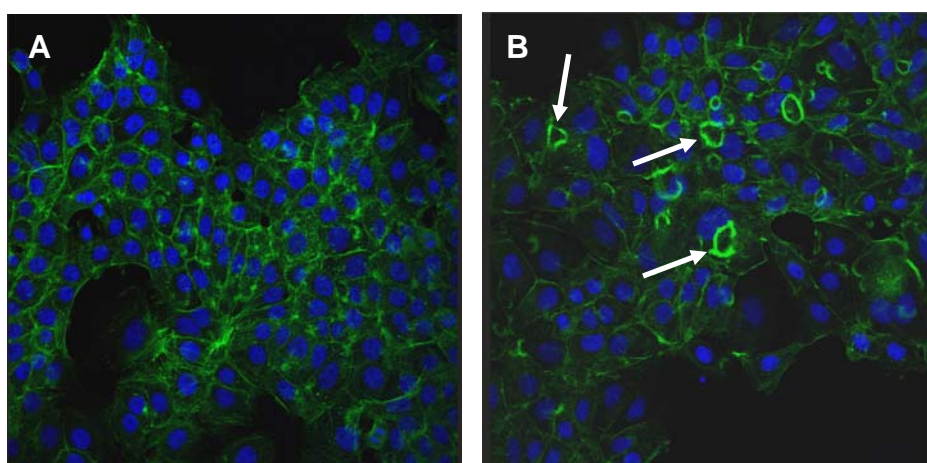


**Fig. 11. Repression of FoxQ1 results in the formation of 'actin rings' in NM18 cells.**

Control transfected cells (A) and FoxQ1 siRNA transfected cells (B) were fixed with acetone and stained for actin (phalloidin, green, 488 nm) and the nucleus (DRAQ5, blue, 633 nm). Actin accumulated in ring-like structures (white arrows) in FoxQ1 knock-down cells (48 hrs).

The increase in cell size, in combination with the formation of 'actin rings' suggested that FoxQ1 may play a role in the regulation of actin dynamics.

A class of proteins which is crucially involved in regulating actin dynamics by capping the pointed end of actin filaments is the Tropomodulin (Tmod) family of proteins. So far, four isoforms (Tmod1-4) have been identified. Whereas the expression of Tmod1, Tmod2 and Tmod4 is restricted to specific cells (erythrocytes, neuronal and skeletal cells), Tmod3 is ubiquitously expressed (Kostyukova, 2008). Additionally, Tmod3 has recently been shown to regulate cell morphology of polarized epithelial cells by stabilizing F-actin on lateral membranes (Weber et al., 2007).

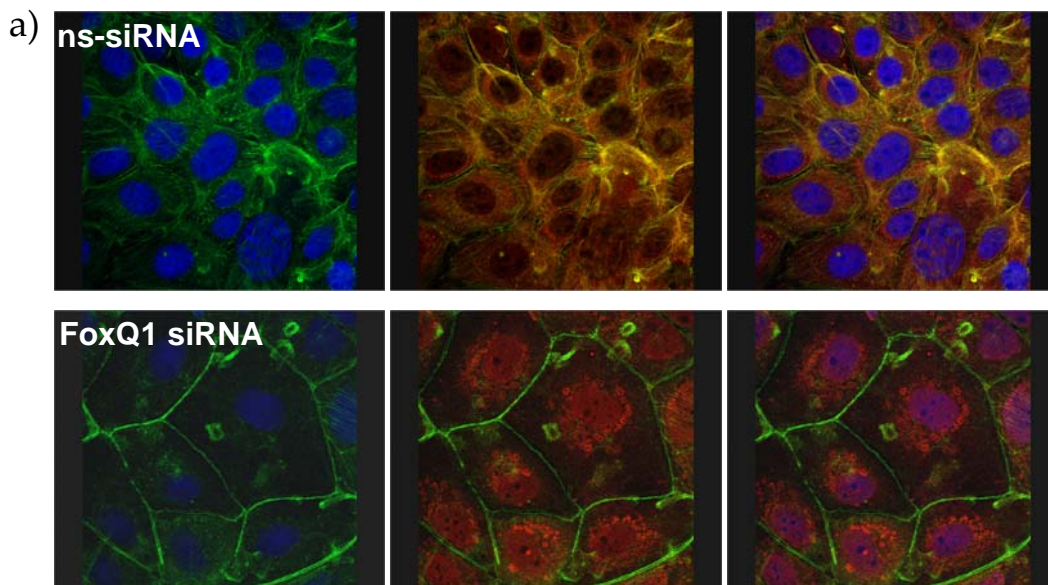
To check if the Forkhead factor FoxQ1 affects the expression of Tmod3, FoxQ1 knock-down cells were stained for Tmod3.

Whereas the Tmod3 protein showed a diffuse and predominantly cytosolic staining pattern in the ns-siRNA transfected cells (Fig. 12a, upper panel), cells with reduced FoxQ1 expression revealed a pronounced nuclear accumulation of Tmod3 (Fig. 12a, lower panel).

In addition, Tmod3 staining overlapped with the staining of F-actin in ns-siRNA transfected cells, whereas the overlap was reduced in FoxQ1 knock-down cells.

The different localisation of Tmod3 was accompanied by only a slight reduction in the total amount of Tmod3 protein expression as analysed by Western blot of total protein lysates (Fig. 12b).

In summary, the morphological changes of FoxQ1 knock-down cells are accompanied by changes in cytoskeletal rearrangements and differences in the localisation of the actin-filament associated protein Tmod3.



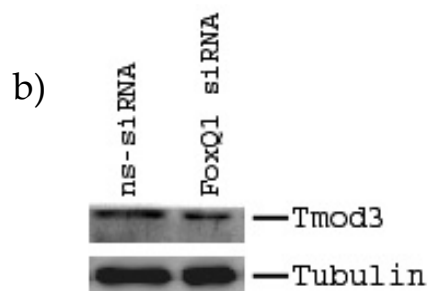


**Fig. 12. Repression of FoxQ1 expression leads to changes in Tmod3 protein localisation.**

NM18 cells were transfected with ns-siRNA (upper panel) or FoxQ1 siRNA (lower panel) for 48 hrs and stained for actin (phalloidin, green, 488 nm), Tmod3 (anti-Tmod3-antibody, red, 546 nm) and DRAQ5 (blue, 633 nm). Whereas control transfected cells showed a diffuse and cytosolic Tmod3 staining overlapping with F-actin staining (upper panel, middle), FoxQ1 knock-down cells (48 hrs) revealed a pronounced nuclear Tmod3 staining and less overlap with F-actin (lower panel, middle). The experiment was performed twice (a).

Western blot analysis of Tmod3 expression in FoxQ1 siRNA transfected cells. Tmod3 protein levels were only marginally reduced, comparing ns-siRNA and FoxQ1 siRNA transfected cells (48 hrs) (b).

#### 4.2.3 FoxQ1 suppression enhances the migratory capacity of NM18 cells

Remodelling of the actin cytoskeleton might modulate cell motility (Krause et al., 2003).

Since the repression of FoxQ1 led to changes in the cells cytoskeleton as revealed by the analysis of F-actin and Tmod3, cells were further tested for their migratory capacity using a classical wound assay (Rodriguez et al., 2005).

Reverse-transfected cells (24 hrs) were scratched to introduce an artificial wound ( $t = 0$  hrs) and monitored for another 48 hrs.

The wounds introduced in FoxQ1 siRNA transfected cell sheets closed faster compared to control transfected cells (Fig. 13a). The differences were quantified and statistically significant (Fig. 13b). These results indicate that the repression of FoxQ1 leads to an enhanced migratory capacity of NM18 cells.

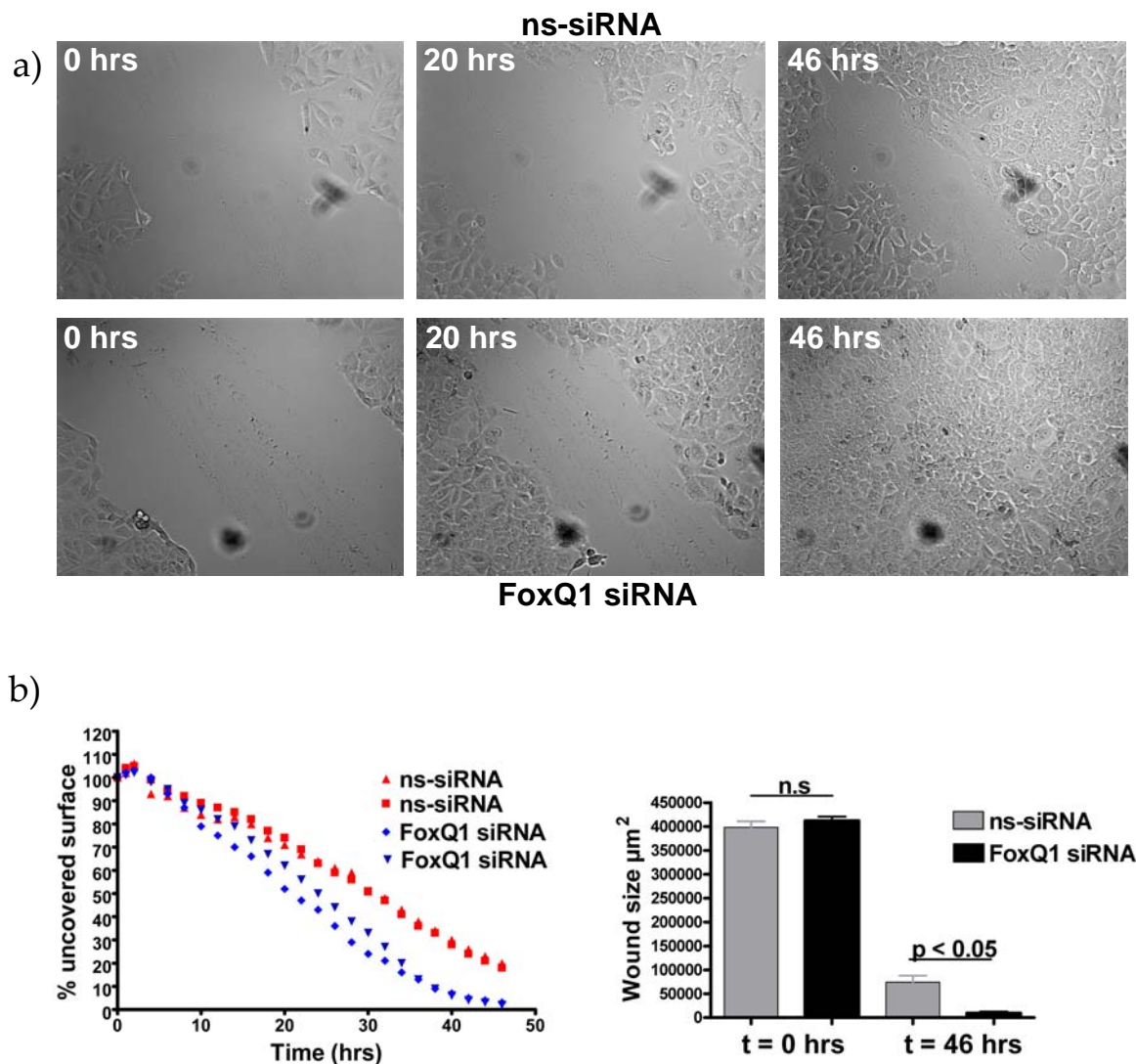


**Fig. 13. FoxQ1 repression enhances the migratory capacity of NM18 cells.**

Microscopic pictures of NM18 cells transfected with ns-siRNA or FoxQ1 siRNA at the indicated time points (a).

Statistical evaluation of wound closure at the indicated time points. Two independent wells per siRNA, each monitored at 4 separated spots were analysed (n=8). Results are shown as uncovered surface in percent (left panel) or remaining wound size (in  $\mu\text{m}^2$ ) (right panel). Statistical significance was calculated using student's t-test (two-tailed, unpaired) (b).

#### **4.2.4 Cellular proliferation and G1/S-cell cycle transition is impaired upon FoxQ1 repression – FoxQ1 suppression affects the expression of Cyclin-dependent kinases (CDKs)**

Cells with an impaired expression of FoxQ1 seemed to proliferate less.

To confirm this observation, transfected cells were subjected to a MTT-assay. In addition, cell numbers of FoxQ1 siRNA and control transfected cells were determined 48 hrs after transfection. The suppression of FoxQ1 led to a lower MTT-reading (Fig. 14a) and decreased cell numbers (Fig. 14b), indicating that FoxQ1 affects the proliferative capacity of NM18 cells. Therefore, FoxQ1 knock-down cells were analysed for possible alterations in their cell cycle phases using flow-cytometry. The repression of FoxQ1 resulted in an increase of cells present in the G0/G1-phase and a concomitant decrease of cells in the S-phase and G2/M-phase of the cell cycle (Fig. 14c). This indicated that the reduced expression of FoxQ1 led to a retarded progression through the G1-phase.

The cyclin-dependent kinases (CDKs) CDK4 and CDK6 together with the cyclin D proteins are specifically involved in the progression of cells through the G1-phase and the entry into the S-phase. CDK4 and CDK6 function as a subunit of a catalytically active protein complex, including the D cyclins. This protein complex phosphorylates the RB-protein (Retinoblastoma-protein), which results in the release of the sequestered E2F-transcription factor and subsequent expression of cell cycle target genes by E2F (Sherr, 1996; Sherr and Roberts, 1999).

Therefore, the protein expression of CDK4, CDK6 and Cyclin D1 was analysed in total protein lysates after knock-down of FoxQ1. The analysis revealed a strongly reduced protein expression of CDK4 and a reduction of CDK6 protein expression (Fig. 14d).

In contrast, the protein expression of Cyclin D1 did not change upon FoxQ1 knock-down.

In summary, these results suggest that FoxQ1 is involved in mediating the transition of cells through the G1-phase of the cell cycle by regulating the expression of CDK4 and CDK6.

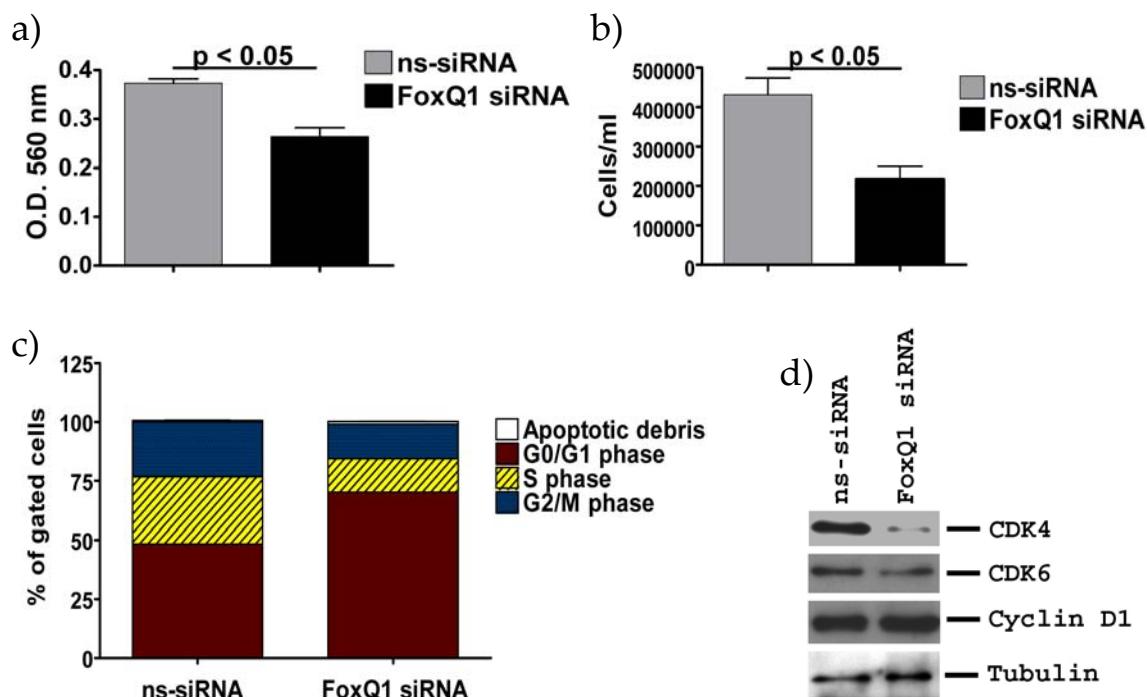


**Fig. 14. FoxQ1 suppression reduces cell proliferation, potentially via the regulation of G1/S-phase cell cycle transition.**

Control and FoxQ1 siRNA transfected cells were subjected to an MTT-assay 24 hrs after transfection (n=9). The p-value was determined by applying student's t-test (unpaired, two-tailed) (a).

Transfected cells were further counted 48 hrs after transfection (n=3). Significance was tested by student's t-test (unpaired, two-tailed) (b).

Cell cycle analyses of transfected cells via flow-cytometry. FoxQ1 siRNA transfected cells accumulate in the G0/G1-phase with a concomitant reduction of cells in the S- and G2/M-phase of the cell cycle (n=3) (c).

Western blot analysis of CDK4, CDK6 and Cyclin D1 expression. CDK6 and especially CDK4 revealed a decreased expression in FoxQ1 siRNA transfected cells, whereas the expression of Cyclin D1 remained unaffected (d).

#### 4.2.5 FoxQ1 repression results in the establishment of pronounced cell-cell contacts

NM18 cells with a reduced FoxQ1 expression revealed changes in their morphology as demonstrated in the previous sections.

For the further analysis of FoxQ1-dependent phenotypic alterations, NM18 cells transfected with FoxQ1 siRNAs were subjected to transmission-electron microscopy.

Compared to control transfected cells, the knock-down of FoxQ1 resulted in the establishment of pronounced cell-cell contacts, suggesting that FoxQ1 not only modifies the cytoskeletal integrity, but also leads to a reorganisation of cell-cell contacts by potentially regulating the expression of genes encoding junctional proteins (Fig. 15).

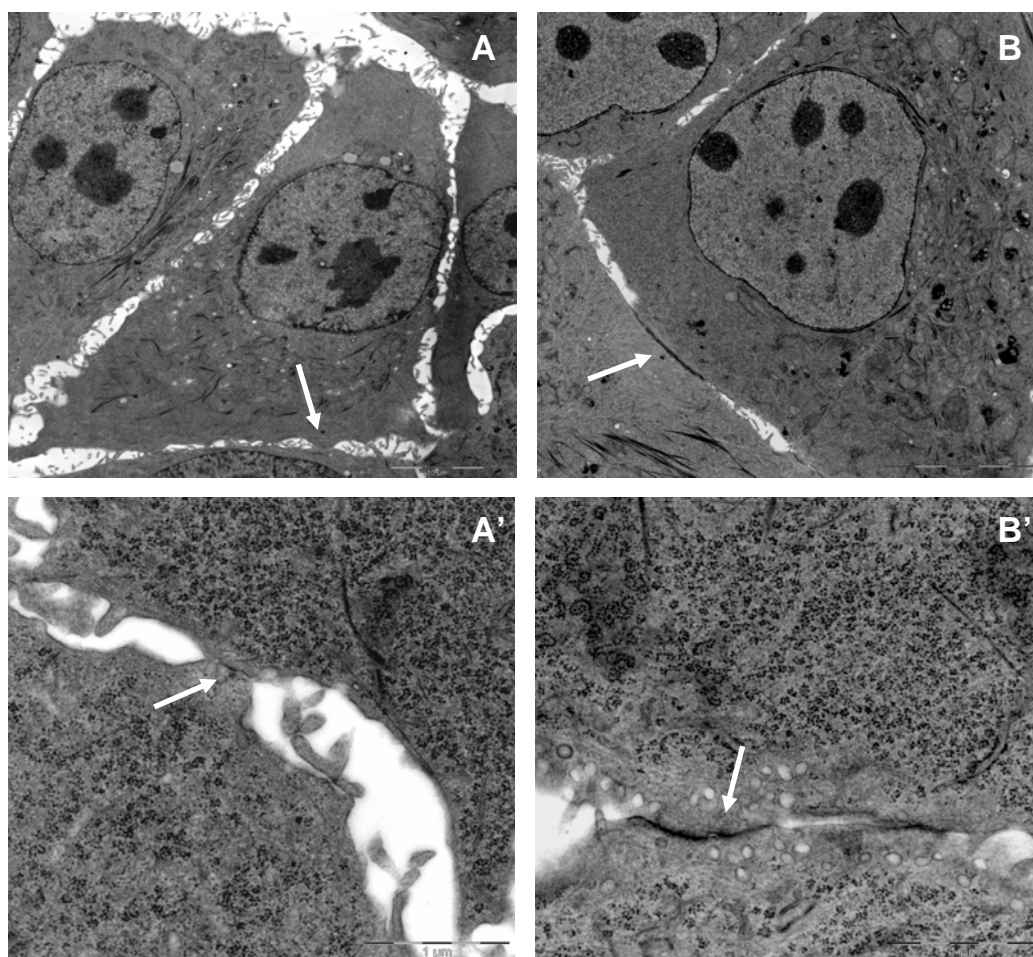


**Fig. 15. Cell-cell contacts are reorganized upon FoxQ1 knock-down.**

NM18 cells were transfected on glass-slides for 48 hrs and subjected to transmission-electron microscopy. Compared to control transfected cells (A/A' – ns-siRNA), FoxQ1 siRNA transfected cells (B/B') revealed pronounced cell-cell contacts (white arrows) and reduced intercellular clefts. Panels A and B show an overview of the cells, whereas panels A' and B' provide details of selected areas.

#### **4.2.6 FoxQ1 repression alters the outcome of TGF- $\beta$ 1-induced EMT-like progression and affects EMT-associated marker expression**

The Forkhead factor FoxQ1 was found to be increased in expression during TGF- $\beta$ 1-induced EMT-like progression and putatively regulates the cytoskeletal homeostasis as well as cell-cell contacts in NM18 cells.

Since the disruption of cell-cell contacts is crucial for the dissolution of the epithelial sheet-structure during TGF- $\beta$ 1-induced EMT-like progression, the effect of inhibiting TGF- $\beta$ 1-dependent induction of FoxQ1 was analysed during EMT-progression.

For this purpose, NM18 cells were reverse-transfected with FoxQ1 siRNA for eight hours and subsequently treated with TGF- $\beta$ 1 for another 40 hrs.

The efficiency of FoxQ1 knock-down during TGF- $\beta$ 1 signalling was first tested by the analysis of FoxQ1 mRNA expression and showed efficient repression of FoxQ1 also during TGF- $\beta$ 1 signalling (Fig. 16a).

TGF- $\beta$ 1 treatment resulted in changes in cellular morphology in control- and FoxQ1-siRNA transfected cells. However, compared to control transfected cells treated with TGF- $\beta$ 1, cells with a decreased FoxQ1 expression remained more attached to each other and seemed to resist the TGF- $\beta$ 1-dependent dissolution of the sheet structure (Fig. 16b).

In line with this, Western blot analysis of the EMT-markers E-cadherin and fibronectin showed that FoxQ1-repression results in an increased expression of E-cadherin, whereas the expression of fibronectin remained unaffected (Fig. 16c).

In summary, these results argue that endogenously expressed FoxQ1 represses E-cadherin expression and suggest that the TGF- $\beta$ 1-dependent increase in FoxQ1 expression contributes to the EMT-like progression by the repression of E-cadherin expression.

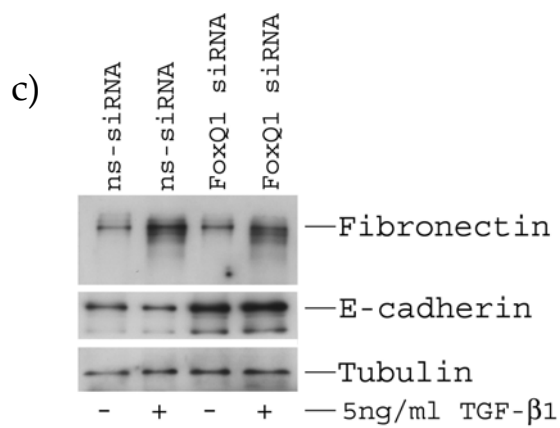
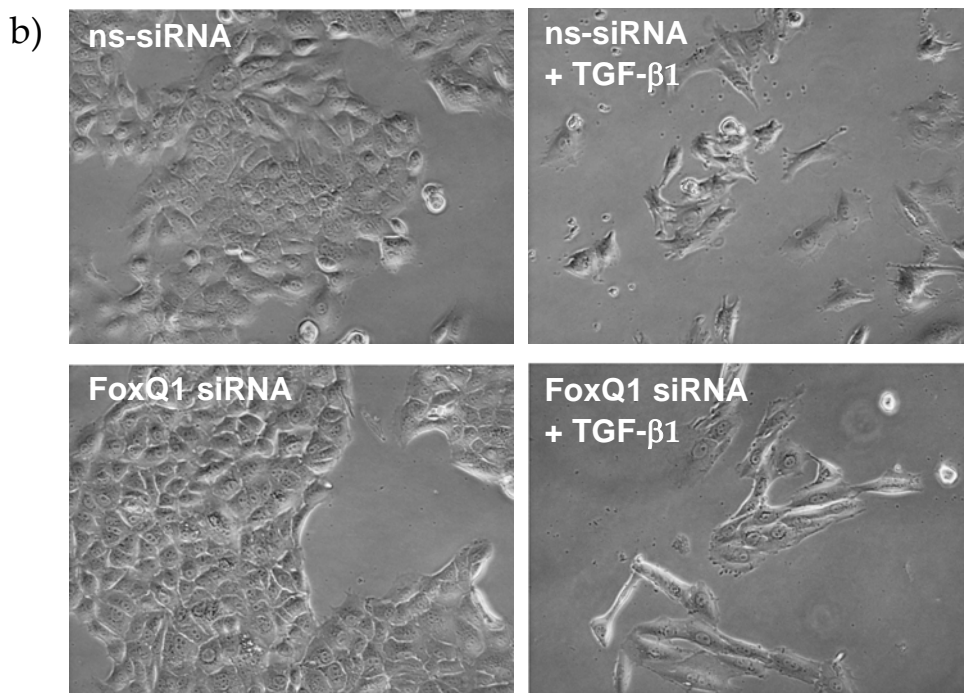
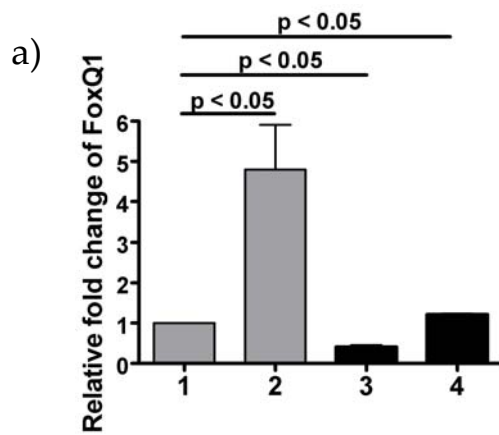


**Fig. 16. Repression of FoxQ1 reduces cell dissociation and repression of E-cadherin during TGF- $\beta$ 1-induced EMT-like progression.**

NM18 cells were transfected with ns-siRNA or FoxQ1 siRNA for 8 hrs and subsequently treated with 5ng/ml TGF- $\beta$ 1 or respective solvent for additional 40 hrs.

LightCycler analyses of FoxQ1 mRNA expression of three independent experiments (1 – ns-siRNA; 2 – ns-siRNA + 5ng/ml TGF- $\beta$ 1; 3 – FoxQ1 siRNA; 4 – FoxQ1 siRNA + 5ng/ml TGF- $\beta$ 1). The FoxQ1 siRNA effectively counteracted the induction of FoxQ1 expression during TGF- $\beta$ 1-induced EMT (lanes 2 and 4). Student's t-test was applied to calculate significance (n=3; paired, two-tailed) **(a)**.

Light microscopy analysis of ns-siRNA or FoxQ1 siRNA transfected cells treated with TGF- $\beta$ 1. Compared to TGF- $\beta$ 1 treated control transfected cells, FoxQ1 siRNA transfected cells induced with TGF- $\beta$ 1 remained attached to each other and appeared to remain more epithelial-like **(b)**.

Western blot analysis of EMT-markers E-cadherin and fibronectin. Compared to ns-siRNA transfected cells, the repression of FoxQ1 increased the expression of E-cadherin **(c)**.

### **4.3 Functional analyses of NM18 cells overexpressing FoxQ1**

#### **4.3.1 Establishment of FoxQ1 overexpressing NM18 cells**

Endogenously expressed FoxQ1 is involved in the regulation of various cellular features of NM18 cells, including proliferation, epithelial morphology and epithelial marker expression.

In order to analyse if the exclusive overexpression of FoxQ1 would be sufficient to induce aspects of an EMT-like progression and enhance cellular proliferation, NM18 cells stably expressing C-terminally- Myc/DDK-tagged FoxQ1 were established.

NM18 cells transfected with pIRESpuro3-FoxQ1-Myc/DDK or pIRESpuro3 were selected in puromycin-containing media for several days. Single colonies were isolated and tested for the expression of FoxQ1 via Western blot using an anti-DDK antibody.

As shown in Fig. 17a, several FoxQ1-overexpressing clones with varying degrees of FoxQ1 expression were obtained after puromycin selection.

Furthermore, the localisation of the FoxQ1 protein was tested via confocal microscopy in all clones using an anti-DDK antibody. The expression of FoxQ1 was restricted to the nucleus (Fig. 17b).

Since the clones 'pIRESpuro3-FoxQ1-Myc/DDK-7, -9 and -10' revealed a comparable expression of FoxQ1, subsequent experiments were primarily performed with these clones.

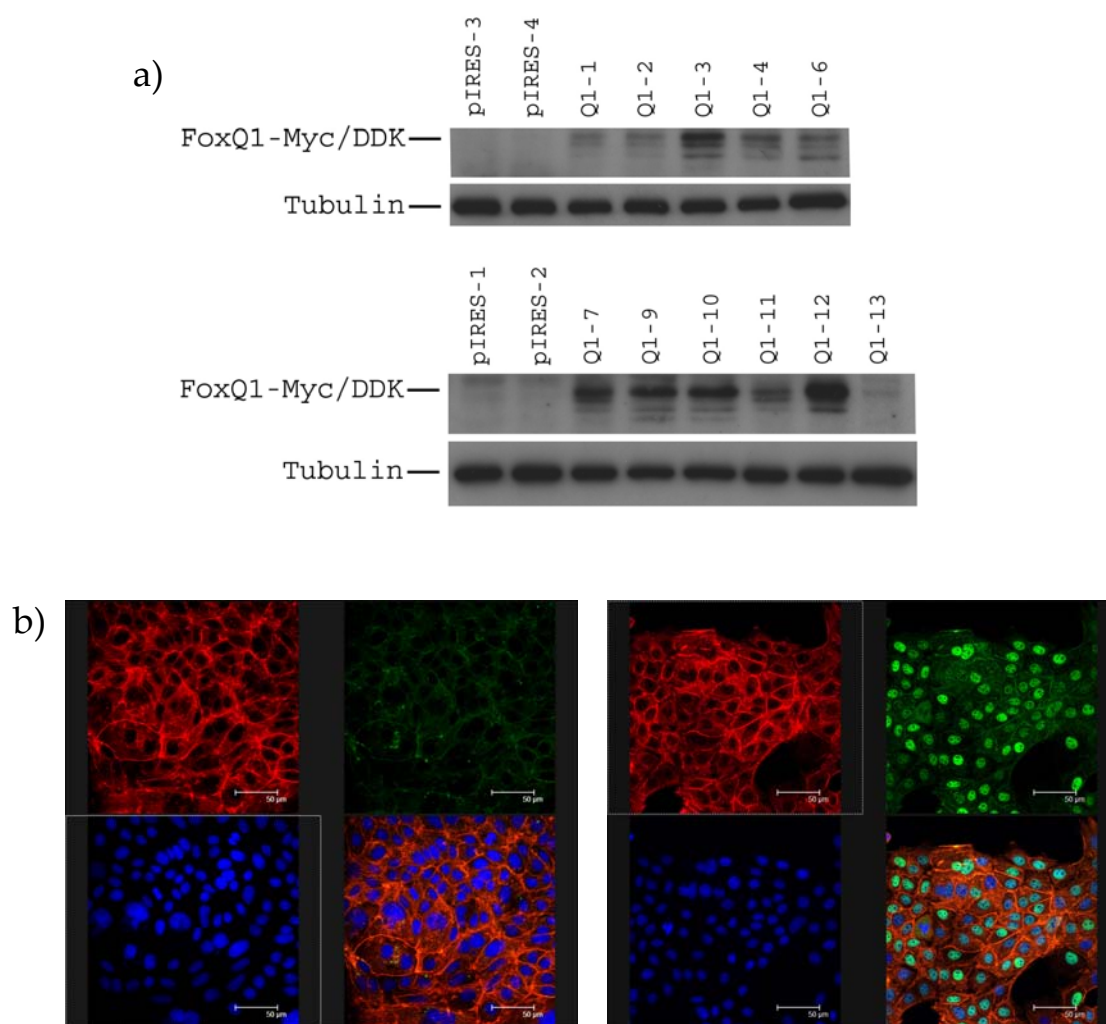


**Fig. 17. Stable overexpression of FoxQ1 in NM18 cells.**

Western blot analysis of FoxQ1 expression using an anti-DDK antibody in control- and FoxQ1-transfected cells. Several clones with varying degrees of FoxQ1 expression were obtained after puromycin selection. The FoxQ1-expressing clones 7, 9 and 10 (Q1-7, Q1-9 and Q1-10) revealed a comparable expression of FoxQ1 and were primarily used for further studies (a).

Immunofluorescent analysis of FoxQ1 protein localisation. Cells were fixed with acetone and stained for actin (phalloidin red, 546 nm), the nucleus (DRAQ5, blue, 633 nm) and FoxQ1 (anti DDK-antibody, green, 488 nm). The staining is shown for the control clone pIRESpuro3-clone 3 (left panel) and the FoxQ1-expressing clone pIRESpuro-FoxQ1-Myc/DDK-clone 7 (right panel) (b).

### 4.3.2 Enhanced expression of FoxQ1 does not induce proliferation and only modestly alters cell sheet organisation

To test if the overexpression of FoxQ1 results in an enhanced proliferation of NM18 cells, equal cell numbers of clones overexpressing FoxQ1 and respective control clones were seeded, cultured for further 48 hrs and subsequently counted. The overexpression of FoxQ1 neither enhanced the proliferative capacity of NM18 cells (Fig. 18a), nor did it increase the protein expression of CDK4 (Fig. 18b).

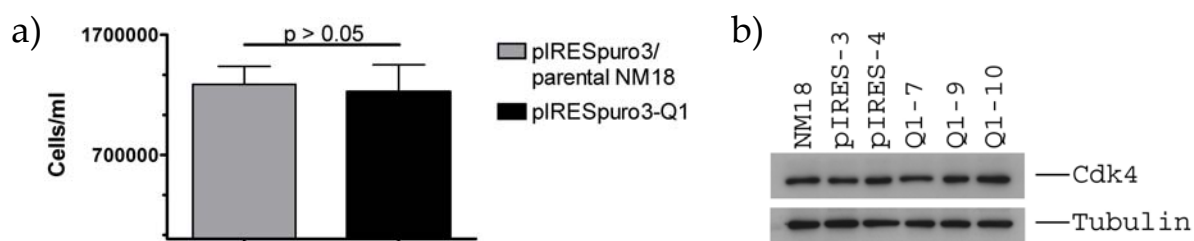


**Fig. 18 Overexpression of FoxQ1 does not enhance the proliferative capacity of NM18 cells.**

Equal cell numbers of control clones pIRESpuro3-clone 3 and 4, the parental cell line NM18 and the FoxQ1-overexpressing clones 7, 9 and 10 were seeded in 6-well dishes. Cells were counted 48 hrs later. The proliferation of control clones and parental NM18 cells were compared to cell numbers of FoxQ1-overexpressing cells (a) and stained for Cdk4 expression (b). The p-value was determined by applying student's t-test (unpaired, two-tailed).

Also, in contrast to the RNAi-mediated knock-down of endogenously expressed FoxQ1, NM18 cells overexpressing FoxQ1 did not reveal explicit alterations in cellular morphology based on sheer light microscopy observations and standard cell culture conditions. However, the analyses of Tmod3 and F-actin expression by confocal microscopy supported the impression that FoxQ1-overexpressing cells were organized in more distinct 'cobblestone-like' sheet structures compared to control cells (Fig. 19).

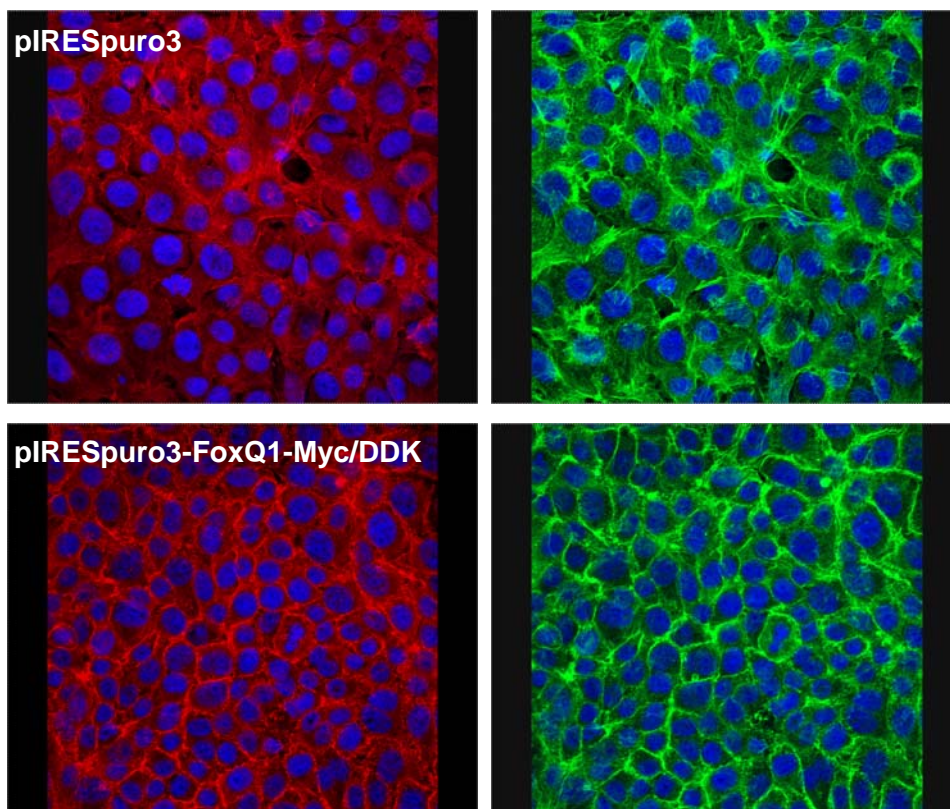


**Fig. 19. Tmod3 and F-actin distribution in FoxQ1-overexpressing cells.**

pIRESpuro3-clone 4 (upper panel) and pIRESpuro3-FoxQ1-Myc/DDK-clone 9 (lower panel) were stained for Tmod3 (anti-Tmod3 antibody, red, 546 nm), nucleus (DRAQ5, blue, 633 nm) and F-actin (phalloidin, green, 488 nm) and subjected to confocal microscopy.

#### **4.3.3 Overexpression of FoxQ1 modulates TGF- $\beta$ 1 induced alterations in epithelial morphology and results in a modified ECM**

The functional impact of FoxQ1 overexpression was further tested in relation to TGF- $\beta$ 1 signalling.

Equal cell numbers of control clones and FoxQ1-overexpressing clones were seeded and either treated with TGF- $\beta$ 1 or solvent, respectively.

TGF- $\beta$ 1 treatment resulted in morphological alterations of control- and FoxQ1-overexpressing clones.

However, as shown in Fig. 20a, the enhanced expression of FoxQ1 influenced the outcome of TGF- $\beta$ 1 signalling with regard to cellular morphology and cell dissociation. FoxQ1-overexpressing cells treated with TGF- $\beta$ 1 remained organized in a sheet-like structure (Fig. 20a, lower right panel), whereas cells of control clones apparently dissociated from each other (Fig. 20a, lower left panel).

Supplementary Fig. 3 shows comparable phenotypic differences for pIRESpuro3-clone 3 and selected FoxQ1-overexpressing clones pIRESpuro-FoxQ1-Myc/DDK-clone 7 and 10, which verifies the TGF- $\beta$ 1-dependent morphological differences between control and FoxQ1-overexpressing cells in independent clones.

Additionally, whereas control clones treated with TGF- $\beta$ 1 regularly showed several lateral cellular protrusions (Fig. 20b, black arrows), FoxQ1-overexpressing cells essentially lacked these structures.

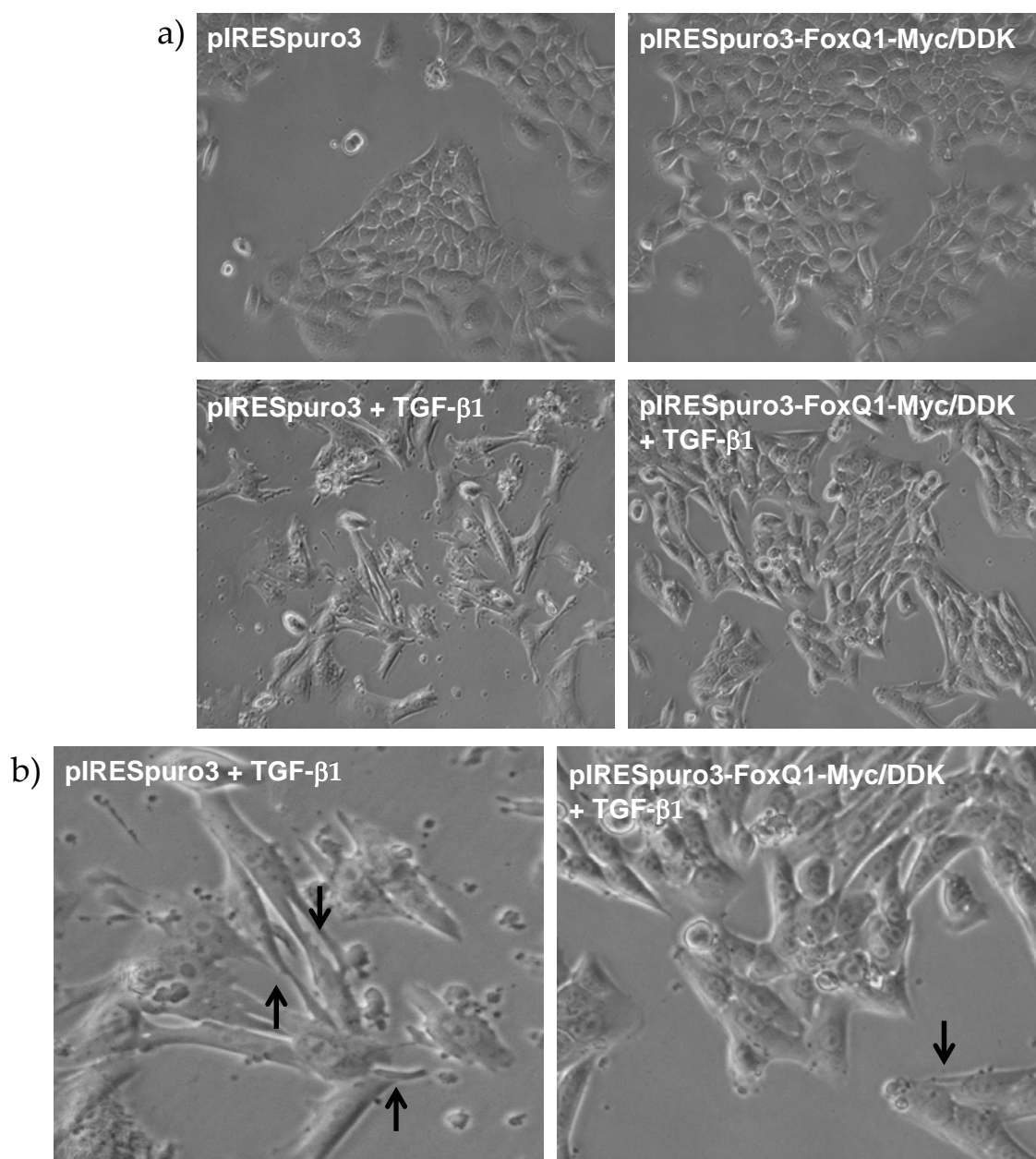
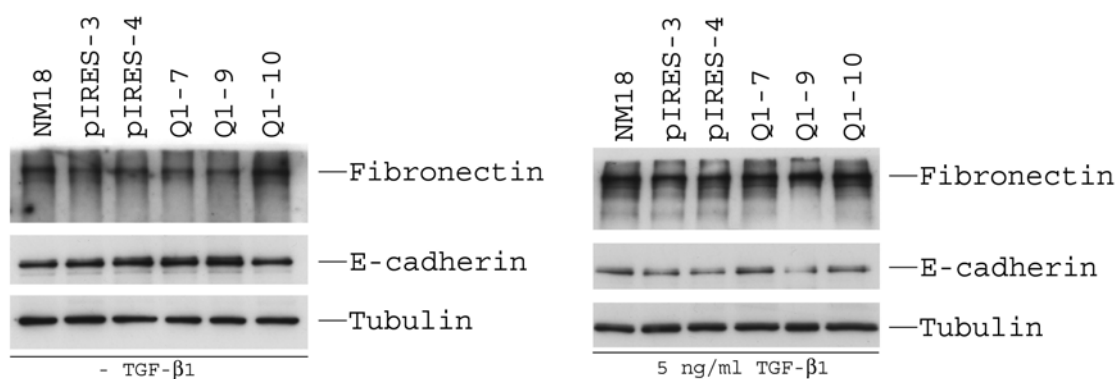


Fig. 20. Enhanced expression of FoxQ1 influences the outcome of TGF- $\beta$ 1-induced changes in cell morphology.

Control clones (shown for pIRESpuro3-clone 4) as well as FoxQ1-overexpressing cells (shown for pIRESpuro3-FoxQ1-Myc/DDK-clone 9) respond to TGF- $\beta$ 1 treatment. Whereas in control clones the epithelial sheet structure was disrupted (lower left), FoxQ1-overexpressing cells seemed to remain attached to each other in a sheet-like structure (lower right) (a).

In addition, TGF- $\beta$ 1 treatment of control clones resulted in the formation of cellular protrusions (black arrows), which were much less abundant in FoxQ1-overexpressing cells (b).

Protein expression analyses of the EMT-associated markers E-cadherin and fibronectin did not reveal any consistent differences between control and FoxQ1-overexpressing cells (Fig. 21).



**Fig. 21. The EMT-markers E-cadherin and fibronectin are not differentially expressed between control and FoxQ1-overexpressing cells upon TGF- $\beta$ 1-induced EMT.**

Equal numbers of the indicated cell-clones were treated with 5 ng/ml TGF- $\beta$ 1 for 48 hrs and analysed for the expression of E-cadherin and fibronectin. FoxQ1-overexpressing cells did not reveal apparent differences in EMT-marker expression compared to control cells (left panel – untreated; right panel – 5 ng/ml TGF-  $\beta$ 1)

However, immunofluorescent staining of fibronectin revealed a difference in its localisation in cells overexpressing FoxQ1 and respective controls (Fig. 22).

Both, control- and FoxQ1-overexpressing cells revealed fibronectin expression in their cytoplasm. Additionally, control cells showed an extracellular deposition of fibronectin (Fig. 22, white arrows in left upper panel) that was markedly reduced in FoxQ1-overexpressing cells (Fig. 22, right upper panel).

Fibronectin expression could equally be induced in control-, as well as FoxQ1-overexpressing clones upon TGF- $\beta$ 1-treatment (Fig. 22, lower panel and Fig. 21).

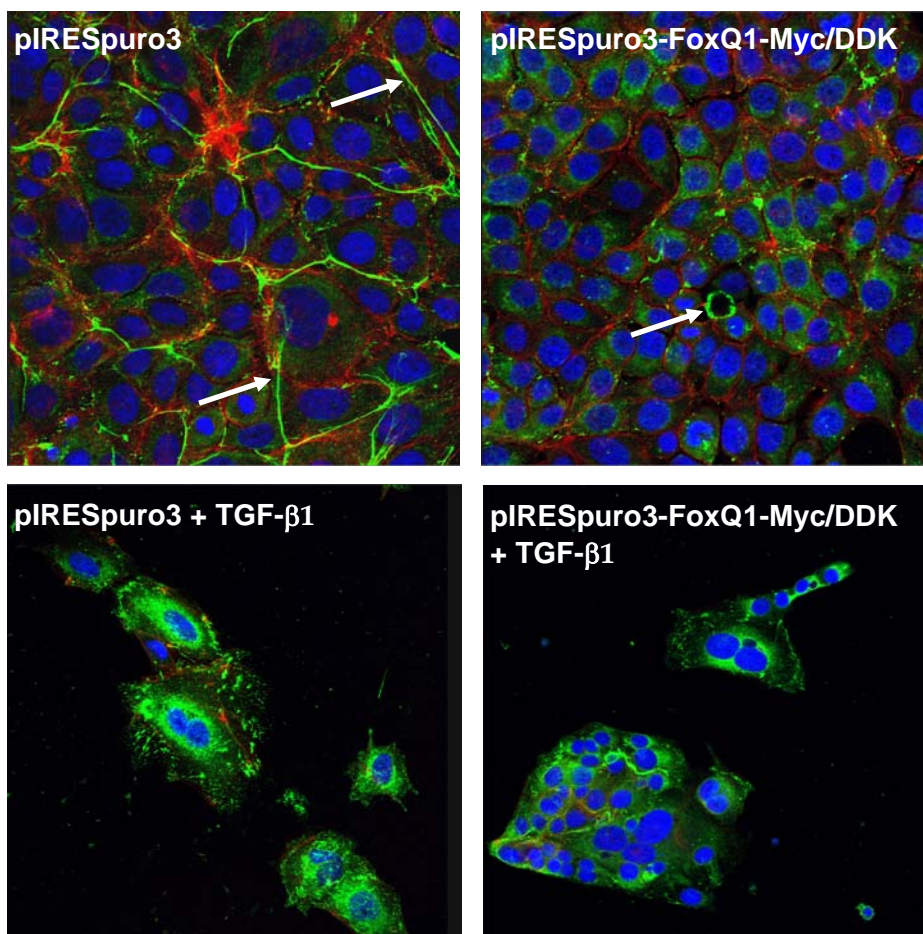


**Fig. 22. Overexpression of FoxQ1 alters extracellular distribution of the ECM component fibronectin.**

Equal cell numbers of control and FoxQ1-overexpressing cells were cultured on glass plates and treated with TGF- $\beta$ 1 for 48 hrs. Cells were stained for fibronectin (anti-fibronectin antibody, green, 488 nm), DRAQ5 (blue, 633 nm) and actin (phalloidin red, 546 nm). Results are shown for control clone 4 (left panel) and FoxQ1-overexpressing clone 9 (right panel). Whereas control cells (pIRESpuro3) revealed an extracellular accumulation of fibronectin (white arrows), FoxQ1-overexpressing cells essentially lacked this extracellular deposition. However, fibronectin expression was induced in control- and FoxQ1-overexpressing cells upon treatment with TGF- $\beta$ 1 (lower panel).

Together, these results suggest that overexpression of FoxQ1 modulates the secretion and/or proper assembly of extracellular fibronectin and thereby modifies the ECM.

## **4.4 A role of FoxQ1 in TGF- $\beta$ 1-dependent gene expression changes associated with EMT-like progression**

### **4.4.1 FoxQ1 repression alters the expression of transcription factors and genes encoding junction proteins which are associated with TGF- $\beta$ 1-dependent EMT-like progression**

The mRNA expression of FoxQ1 was found to be increased in a TGF- $\beta$ 1-dependent manner in NMuMG cells undergoing an EMT-like process. Furthermore, the expression of E-cadherin was increased upon FoxQ1 knock-down (Fig. 16c).

In order to analyse how FoxQ1 potentially influences the outcome of TGF- $\beta$ 1-induced gene expression changes during EMT-like progression, the gene expression profile of FoxQ1 knock-down cells treated with TGF- $\beta$ 1 was analysed.

Therefore, NM18 cells were transfected with ns-siRNA or FoxQ1 siRNA for eight hours and subsequently treated with 5 ng/ml TGF- $\beta$ 1 for an additional 40 hrs.

The total RNA was isolated, processed as described and hybridized onto GeneChip® Mouse Genome 430A\_2.0 Arrays. Differential expressed genes were identified with a FDR < 0.05.

Changes in gene expression were compared to control transfected cells (ns-siRNA). Only genes with a fold change of at least 1.45 x fold were considered for further analyses.

Treatment of ns-siRNA transfected cells with TGF- $\beta$ 1 resulted in the differential expression of 1636 genes (ns-siRNA vs. ns-siRNA + TGF- $\beta$ 1), whereas 2201 genes were differentially expressed upon FoxQ1 knock-down and TGF- $\beta$ 1 treatment (ns-siRNA vs. FoxQ1 siRNA + TGF- $\beta$ 1).

Both analyses were merged to identify genes which are differentially expressed in a FoxQ1-dependent manner with a fold change of at least 1.45 x fold. This resulted in the identification of 721 genes considered to be regulated in a FoxQ1-dependent manner during TGF- $\beta$ 1 signalling (Fig. 23).

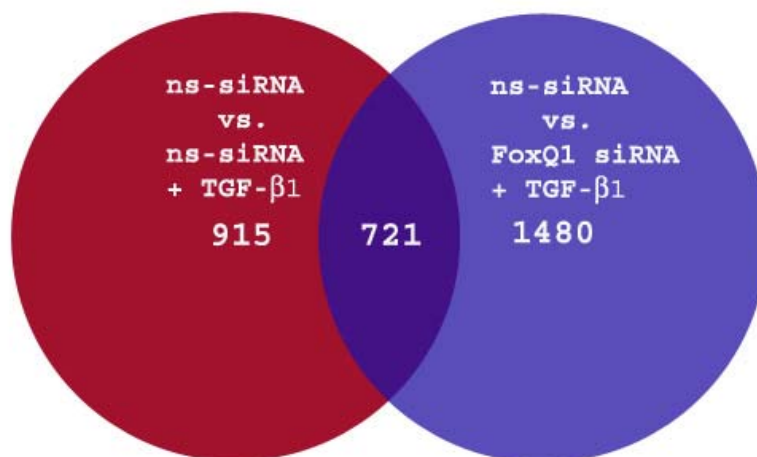


**Fig. 23. Summary of differentially expressed genes during TGF-β1 signalling in dependency of FoxQ1 expression.**

The Venn-diagram depicts the number of differentially expressed genes (FDR < 0.05 and at least -/+1.45 x fold change) during TGF-β1 signalling (red circle, left) and during TGF-β1 signalling with impaired FoxQ1 induction (blue circle, right). The diagram depicts that 721 genes, which are regulated by TGF-β1 signalling, are altered in their expression by at least 1.45 x fold when the TGF-β1-dependent induction of FoxQ1 is inhibited. In contrast, 915 genes differentially expressed in a TGF-β1-dependent manner, remain unaffected in their expression upon FoxQ1 knock-down.

These 721 genes were subsequently functionally categorized into the GO-terms ‘Intercellular junctions’, ‘Cytoskeleton organization and biogenesis’ and ‘Transcription factor activity’ using Cytoscape/BINGO. Definitions for these GO-terms are found in Tab. 7. These exemplary categories were chosen due to their functional relevance for TGF-β1-dependent alterations of epithelial differentiation of NMuMG cells. The result of the Cytoscape analysis is summarized in Supplementary Tab. 2.

Among several transcription factors differentially expressed in a FoxQ1-dependent manner, a decreased expression of Ets-1 was found, while the TGF-β1-dependent repression of several genes encoding junction proteins was impaired upon FoxQ1 knock-down (e.g. Crb3, MarvelD2, Occludin, Jup and E-cadherin), indicating that the repression of FoxQ1 leads to an elevated expression of several junction proteins.

The putatively FoxQ1-dependent regulation of Ets-1, Occludin, Jup, and MarvelD2 in addition to E-cadherin was tested on protein level. As shown in Fig. 24, the knock-down of FoxQ1 resulted in the decreased expression of Ets-1 and a concomitant increase in expression of E-cadherin, Jup, Occludin and MarvelD2 on protein level.

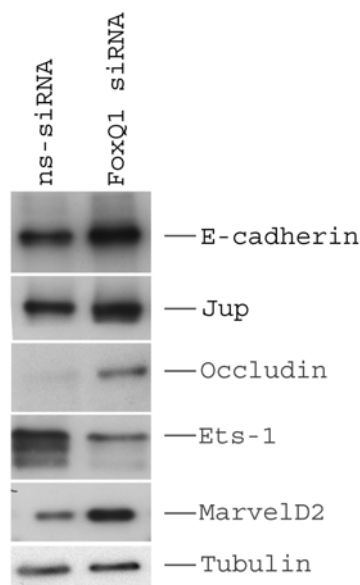


**Fig. 24. Western blot analyses of protein expression of intercellular junction proteins and the transcription factor Ets-1 upon FoxQ1 knock-down.**

NM18 cells were transfected with ns-siRNA or FoxQ1 siRNA and incubated for 68 hrs. Total protein lysates were analysed for the expression of the junction proteins E-cadherin, Jup, Occludin, and MarvelD2 and for the expression of the transcription factor Ets-1. Tubulin was stained as loading control.

In summary, this data suggests that FoxQ1 modulates epithelial plasticity and TGF- $\beta$ 1-mediated changes in epithelial differentiation, at least partially via the regulation of other transcription factors (e.g. Ets-1, Zeb1 and Zeb2), some of which have previously been demonstrated to influence TGF- $\beta$ 1-induced EMT in NMuMG cells (Shirakihara et al., 2007).

## 4.5 Regulatory aspects of FoxQ1

### 4.5.1 FoxQ1 is induced independently of TGF- $\beta$ 1-induced Smad4 signalling and is a downstream target of Zeb1

The Forkhead factor FoxQ1 has previously been shown to be repressed in a Smad4-dependent manner during TGF- $\beta$ 1 signalling in HaCat cells (Levy and Hill, 2005).

In order to test if the increased expression of FoxQ1 in NM18 cells was dependent on functional Smad4 signalling, NM18 cells stably-transfected with a shRNA against Smad4 (pRS-S4kd), were treated with TGF- $\beta$ 1 and analysed for FoxQ1 expression. As an additional Forkhead factor, the repression of FoxA2 was analysed.

As shown in Fig. 25a, the TGF- $\beta$ 1-dependent induction of FoxQ1 was not inhibited in Smad4-knock-down cells compared to control cells (pRS). In contrast, the repression of FoxA2 was dependent on functional Smad4 signalling.

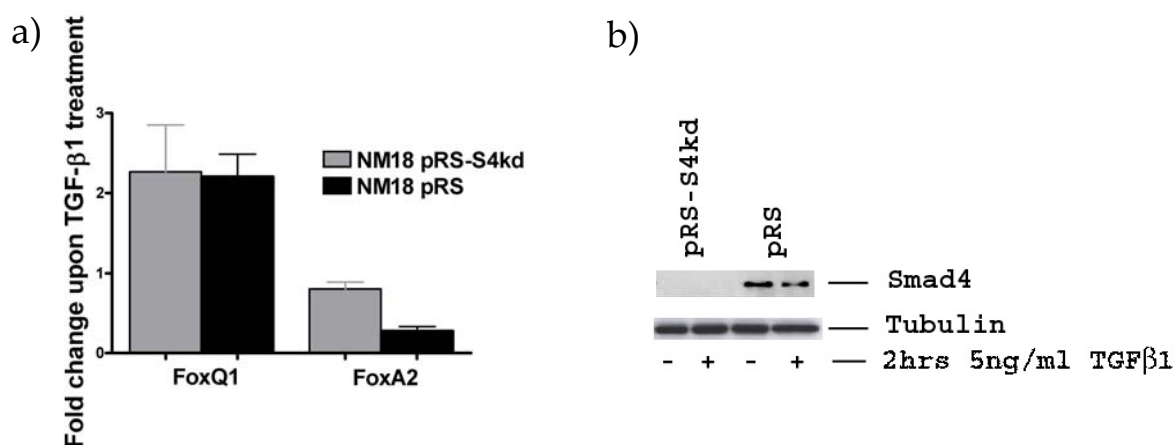


**Fig. 25. TGF- $\beta$ 1-dependent induction of FoxQ1 is independent of Smad4 signalling in NM18 cells.**

NM18 cells stably-transfected with a shRNA against Smad4 (pRS-S4kd) or respective control cells (pRS) were treated with TGF- $\beta$ 1 for 2 hrs and analysed for the expression of FoxQ1 and FoxA2 mRNA expression. Whereas the induction of FoxQ1 was comparable in cells with a reduced expression of Smad4 and respective controls, the repression of FoxA2 was inhibited in cells with a reduced Smad4 protein expression (a).

Western blot analysis of Smad4 expression in pRS-S4kd and pRS NM18 cells (b).

Based on the results of differentially expressed transcription factors identified via *NIAC-NTR* gene expression profiling (Supplementary Tab. 1a/b), a putative impact of Zeb1 on the expression of FoxQ1 was tested.

The choice of Zeb1 was based on the following considerations:

- 1) *NIAC-NTR*-based gene expression profiling indicated that Zeb1 was induced via post-transcriptional mechanisms during early TGF- $\beta$ 1 signalling, whereas FoxQ1 was transcriptionally induced, suggesting that Zeb1 might act upstream of FoxQ1.
- 2) FoxQ1 repression led to an enhanced expression of E-cadherin (Fig. 16c), which resembles the situation of Zeb1 knock-down cells (Shirakihara et al., 2007). Hence, the increase of E-cadherin in Zeb1 knock-down cells might partially occur via the repression of FoxQ1.
- 3) Putative Zeb1 binding sites were identified within the 3kb region upstream of the TSS in the FoxQ1 promoter using TFM-Scan.

In order to analyse if Zeb1 affects FoxQ1 expression, NMuMG cells were reverse-transfected with Zeb1 siRNA and analysed for the expression of FoxQ1.

As shown in Fig. 26, FoxQ1 RNA expression was decreased upon Zeb1 knock-down.

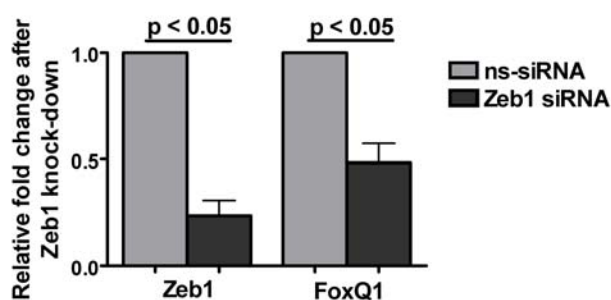


**Fig. 26. RNAi-mediated repression of Zeb1 leads to a decreased expression of FoxQ1.**

NMuMG cells were reverse-transfected with siRNA against Zeb1 and cultured for further 48 hrs. Total RNA was isolated and analysed for the expression of Zeb1 and FoxQ1 (n=3).

## 5. DISCUSSION

The cytokine TGF- $\beta$ 1 regulates a plethora of biological processes in mammalian cells, including proliferation, apoptosis and differentiation. Furthermore, TGF- $\beta$ 1 is a main inducer of EMT-like processes, a dedifferentiation process of epithelial cells into motile mesenchymal cells.

EMT-like processes involve considerable changes in the cytoskeletal arrangements and the dissolution of several epithelial junctional proteins, including tight- and adherens junctions, and are a remarkable example of the plasticity of epithelial cells.

The outcome of TGF- $\beta$ 1 signalling is cell context-specific and largely depends on the cellular expression of TGF- $\beta$ 1 effector molecules.

Transcription factors are crucial mediators of TGF- $\beta$ 1 signalling. Several transcription factors involved in the regulation of epithelial plasticity and EMT-like progression have been identified through gene expression profiling using TGF- $\beta$ 1-responsive *in-vitro* cell culture models. Prominent members of this set of transcription factors belong to the Snail transcription factor family (Snail1 and Snail2) and the Zeb family (Zeb1 and Zeb2).

The work presented here identified the transcription factor FoxQ1 as transcriptionally increased in expression in a TGF- $\beta$ 1-dependent manner in NMuMG cells, a 'classical' cell model to study cytokine induced changes in epithelial differentiation.

Since the cellular functions of FoxQ1 have not been thoroughly elucidated so far, the functions of FoxQ1, its putative impact on TGF- $\beta$ 1-induced EMT-like progression and regulatory aspects of FoxQ1 were studied in this work.

The presented results provide new insights into functional aspects of FoxQ1 and TGF- $\beta$ 1-induced EMT-like progression *in-vitro*.

## 5.1 Several Forkhead transcription factors are regulated during TGF- $\beta$ 1 signalling

In this work, a novel-type of microarray analysis was utilized (*NIAC-NTR*) to identify differentially expressed genes during TGF- $\beta$ 1 signalling in NMuMG cells.

In contrast to standard microarray techniques, which measure the differential expression of genes in steady-state RNA, *NIAC-NTR*-based gene expression profiling measures relative differences of nascent RNA, hence transcriptionally regulated gene expression changes.

The method relies on the incorporation of 4sU into nascent RNA, which can further be isolated and enriched via mercury-based chromatography. The method is applicable for all cells that incorporate 4sU into their RNA and possess an active 'pyrimidine salvage pathway' (Kenzelmann et al., 2007).

As summarized in Fig. 7b/c, NMuMG cells incorporate 4sU into nascent RNA. Only RNA from cells incubated with 4sU and  $^3\text{H}$ -cytidine was significantly enriched, compared to RNA isolated from cells only treated with  $^3\text{H}$ -cytidine, proving that NMuMG cells are suitable for *NIAC-NTR*-based gene expression profiling.

The analysis of differentially expressed genes was performed for cells treated with TGF- $\beta$ 1 for 2 hrs. This early time point was chosen based on previous studies which indicated that several transcription factors are already differentially expressed in a TGF- $\beta$ 1-dependent manner within a short time frame in NMuMG cells, some of which mediate epithelial plasticity (Ishikawa et al., 2008; Shirakihara et al., 2007).

As shown in Fig. 8, the application of *NIAC-NTR* resulted in the identification of additional differentially expressed genes which would have escaped their detection when only steady-state RNA would have been analysed. In contrast, other genes were only detected by the analysis of steady-state RNA. These results are in agreement with studies from Kenzelmann et al., who has previously shown that genes found differentially expressed through the analysis of 4sU labelled and enriched RNA are regulated transcriptionally (Kenzelmann et al., 2007). In contrast, differentially expressed genes that are exclusively detected through the analysis of steady-state RNA are regulated by post-transcriptional mechanisms, hence independent of transcriptional regulation.

Therefore, the gene expression profile conducted in this work is the first high-throughput profile of early TGF- $\beta$ 1-dependent gene expression changes, thus providing insight into transcriptional versus non-transcriptional gene regulation.

The gene expression data was analysed for differentially expressed transcription factors using the plug-in BINGO in Cytoscape and led to the identification of 116 transcription factors (Supplementary Tab.1 a/b). Some of those transcription factors have previously been shown to be regulated in a TGF- $\beta$ 1-dependent manner in NMuMG cells, including Klf5, Ets1 and Zeb1 (Ishikawa et al., 2008; Nogai et al., 2008; Shirakihara et al., 2007).

However, of particular interest was the identification of several transcription factors belonging to the Forkhead family (summarized in Fig. 9), indicating potential impact of Forkhead factors for epithelial differentiation/plasticity and TGF- $\beta$ 1-induced EMT-like progression in NMuMG cells.

Several recently published studies have shown that different Forkhead factors influence the plasticity of epithelial cells. Mani et al. have shown that the Fox-factor FoxC2 is induced in cells undergoing an EMT-like progression and is involved in promoting the mesenchymal differentiation process. The authors further revealed, that FoxC2 relocates the prototypical epithelial marker E-cadherin from the membrane to the cytoplasm (Mani et al., 2007).

Additionally, the Fox-factor FoxA2 has recently been proposed to regulate the polarity of epithelial cells *in-vivo* and to induce an epithelial cellular phenotype (Burtscher and Lickert, 2009). Furthermore, Song et al. have recently shown that the loss of FoxA1/FoxA2 expression is mandatory and sufficient to induce an EMT in pancreatic ductal adenocarcinoma cells (Song et al.).

Also, based on gene expression analysis of Forkhead-factors, the Fox-factors FoxF1 and FoxF2 have been proposed to play a role in EMT in prostate cancer (van der Heul-Nieuwenhuijsen et al., 2009).

However, not much has been reported yet on a potential impact of the Forkhead factor FoxQ1 with regard to its cellular functions, including EMT-like processes.

Studies on mice with mutated FoxQ1 (also known as 'satin' mice) have provided evidence that FoxQ1 plays a role in hair follicle differentiation (Hong et al., 2001).

FoxQ1-deficient mice reveal differences in the function of gastric mucosa and exhibit a lack of gastric acid secretion in response to stimuli (Goering et al., 2008; Verzi et al., 2008).

Moreover, FoxQ1 has recently been identified as functionally relevant for an enhanced tumourgenecity and tumour growth in colorectal carcinoma (Kaneda et al.).

## 5.2 Functional analyses of FoxQ1 in mammary epithelial cells

### 5.2.1 FoxQ1 regulates cell size/morphology, cytoskeletal arrangements, cell migration and intercellular adherence

The siRNA-mediated knock-down of FoxQ1 resulted in an apparent change of cellular morphology in NM18 cells (Fig. 10b). These morphological alterations were associated with a gain of cell size (Fig. 10c), an increase in the expression of several junction proteins (Fig. 24) and cytoskeletal alterations as documented by the formation of 'actin rings' (Fig. 11) and the different localisation of the actin associated protein Tmod3 (Fig. 12a). The cytoskeletal rearrangements, in addition to the establishment of pronounced cell-cell contacts are likely to cause the alterations in cell morphology.

'Actin rings' have been described in yeast cells overexpressing actin. The formation of the ring-like structures was shown to be dependent on septins, a class of proteins which links microtubules with the actin cytoskeleton and are critical for maintaining cell shape (Field and Kellogg, 1999; Norden et al., 2004; Silverman-Gavrila and Silverman-Gavrila, 2008). In this regard it might be of interest to note, that Acta1, Acta2 (actin-alpha 1 and 2) and Sept9 (Septin 9) were found to be increased in RNA expression in a FoxQ1-dependent manner using gene expression profiling (3.2.1.15). This might provide an indication for the formation of 'actin rings' in FoxQ1 knock-down cells. It remains to be elucidated if these ring-like structures have a functional role or if they are merely accumulated actin (Norden et al., 2004).

Tmod3 is an actin-associated protein which binds to the pointed-end of actin. Repression of Tmod3 expression has been shown to cause the loss of F-actin from lateral membranes which is thought to be involved in the regulation of cell morphology (Weber et al., 2007).

The analysis of Tmod3 expression in NM18 cells revealed, that Tmod3 expression is not profoundly affected on the overall protein expression level within the analysed time frame upon FoxQ1 repression. However, the knock-down of FoxQ1 resulted in a different localisation of the Tmod3 protein, from a predominantly cytoplasmatic staining to a more nuclear staining pattern. Furthermore, as indicated by co-staining, the repression of FoxQ1 led to a reduced overlap of F-actin and Tmod3 (Fig. 12a).

Tmod proteins contain a conserved NLS and NES sequence and have been found to naturally shuttle between nucleus and cytoplasm. The functional role of Tmods in the nucleus remains largely unknown. However, it has been proposed that increased nuclear

expression of Tmod1 (also known as E-Tmod) impairs myogenic differentiation by the selective repression of muscle-specific genes (Kong and Kedes, 2004).

The cellular mechanisms of FoxQ1-dependent translocation of Tmod3 in NM18 cells remain open as well as the analyses if nuclear Tmod3 contributes to gene expression control in NM18 cells. It is interesting to speculate though that FoxQ1 potentially links cytoskeletal rearrangements and gene expression control via the regulation of Tmod3 expression and protein localisation.

Changes in cytoskeletal dynamics may modulate the migratory capacity of cells (Pollard and Cooper, 2009). Additionally, Tmod3 modulates cell motility in endothelial (HMEC-1) cells (Fischer et al., 2003).

The repression of FoxQ1 led to an enhanced migratory capacity of NM18 cells as shown by a classical wound assay (Fig. 13).

A few Forkhead transcription factors have been linked to cellular migration. However, in contrast to the Fox-factors FoxF1 and FoxC2 which enhance the migration of mesenchymal and endothelial cells by the induction of integrin- $\beta$ 3 transcription (Hayashi and Kume, 2009; Malin et al., 2007), FoxQ1 limits the migratory capacity of NM18 cells.

Interestingly, FoxQ1 knock-down cells revealed an elevated protein expression of several junction proteins, including E-cadherin, Jup (Plakoglobin), MarvelD2 and Occludin (Fig. 24) and showed increased cell-cell contacts (Fig. 15). Therefore, these results argue that FoxQ1 suppression leads to an enhanced migration of whole epithelial sheets by enhancing the migratory capacity and the concomitant increase of intercellular adherence through the *de novo* synthesis of junction proteins.

### 5.2.2 FoxQ1 regulates cell cycle G1/S-transition in NM18 cells by regulating the expression of CDKs

Downregulation of FoxQ1 expression resulted in a reduced proliferative capacity of NM18 cells, as indicated by a MTT-assay and the analyses of cell numbers (Fig 14a/b).

Subsequent cell cycle analyses confirmed this finding and proposed that a decrease in FoxQ1 expression leads to an accumulation of cells in the G0/G1 phase of the cell cycle (Fig. 14c).

In line with this, the protein expression of CDK4 and CDK6, cyclin-dependent kinases which are involved in the transition through the G1-phase and the transition towards the S-phase, was reduced in FoxQ1 knock-down cells. In contrast, Cyclin D1 protein expression remained unaffected (Fig 14d).

FoxQ1 has previously been shown to regulate cell proliferation. However, our findings are in contrast to the results of Kaneda et al., who showed that a reduction of FoxQ1 expression leads to a reduced expression of the CDK-inhibitor p21<sup>Cip1/Waf1</sup>, thereby enhancing proliferation of the lung-carcinoma cell line H1299 (Kaneda et al.). Together, these findings demonstrate that FoxQ1 may have opposing and cell-context specific functions with regard to proliferation. Such opposing cell-context specific functions of transcription factors were demonstrated also for other transcription factors, including the Myb proteins and c-jun homodimers (Grondin et al., 2007; Ness, 2003). Potential mechanisms which contribute to cell-context specific functions of FoxQ1 might involve different post-translational protein modifications and/or the interaction with different FoxQ1 effector proteins, thus changing target gene specificity.

### 5.2.3 Overexpression of FoxQ1 modulates TGF- $\beta$ 1-mediated formation of cell protrusions/ morphology and results in a modified ECM

The TGF- $\beta$ 1-dependent increase in FoxQ1 expression suggested that FoxQ1 might elicit aspects of EMT-like processes *in-vitro*.

To test this hypothesis, NM18 cells constitutively overexpressing FoxQ1 were established.

Overexpressed FoxQ1 was exclusively localized in the nucleus as analysed by immunofluorescence analyses (Fig. 17b).

However, FoxQ1 overexpression did not result in the regulation of E-cadherin or CDK4 expression, downstream target genes that were affected by the knock-down of FoxQ1 and harbour putative FoxQ1 binding sites in their 3kb promoter region.

Quite contrary to expectations, cells overexpressing FoxQ1 revealed only modest phenotypic differences compared to control cells and merely seemed organized in more distinct 'cobblestone'-like sheets. Surprisingly, the overexpression of FoxQ1 led to an impaired TGF- $\beta$ 1-dependent cell dissociation (Fig. 20 and Supplementary Fig. 3), which partially resembles the phenotype of cells with a decreased FoxQ1 expression (Fig. 16b).

These results show that the exclusive overexpression of FoxQ1 is not sufficient to elicit an EMT-like progression in NM18 cells. Nevertheless, TGF- $\beta$ 1-induced changes in cell morphology as well as cell dissociation are altered in a FoxQ1-dependent manner.

Especially, the difference between TGF- $\beta$ 1 treated control and FoxQ1-overexpressing cells with regard to the formation of cellular protrusions might shed light on the functional impact of FoxQ1 overexpression.

Whereas control transfected cells (pIRESpuro3) treated with TGF- $\beta$ 1 regularly formed multiple lateral protrusions, FoxQ1-overexpressing cells showed a restricted formation of these membrane ruffles, letting these cells appear more homogenous and spindle-shaped in morphology (Fig. 20b and Supplementary Fig. 3). The formation of multiple 'lateral'- versus 'single'-protrusions is a characteristic of randomly- vs. directionally migrating cells in response to the stimulation of a cells motility machinery (in this case via TGF-  $\beta$ 1 signalling). Cells with a dominant leading edge usually display an enhanced directional migration whereas cells with multiple lateral membrane ruffles typically have a restricted capability of directional migration (Fig. 27) (Petrie et al., 2009). Hence, our results argue that the overexpression of FoxQ1 might take effect on migratory characteristics of NM18 cells, especially in response to motility inducing cues.

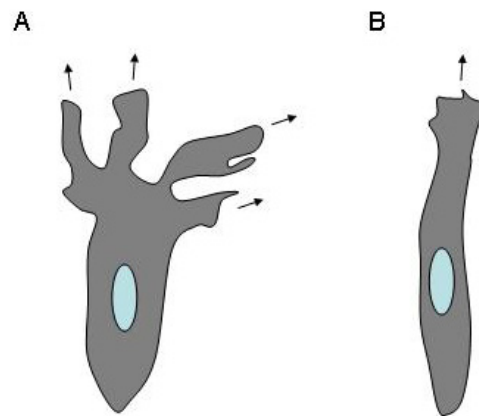


**Fig. 27. Control of cellular protrusions takes effect on migratory characteristics of cells.**

The formation of multiple lateral cell protrusions (A) or of one dominant leading edge by restricting the formation of multiple protrusions (B) modulates the migratory characteristics of cells. The different 'mode' of protrusion formation is controlled by complex mechanisms, e.g. RhoGTPase signalling, Integrin-mediated signalling and the constitution of the ECM. Modified from (Petrie et al., 2009).

Though it remains to be further resolved as to why the overexpression of FoxQ1 impairs TGF- $\beta$ 1-dependent cell dissociation and the formation of cellular protrusions, confocal microscopy provided evidence that the constitutive overexpression of FoxQ1 results in the modification of the ECM as indicated by an impaired extracellular localisation of fibronectin (Fig. 22), a known ligand of integrin receptors (White et al., 2008).

The composition of the ECM and its topography provides structural support for cells and may affect the mode of cellular migration and cell morphology by multiple mechanisms, including differences in cell-matrix adhesion and geometrical arrangements of the ECM. Therefore, the different outcome of TGF- $\beta$ 1 signalling in FoxQ1-overexpressing compared to control cells might indeed be related to FoxQ1-dependent alterations of the ECM.

However, it is also conceivable that overexpressed FoxQ1 alters TGF- $\beta$ 1 responses by synergizing with further factors whose expression or activity depend on TGF- $\beta$ 1 signalling (see also 5.2.4).

Though both ideas provide an explanation why FoxQ1-dependent phenotypes emerge more apparent in cells treated with TGF- $\beta$ 1, future work will need to explore these assumptions.

#### 5.2.4 TGF- $\beta$ 1-dependent increase in FoxQ1 expression is independent of Smad4

The knowledge about regulatory aspects of FoxQ1 is scarce.

FoxQ1 was proposed as a putative target gene of the homeobox transcription factor Hoxa1 in embryonic stem cells (Martinez-Ceballos et al., 2005). Furthermore, Hoxc13 was shown to be a direct regulator of FoxQ1 expression during hair follicle differentiation, indicating potential cross-talk of Hox- and Fox-transcription factors (Potter et al., 2006).

With regard to TGF- $\beta$ 1 signalling, FoxQ1 is repressed in a Smad4-dependent manner in TGF- $\beta$ 1 treated HaCat cells. Smad4 expression was further shown to be dispensable for TGF- $\beta$ 1-induced EMT-like progression in these cells (Levy and Hill, 2005), which is contrary to the findings in NM18 cells, which crucially depend on Smad4 expression for TGF- $\beta$ 1-induced EMT-like progression, cell growth arrest and apoptosis (Deckers et al., 2006).

The TGF- $\beta$ 1-dependent induction of FoxQ1 expression in NM18-pRS-S4kd cells strongly argues that FoxQ1 induction is independent of Smad4 signalling (Fig. 25). This finding is of interest since it indicates that the TGF- $\beta$ 1-driven induction of FoxQ1 itself is apparently insufficient to elicit major phenotypes in NM18 cells. Hence, cellular phenotypes that depend on the induction of FoxQ1 might thus, at least partially, also depend on functional Smad4 signalling.

A potential cross-talk of FoxQ1 and Smad4 signalling in relation to TGF- $\beta$ 1 signalling would need to be further evaluated; however other Forkhead factors have been shown to functionally interact with Smad-factors in different cell systems. Studies in *Xenopus* identified Fast1 (*forkhead activin signal transducer*, also known as FoxH1) as the first DNA binding partner for Smads (Attisano et al., 2001; Chen et al., 1996).

Also, it has been shown that several TGF- $\beta$ 1-responsive genes in keratinocytes are dependent on the synergism of FoxO factors (FoxO1, FoxO3 and FoxO4) and Smad proteins (Gomis et al., 2006).

In principle agreement with this explanation, and already mentioned above, NM18 cells overexpressing FoxQ1 reveal only a very modest phenotype, which is pronounced upon TGF- $\beta$ 1 treatment and thus potentially due to the synergism of FoxQ1 with additional TGF- $\beta$ 1/Smad-dependent signalling.

### 5.2.5 Suppression of FoxQ1 affects the expression of genes associated with TGF- $\beta$ 1-induced EMT-like processes

Gene expression profiling of TGF- $\beta$ 1-induced FoxQ1-knock-down cells suggests that FoxQ1 is a potent modulator of TGF- $\beta$ 1-dependent gene expression changes, some of which are known mediators of EMT-like processes (Fig. 23 and Supplementary Tab. 2).

The expression of the transcription factors Zeb1, Zeb2 and Ets-1 has previously been shown to be induced in TGF- $\beta$ 1 treated NMuMG cells and to contribute to the repression of the epithelial marker protein E-cadherin. The same study also revealed that the increased expression of Zeb1 and Zeb2 is impaired upon Ets-1 suppression (Shirakihara et al., 2007).

Here it is shown that Ets-1 expression is decreased in TGF- $\beta$ 1 treated FoxQ1 knock-down cells. In line with this, TGF- $\beta$ 1-dependent induction of Zeb1 and Zeb2 expression is impaired. These data suggest that FoxQ1 acts upstream of the transcription factors Ets-1, Zeb1 and Zeb2 and potentially induces their expression during TGF- $\beta$ 1 signalling.

This interpretation however would be in contradiction to results from the *NIAC-NTR*-based gene expression profiling. *NIAC-NTR* profiling provided evidence that initially after TGF- $\beta$ 1 treatment (2 hrs), only FoxQ1 and Ets-1 are transcriptionally induced, whereas the increase in Zeb1 expression is putatively regulated post-transcriptionally, hence independent of transcriptional mechanisms (Supplementary Tab. 1b).

These seemingly opposing results might be explained by a potential feedback mechanism involving Zeb1 and FoxQ1 expression during early and late TGF- $\beta$ 1 signalling.

The model shown in Fig. 28 provides a hypothesis of regulatory cross-talk between these factors during TGF- $\beta$ 1 signalling, also taking into account putative Zeb1 and FoxQ1 binding sites in the promoters of the considered factors.

This hypothetical model is inferred from the following findings:

- 1) Shirakihara and colleagues have shown that the repression of Ets-1 impaired TGF- $\beta$ 1-dependent induction of Zeb1 and Zeb2 expression.
- 2) *NIAC-NTR*-based gene expression profiling indicated that Zeb1 was induced by post-transcriptional mechanisms during early TGF- $\beta$ 1 signalling (black arrows in Fig. 28), whereas Ets-1 and FoxQ1 were transcriptionally increased.
- 3) Knock-down of Zeb1 in NMuMG cells led to a decrease of FoxQ1 expression, demonstrating that Zeb1 affects FoxQ1 expression.
- 4) Repression of FoxQ1 during TGF- $\beta$ 1 signalling, led to a reduced expression of Ets-1, Zeb1 and Zeb2 compared to TGF- $\beta$ 1 treated control cells, showing that FoxQ1 is acting upstream of these factors. However, a putative FoxQ1 binding site could be found only in the 3kb promoter region of Zeb1, indicating that any direct effect of FoxQ1 might be exerted through the regulation of Zeb1.

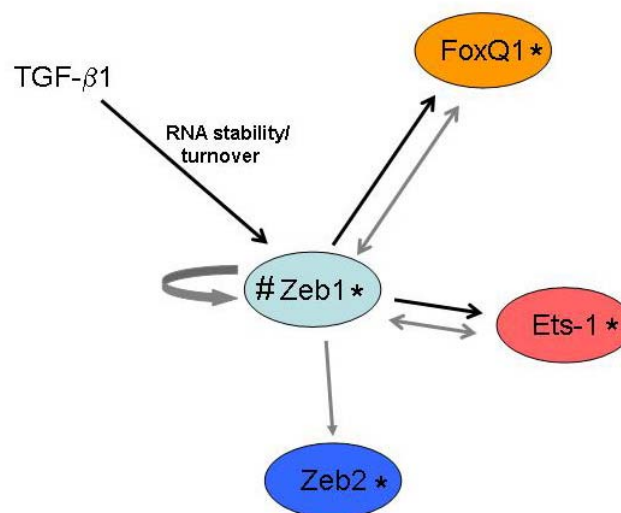


**Fig. 28. Hypothetical model of potential cross-talk between FoxQ1, Zeb1, Zeb2 and Ets-1 during TGF- $\beta$ 1 signalling.**

In this model, early TGF- $\beta$ 1 signalling (black arrows) leads to the post-transcriptionally mediated increase in Zeb1 expression, which results in the transcriptionally regulated increase in Ets-1 as well as FoxQ1 expression. The increase in FoxQ1, Ets-1 and also Zeb1 expression itself might then lead to a transcriptionally regulated expression of Zeb1 during late TGF- $\beta$ 1 signalling via feedback mechanisms (grey arrows). This model would also be in principle agreement with a Smad4-independent induction of FoxQ1 upon TGF- $\beta$ 1 treatment.

\* - factor contains potential Zeb1 binding sites in the 3kb promoter region upstream of the TSS. # - factor contains putative FoxQ1 binding site in the 3kb promoter region upstream of the TSS.

In any case, the presented results argue that FoxQ1 exerts its cellular functions partially through the regulation of other transcription factors, some of which have previously been shown to play a role in the regulation of epithelial junction complexes and EMT-like progression.

Though the direct targets of FoxQ1 in NM18 cells remain to be elucidated, the FoxQ1-dependent regulation of several genes which are considered to be putative markers of an EMT-like progression (e.g. Zeb1, Zeb2 and E-cadherin/Cdh1) argues that FoxQ1 modifies TGF- $\beta$ 1-induced EMT-like progression in NM18 cells.

## 6. SUPPLEMENTS

**Supplementary Tab. 1a. Summary of differentially expressed transcription factors, detected in the newly-transcribed RNA fraction 2 hrs after TGF- $\beta$ 1 treatment.**

GO term	Gene	Fold change Mock treated vs. TGF- $\beta$ 1 treated
<i>Transcription factor activity</i>	Ankrd10	1.36
	Ankrd54	1.44
	Ankrd56	1.39
	Arid3a	1.56
	Atf6	-1.44
	Bach1	1.70
	Bcor	1.50
	Bpnt1	-1.26
	Btbd11	3.67
	Cebpd	-1.76
	Creb3l2	2.92
	Crebl1	-1.35
	Dbp	-1.81
	Dlx2	1.39
	Egr1	-1.35
	Egr2	7.01
	Elf3	1.53
	Eomes	1.60
	Ets1	1.63
	Ets2	-1.50
	Fank1	1.54
	Fbxw7	1.96
	Fos	1.46
	Fosl2	1.33
	Foxa2	-3.27
	Foxa3	2.21
	Foxc1	1.29
	Foxd1	1.52
	Foxf2	1.89
	Foxk1	1.36
	Foxo1	1.65
	Foxq1	1.86
	Gata6	-1.55
	Hhex	-1.83
	Irf2	-1.46
	Irx3	1.97
	Jun	1.81
	Jundm	1.46
	Klf7	1.41
	Lhx6	1.21
	Mkx	2.07
	Mril	-1.28
Mycn	1.24	
Nfatc1	1.69	
Nfatc2	1.37	
Nfe2l2	-1.94	
Nfib	-1.29	
Notch1	-1.59	
Nr1h4	-2.35	

Nr4a2	-1.29
Nr6a1	-1.39
Ripk4	1.29
Runx1	1.95
Runx2	1.37
Smad7	2.03
Sox11	2.33
Tfdp2	1.37
Tsc22d3	-1.32
Xbp1	1.73
Zfhx4	-1.60

**Supplementary Tab. 1b. Summary of differentially expressed transcription factors, exclusively detected in the steady-state RNA fraction 2 hrs after TGF- $\beta$ 1 treatment.**

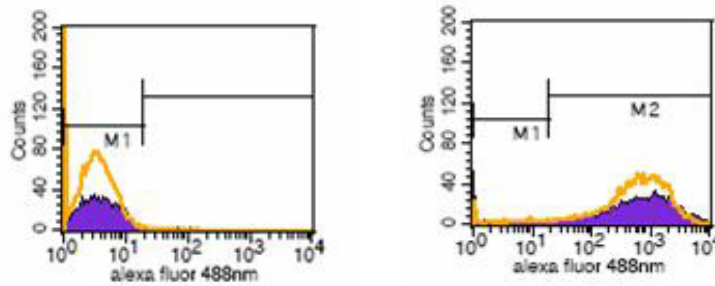
GO term	Gene	Fold change Mock treated vs. TGF- $\beta$ 1 treated
<i>Transcription factor activity</i>	Aebp2	1.29
	Aff1	1.44
	Ahr	-1.68
	Ankrd1	-1.63
	Axud1	1.45
	Btg2	-1.43
	Ccnt2	-1.23
	Cebpb	1.40
	Ddit3	-1.53
	E2f2	-1.50
	Elk3	1.55
	Eya2	1.34
	Fhl2	1.27
	Fosb	1.50
	Gatad2b	1.19
	Glis2	1.25
	Gzf1	-1.33
	Hes1	-1.37
	Hmga2	1.36
	Irf2bp2	-1.34
	Irx5	1.53
	Junb	1.76
	Klf5	-1.64
	Klf9	1.22
	Lif	1.38
	Lmo4	-1.35
	Maf	-1.30
	Maff	1.55
	Mafk	1.31
	Myc	-1.29
	Ncor2	1.30
	Nfkbiz	-1.53
Nr2f2	1.20	
Pax4	1.19	
Pcgf5	1.35	
Phf17	-1.43	
Phf20	-1.35	
Prdm8	1.45	
Psrc1	-1.35	

Rai1	1.26
Rbak	-1.34
Rere	-1.25
Sin3a	-1.15
Sirt7	-1.22
Smad3	1.25
Snai3	1.23
Sox4	1.29
Taf9b	-1.22
Timeless	-1.19
Tshz1	1.30
Tshz2	-1.29
Zeb1	1.41
Zfp189	-1.41
Zfp462	-1.37
Zfp707	-1.28
Zmym2	1.71

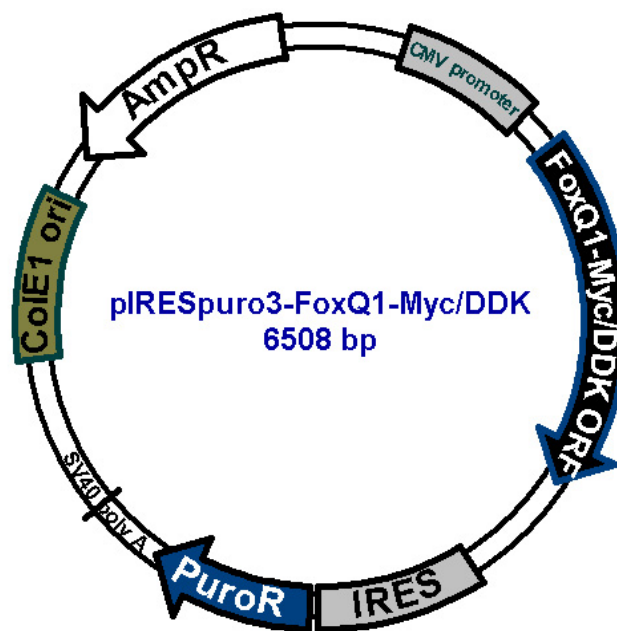
**Supplementary Tab. 2. Summary of differentially expressed genes categorized into selected GO-terms. The differential expression of genes was analysed in the indicated expression profiles. (n.s – not significant FDR < 0.05)**

GO term	Gene	Fold change ns-siRNA vs. ns-siRNA + TGF- $\beta$ 1	Fold change ns-siRNA vs. FoxQ1 siRNA + TGF- $\beta$ 1
<i>Intercellular junction</i>	Cdh1	-2.08	n.s
	Cldn2	-2.07	n.s
	Cldn4	6.33	11.09
	Crb3	-1.61	n.s
	F11r	1.53	n.s
	Inadl	-1.77	n.s
	Jup	1.58	2.58
	Lin7c	-1.63	n.s
	MarvelD2	-1.60	n.s
	Ocln	-1.52	n.s
	Pcdh1	1.56	n.s
	Wnk4	-5.10	-1.73
	<i>Transcription factor activity</i>	Ankrd10	1.55
Atf3		1.56	n.s
Cdkn2c		-2.40	-4.11
Creb3		1.89	n.s
Dbp		-2.57	-1.64
E2f8		-3.34	-10.50
Ehf		-4.72	-2.98
Ets1		1.50	-1.50
Foxa3		-1.91	n.s
FoxQ1		1.94	n.s
Hhex		-2.63	n.s
Hivep2		1.71	n.s
Hnf4a		-2.70	n.s
Irf6		-2.68	-1.74
Klf2		2.11	n.s
Nfatc1	1.83	3.88	
Nfil3	1.83	n.s	
Nfyb	-1.47	n.s	

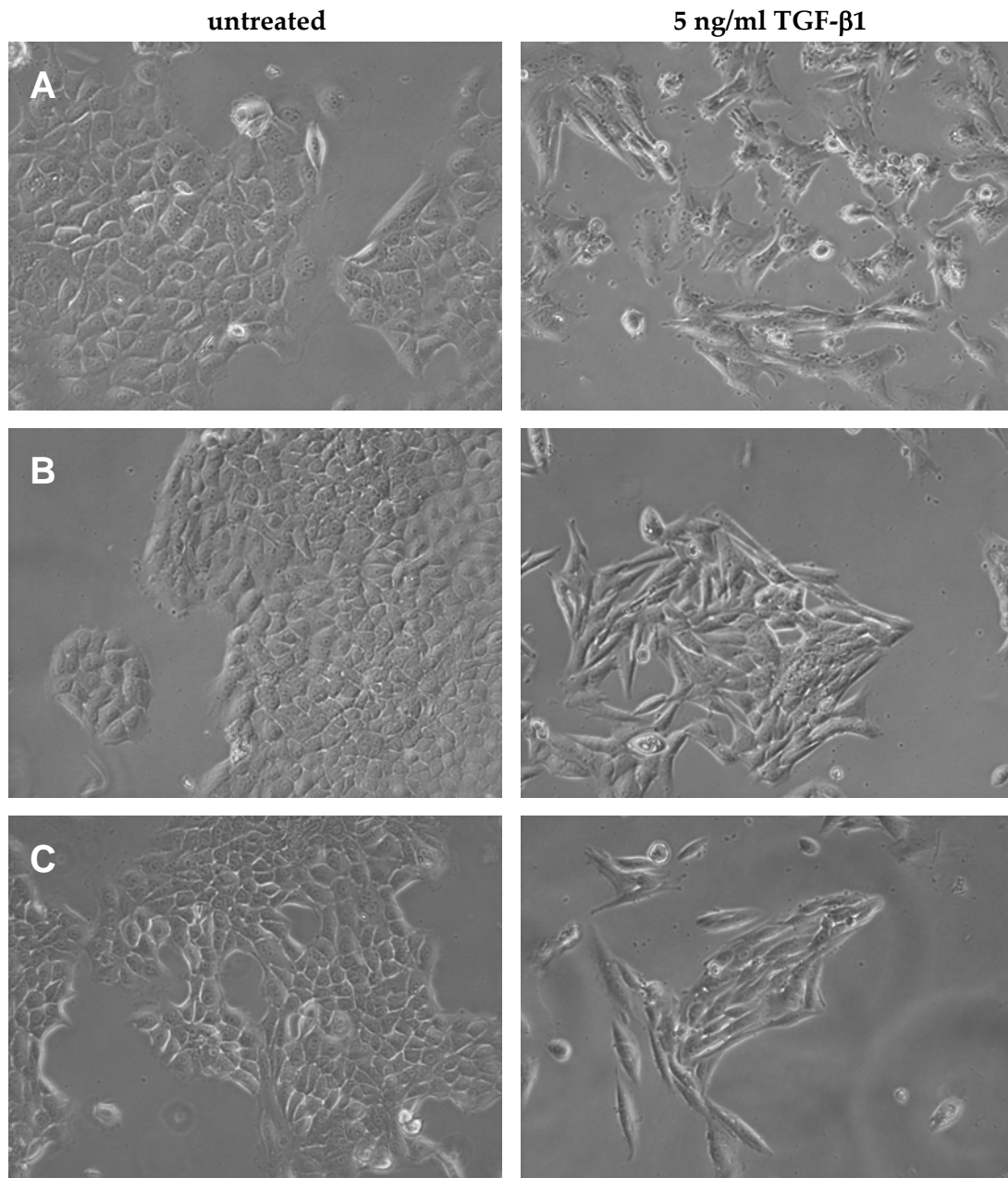
	Nr1h3	-1.63	n.s
	Pbx1	1.58	2.40
	Ripk4	-1.79	n.s
	Runx1	1.51	n.s
	Smad5	1.47	n.s
	Srf	1.58	n.s
	Tfam	1.72	-2.64
	Zeb1	1.98	n.s
	Zeb2	2.16	n.s
<i>Cytoskeletal organization and biogenesis</i>	Apbb2	2.99	4.73
	Bircd2	1.63	n.s
	Birc5	-2.84	-14.61
	Bra1	-1.83	-3.53
	Cenpe	-1.88	-9.65
	Diap3	-1.74	-4.68
	Dlc1	2.72	n.s
	Epb4.1l2	1.62	n.s
	Fhdc1	-1.66	n.s
	Fhod3	4.14	n.s
	Flnc	1.62	n.s
	Kif11	-2.41	-10.22
	Kif18a	-1.77	-4.22
	Kif20a	-2.08	-9.19
	Kif22	-2.27	-7.20
	Kif2c	-1.52	-2.38
	Kif4	-1.92	-5.58
	Myo9b	1.55	n.s
	Nuf2	-2.52	-14.18
	Nusap1	-2.07	-12.19
	Pdgfb	3.65	2.25
	Pdlim7	1.62	4.41
	Pfn2	-1.49	1.62
	Rhoq	4.11	2.32
	Tacc3	-2.28	-8.41
	Tln1	1.55	n.s
	Tpx2	-1.47	-4.65
Vil1	-1.96	1.89	



**Supplementary Fig. 1.** Efficiency of transfection of siRNAs into NMuMG cells and NM18 subclone. NMuMG cells (purple) and NM18 cells (orange) were transfected with 25 nM unconjugated non-silencing siRNA (left panel) or alexa-fluor 488 nm conjugated siRNA (right panel). More than 90% of the cells were transfected with siRNAs according to flow-cytometry analyses (24 hrs).



**Supplementary Fig. 2.** Plasmid map of pIRESpuro3-FoxQ1-Myc/DDK. The FoxQ1-Myc/DDK transcript and the Puromycin resistance cassette are transcribed as a fusion mRNA. Whereas FoxQ1-Myc/DDK is translated in a 5'-Cap-dependent manner, the translation of the puromycin-cassette is regulated via an IRES-sequence (*Internal ribosome entry site*). The sequence of the FoxQ1-Myc/DDK-cassette was verified by sequencing in the core sequencing facility of the DKFZ.



**Supplementary Fig. 3. Overexpression of FoxQ1 modifies TGF- $\beta$ 1-induced alterations in epithelial cell morphology.** The figure shows the outcome of TGF- $\beta$ 1 treatment of control clone pIRESpuro3-clone 3 (A) and FoxQ1 overexpressing clones pIRESpuro3-FoxQ1-Myc/DDK-clone 7 (B) and 10 (C) (see also Fig. 20 in the main text).

## 7. LITERATURE

- Acloque H, Adams MS, Fishwick K, Bronner-Fraser M, Nieto MA. 2009. Epithelial-mesenchymal transitions: the importance of changing cell state in development and disease. *J Clin Invest* 119(6):1438-1449.
- Aigner K, Dampier B, Descovich L, Mikula M, Sultan A, Schreiber M, Mikulits W, Brabletz T, Strand D, Obrist P, Sommergruber W, Schweifer N, Wernitznig A, Beug H, Foisner R, Eger A. 2007a. The transcription factor ZEB1 (deltaEF1) promotes tumour cell dedifferentiation by repressing master regulators of epithelial polarity. *Oncogene* 26(49):6979-6988.
- Aigner K, Descovich L, Mikula M, Sultan A, Dampier B, Bonne S, van Roy F, Mikulits W, Schreiber M, Brabletz T, Sommergruber W, Schweifer N, Wernitznig A, Beug H, Foisner R, Eger A. 2007b. The transcription factor ZEB1 (deltaEF1) represses Plakophilin 3 during human cancer progression. *FEBS Lett* 581(8):1617-1624.
- Attisano L, Silvestri C, Izzi L, Labbe E. 2001. The transcriptional role of Smads and FAST (FoxH1) in TGFbeta and activin signalling. *Mol Cell Endocrinol* 180(1-2):3-11.
- Batlle E, Sancho E, Franci C, Dominguez D, Monfar M, Baulida J, Garcia De Herreros A. 2000. The transcription factor snail is a repressor of E-cadherin gene expression in epithelial tumour cells. *Nat Cell Biol* 2(2):84-89.
- Bierie B, Moses HL. 2006. Tumour microenvironment: TGFbeta: the molecular Jekyll and Hyde of cancer. *Nat Rev Cancer* 6(7):506-520.
- Bishop AL, Hall A. 2000. Rho GTPases and their effector proteins. *Biochem J* 348 Pt 2:241-255.
- Bollig F, Winzen R, Kracht M, Ghebremedhin B, Ritter B, Wilhelm A, Resch K, Holtmann H. 2002. Evidence for general stabilization of mRNAs in response to UV light. *Eur J Biochem* 269(23):5830-5839.
- Boutet A, De Frutos CA, Maxwell PH, Mayol MJ, Romero J, Nieto MA. 2006. Snail activation disrupts tissue homeostasis and induces fibrosis in the adult kidney. *Embo J* 25(23):5603-5613.
- Brook M, Sully G, Clark AR, Saklatvala J. 2000. Regulation of tumour necrosis factor alpha mRNA stability by the mitogen-activated protein kinase p38 signalling cascade. *FEBS Lett* 483(1):57-61.
- Brunet A, Bonni A, Zigmond MJ, Lin MZ, Juo P, Hu LS, Anderson MJ, Arden KC, Blenis J, Greenberg ME. 1999. Akt promotes cell survival by phosphorylating and inhibiting a Forkhead transcription factor. *Cell* 96(6):857-868.
- Burtscher I, Lickert H. 2009. Foxa2 regulates polarity and epithelialization in the endoderm germ layer of the mouse embryo. *Development* 136(6):1029-1038.
- Cano A, Perez-Moreno MA, Rodrigo I, Locascio A, Blanco MJ, del Barrio MG, Portillo F, Nieto MA. 2000. The transcription factor snail controls epithelial-mesenchymal transitions by repressing E-cadherin expression. *Nat Cell Biol* 2(2):76-83.
- Carballo E, Cao H, Lai WS, Kennington EA, Campbell D, Blackshear PJ. 2001. Decreased sensitivity of tristetraprolin-deficient cells to p38 inhibitors suggests the involvement of tristetraprolin in the p38 signaling pathway. *J Biol Chem* 276(45):42580-42587.
- Chen CY, Shyu AB. 1995. AU-rich elements: characterization and importance in mRNA degradation. *Trends Biochem Sci* 20(11):465-470.
- Chen X, Rubock MJ, Whitman M. 1996. A transcriptional partner for MAD proteins in TGF-beta signalling. *Nature* 383(6602):691-696.
- Chomczynski P, Sacchi N. 1987. Single-step method of RNA isolation by acid guanidinium thiocyanate-phenol-chloroform extraction. *Anal Biochem* 162(1):156-159.
- Clark KL, Halay ED, Lai E, Burley SK. 1993. Co-crystal structure of the HNF-3/fork head DNA-recognition motif resembles histone H5. *Nature* 364(6436):412-420.

- Crawford SE, Stellmach V, Murphy-Ullrich JE, Ribeiro SM, Lawler J, Hynes RO, Boivin GP, Bouck N. 1998. Thrombospondin-1 is a major activator of TGF-beta1 in vivo. *Cell* 93(7):1159-1170.
- Cui Y, Jean F, Thomas G, Christian JL. 1998. BMP-4 is proteolytically activated by furin and/or PC6 during vertebrate embryonic development. *Embo J* 17(16):4735-4743.
- Dai M, Wang P, Boyd AD, Kostov G, Athey B, Jones EG, Bunney WE, Myers RM, Speed TP, Akil H, Watson SJ, Meng F. 2005. Evolving gene/transcript definitions significantly alter the interpretation of GeneChip data. *Nucleic Acids Res* 33(20):e175.
- Dean JL, Sully G, Clark AR, Saklatvala J. 2004. The involvement of AU-rich element-binding proteins in p38 mitogen-activated protein kinase pathway-mediated mRNA stabilisation. *Cell Signal* 16(10):1113-1121.
- Deckers M, van Dinther M, Buijs J, Que I, Lowik C, van der Pluijm G, ten Dijke P. 2006. The tumor suppressor Smad4 is required for transforming growth factor beta-induced epithelial to mesenchymal transition and bone metastasis of breast cancer cells. *Cancer Res* 66(4):2202-2209.
- Defrance M, Touzet H. 2006. Predicting transcription factor binding sites using local over-representation and comparative genomics. *BMC Bioinformatics* 7:396.
- Derynck R, Feng XH. 1997. TGF-beta receptor signaling. *Biochim Biophys Acta* 1333(2):F105-150.
- Derynck R, Zhang YE. 2003. Smad-dependent and Smad-independent pathways in TGF-beta family signalling. *Nature* 425(6958):577-584.
- Field CM, Kellogg D. 1999. Septins: cytoskeletal polymers or signalling GTPases? *Trends Cell Biol* 9(10):387-394.
- Fischer RS, Fritz-Six KL, Fowler VM. 2003. Pointed-end capping by tropomodulin3 negatively regulates endothelial cell motility. *J Cell Biol* 161(2):371-380.
- Franke WW, Schmid E, Osborn M, Weber K. 1978. Different intermediate-sized filaments distinguished by immunofluorescence microscopy. *Proc Natl Acad Sci U S A* 75(10):5034-5038.
- Frevel MA, Bakheet T, Silva AM, Hissong JG, Khabar KS, Williams BR. 2003. p38 Mitogen-activated protein kinase-dependent and -independent signaling of mRNA stability of AU-rich element-containing transcripts. *Mol Cell Biol* 23(2):425-436.
- Furuhashi M, Yagi K, Yamamoto H, Furukawa Y, Shimada S, Nakamura Y, Kikuchi A, Miyazono K, Kato M. 2001. Axin facilitates Smad3 activation in the transforming growth factor beta signaling pathway. *Mol Cell Biol* 21(15):5132-5141.
- Gautier L, Cope L, Bolstad BM, Irizarry RA. 2004. affy--analysis of Affymetrix GeneChip data at the probe level. *Bioinformatics* 20(3):307-315.
- Geiger B, Bershadsky A, Pankov R, Yamada KM. 2001. Transmembrane crosstalk between the extracellular matrix--cytoskeleton crosstalk. *Nat Rev Mol Cell Biol* 2(11):793-805.
- Giannelli G. 2009. The epithelial-mesenchymal transition: fact or fiction in cancer? *Hepatology* 50(5):1344-1346.
- Goering W, Adham IM, Pasche B, Manner J, Ochs M, Engel W, Zoll B. 2008. Impairment of gastric acid secretion and increase of embryonic lethality in Foxq1-deficient mice. *Cytogenet Genome Res* 121(2):88-95.
- Gomis RR, Alarcon C, He W, Wang Q, Seoane J, Lash A, Massague J. 2006. A FoxO-Smad synexpression group in human keratinocytes. *Proc Natl Acad Sci U S A* 103(34):12747-12752.
- Gotzmann J, Mikula M, Eger A, Schulte-Hermann R, Foisner R, Beug H, Mikulits W. 2004. Molecular aspects of epithelial cell plasticity: implications for local tumor invasion and metastasis. *Mutat Res* 566(1):9-20.

- Greenburg G, Hay ED. 1986. Cytodifferentiation and tissue phenotype change during transformation of embryonic lens epithelium to mesenchyme-like cells in vitro. *Dev Biol* 115(2):363-379.
- Grondin B, Lefrancois M, Tremblay M, Saint-Denis M, Haman A, Waga K, Bedard A, Tenen DG, Hoang T. 2007. c-Jun homodimers can function as a context-specific coactivator. *Mol Cell Biol* 27(8):2919-2933.
- Grone HJ, Weber K, Grone E, Helmchen U, Osborn M. 1987. Coexpression of keratin and vimentin in damaged and regenerating tubular epithelia of the kidney. *Am J Pathol* 129(1):1-8.
- Hajra KM, Chen DY, Fearon ER. 2002. The SLUG zinc-finger protein represses E-cadherin in breast cancer. *Cancer Res* 62(6):1613-1618.
- Harris MA, Clark J, Ireland A, Lomax J, Ashburner M, Foulger R, Eilbeck K, Lewis S, Marshall B, Mungall C, Richter J, Rubin GM, Blake JA, Bult C, Dolan M, Drabkin H, Eppig JT, Hill DP, Ni L, Ringwald M, Balakrishnan R, Cherry JM, Christie KR, Costanzo MC, Dwight SS, Engel S, Fisk DG, Hirschman JE, Hong EL, Nash RS, Sethuraman A, Theesfeld CL, Botstein D, Dolinski K, Feierbach B, Berardini T, Mundodi S, Rhee SY, Apweiler R, Barrell D, Camon E, Dimmer E, Lee V, Chisholm R, Gaudet P, Kibbe W, Kishore R, Schwarz EM, Sternberg P, Gwinn M, Hannick L, Wortman J, Berriman M, Wood V, de la Cruz N, Tonellato P, Jaiswal P, Seigfried T, White R. 2004. The Gene Ontology (GO) database and informatics resource. *Nucleic Acids Res* 32(Database issue):D258-261.
- Hartwell KA, Muir B, Reinhardt F, Carpenter AE, Sgroi DC, Weinberg RA. 2006. The Spemann organizer gene, Goosecoid, promotes tumor metastasis. *Proc Natl Acad Sci U S A* 103(50):18969-18974.
- Hay ED. 1990. Role of cell-matrix contacts in cell migration and epithelial-mesenchymal transformation. *Cell Differ Dev* 32(3):367-375.
- Hay ED. 1995. An overview of epithelio-mesenchymal transformation. *Acta Anat (Basel)* 154(1):8-20.
- Hay ED, Zuk A. 1995. Transformations between epithelium and mesenchyme: normal, pathological, and experimentally induced. *Am J Kidney Dis* 26(4):678-690.
- Hayashi H, Kume T. 2009. Foxc2 transcription factor as a regulator of angiogenesis via induction of integrin beta3 expression. *Cell Adh Migr* 3(1).
- Herpin A, Lelong C, Favrel P. 2004. Transforming growth factor-beta-related proteins: an ancestral and widespread superfamily of cytokines in metazoans. *Dev Comp Immunol* 28(5):461-485.
- Hocevar BA, Smine A, Xu XX, Howe PH. 2001. The adaptor molecule Disabled-2 links the transforming growth factor beta receptors to the Smad pathway. *Embo J* 20(11):2789-2801.
- Holian J, Qi W, Kelly DJ, Zhang Y, Mreich E, Pollock CA, Chen XM. 2008. Role of Kruppel-like factor 6 in transforming growth factor-beta1-induced epithelial-mesenchymal transition of proximal tubule cells. *Am J Physiol Renal Physiol* 295(5):F1388-1396.
- Hong HK, Noveroske JK, Headon DJ, Liu T, Sy MS, Justice MJ, Chakravarti A. 2001. The winged helix/forkhead transcription factor Foxq1 regulates differentiation of hair in satin mice. *Genesis* 29(4):163-171.
- Huang X, Saint-Jeannet JP. 2004. Induction of the neural crest and the opportunities of life on the edge. *Dev Biol* 275(1):1-11.
- Huber W, von Heydebreck A, Sultmann H, Poustka A, Vingron M. 2002. Variance stabilization applied to microarray data calibration and to the quantification of differential expression. *Bioinformatics* 18 Suppl 1:S96-104.

- Humphreys BD, Lin SL, Kobayashi A, Hudson TE, Nowlin BT, Bonventre JV, Valerius MT, McMahon AP, Duffield JS. Fate tracing reveals the pericyte and not epithelial origin of myofibroblasts in kidney fibrosis. *Am J Pathol* 176(1):85-97.
- Ishikawa F, Nose K, Shibamura M. 2008. Downregulation of hepatocyte nuclear factor-4alpha and its role in regulation of gene expression by TGF-beta in mammary epithelial cells. *Exp Cell Res* 314(10):2131-2140.
- Iwano M, Plieth D, Danoff TM, Xue C, Okada H, Neilson EG. 2002. Evidence that fibroblasts derive from epithelium during tissue fibrosis. *J Clin Invest* 110(3):341-350.
- Johnson GL, Lapadat R. 2002. Mitogen-activated protein kinase pathways mediated by ERK, JNK, and p38 protein kinases. *Science* 298(5600):1911-1912.
- Kalluri R, Weinberg RA. 2009. The basics of epithelial-mesenchymal transition. *J Clin Invest* 119(6):1420-1428.
- Kaneda H, Arao T, Tanaka K, Tamura D, Aomatsu K, Kudo K, Sakai K, De Velasco MA, Matsumoto K, Fujita Y, Yamada Y, Tsurutani J, Okamoto I, Nakagawa K, Nishio K. FOXQ1 Is Overexpressed in Colorectal Cancer and Enhances Tumorigenicity and Tumor Growth. *Cancer Res*.
- Kenzelmann M, Maertens S, Hergenroth M, Kueffer S, Hotz-Wagenblatt A, Li L, Wang S, Ittrich C, Lemberger T, Arribas R, Jonnakuty S, Hollstein MC, Schmid W, Gretz N, Grone HJ, Schutz G. 2007. Microarray analysis of newly synthesized RNA in cells and animals. *Proc Natl Acad Sci U S A* 104(15):6164-6169.
- Khabar KS. 2005. The AU-rich transcriptome: more than interferons and cytokines, and its role in disease. *J Interferon Cytokine Res* 25(1):1-10.
- Khalil N. 1999. TGF-beta: from latent to active. *Microbes Infect* 1(15):1255-1263.
- Kong KY, Kedes L. 2004. Cytoplasmic nuclear transfer of the actin-capping protein tropomodulin. *J Biol Chem* 279(29):30856-30864.
- Kostyukova AS. 2008. Tropomodulins and tropomodulin/tropomyosin interactions. *Cell Mol Life Sci* 65(4):563-569.
- Krause M, Dent EW, Bear JE, Loureiro JJ, Gertler FB. 2003. Ena/VASP proteins: regulators of the actin cytoskeleton and cell migration. *Annu Rev Cell Dev Biol* 19:541-564.
- Lagnado CA, Brown CY, Goodall GJ. 1994. AUUUA is not sufficient to promote poly(A) shortening and degradation of an mRNA: the functional sequence within AU-rich elements may be UUAUUUA(U/A)(U/A). *Mol Cell Biol* 14(12):7984-7995.
- Lee CS, Friedman JR, Fulmer JT, Kaestner KH. 2005. The initiation of liver development is dependent on Foxa transcription factors. *Nature* 435(7044):944-947.
- Lee JM, Dedhar S, Kalluri R, Thompson EW. 2006. The epithelial-mesenchymal transition: new insights in signaling, development, and disease. *J Cell Biol* 172(7):973-981.
- Levy L, Hill CS. 2005. Smad4 dependency defines two classes of transforming growth factor {beta} (TGF-{{beta}}) target genes and distinguishes TGF-{{beta}}-induced epithelial-mesenchymal transition from its antiproliferative and migratory responses. *Mol Cell Biol* 25(18):8108-8125.
- Liu P, Wakamiya M, Shea MJ, Albrecht U, Behringer RR, Bradley A. 1999. Requirement for Wnt3 in vertebrate axis formation. *Nat Genet* 22(4):361-365.
- Livak KJ, Schmittgen TD. 2001. Analysis of relative gene expression data using real-time quantitative PCR and the 2<sup>-Delta Delta C(T)</sup> Method. *Methods* 25(4):402-408.
- Lyons RM, Keski-Oja J, Moses HL. 1988. Proteolytic activation of latent transforming growth factor-beta from fibroblast-conditioned medium. *J Cell Biol* 106(5):1659-1665.
- Maere S, Heymans K, Kuiper M. 2005. BiNGO: a Cytoscape plugin to assess overrepresentation of gene ontology categories in biological networks. *Bioinformatics* 21(16):3448-3449.

- Mahtani KR, Brook M, Dean JL, Sully G, Saklatvala J, Clark AR. 2001. Mitogen-activated protein kinase p38 controls the expression and posttranslational modification of tristetraprolin, a regulator of tumor necrosis factor alpha mRNA stability. *Mol Cell Biol* 21(19):6461-6469.
- Malin D, Kim IM, Boetticher E, Kalin TV, Ramakrishna S, Meliton L, Ustiyani V, Zhu X, Kalinichenko VV. 2007. Forkhead box F1 is essential for migration of mesenchymal cells and directly induces integrin-beta3 expression. *Mol Cell Biol* 27(7):2486-2498.
- Mani SA, Yang J, Brooks M, Schwaninger G, Zhou A, Miura N, Kutok JL, Hartwell K, Richardson AL, Weinberg RA. 2007. Mesenchyme Forkhead 1 (FOXC2) plays a key role in metastasis and is associated with aggressive basal-like breast cancers. *Proc Natl Acad Sci U S A* 104(24):10069-10074.
- Martinez-Ceballos E, Chambon P, Gudas LJ. 2005. Differences in gene expression between wild type and Hoxa1 knockout embryonic stem cells after retinoic acid treatment or leukemia inhibitory factor (LIF) removal. *J Biol Chem* 280(16):16484-16498.
- Massague J. 1998. TGF-beta signal transduction. *Annu Rev Biochem* 67:753-791.
- Massague J, Blain SW, Lo RS. 2000. TGFbeta signaling in growth control, cancer, and heritable disorders. *Cell* 103(2):295-309.
- Massague J, Seoane J, Wotton D. 2005. Smad transcription factors. *Genes Dev* 19(23):2783-2810.
- Medici D, Hay ED, Olsen BR. 2008. Snail and Slug promote epithelial-mesenchymal transition through beta-catenin-T-cell factor-4-dependent expression of transforming growth factor-beta3. *Mol Biol Cell* 19(11):4875-4887.
- Miettinen PJ, Ebner R, Lopez AR, Derynck R. 1994. TGF-beta induced transdifferentiation of mammary epithelial cells to mesenchymal cells: involvement of type I receptors. *J Cell Biol* 127(6 Pt 2):2021-2036.
- Nawshad A, Lagamba D, Polad A, Hay ED. 2005. Transforming growth factor-beta signaling during epithelial-mesenchymal transformation: implications for embryogenesis and tumor metastasis. *Cells Tissues Organs* 179(1-2):11-23.
- Ness SA. 2003. Myb protein specificity: evidence of a context-specific transcription factor code. *Blood Cells Mol Dis* 31(2):192-200.
- Nieto MA. 2002. The snail superfamily of zinc-finger transcription factors. *Nat Rev Mol Cell Biol* 3(3):155-166.
- Nilsson J, Helou K, Kovacs A, Bendahl PO, Bjursell G, Ferno M, Carlsson P, Kannius-Janson M. Nuclear Janus-Activated Kinase 2/Nuclear Factor 1-C2 Suppresses Tumorigenesis and Epithelial-to-Mesenchymal Transition by Repressing Forkhead Box F1. *Cancer Res*.
- Nogai H, Rosowski M, Grun J, Rietz A, Debus N, Schmidt G, Lauster C, Janitz M, Vortkamp A, Lauster R. 2008. Follistatin antagonizes transforming growth factor-beta3-induced epithelial-mesenchymal transition in vitro: implications for murine palatal development supported by microarray analysis. *Differentiation* 76(4):404-416.
- Norden C, Liakopoulos D, Barral Y. 2004. Dissection of septin actin interactions using actin overexpression in *Saccharomyces cerevisiae*. *Mol Microbiol* 53(2):469-483.
- Ozkaynak E, Schnegelsberg PN, Jin DF, Clifford GM, Warren FD, Drier EA, Oppermann H. 1992. Osteogenic protein-2. A new member of the transforming growth factor-beta superfamily expressed early in embryogenesis. *J Biol Chem* 267(35):25220-25227.
- Pankov R, Yamada KM. 2002. Fibronectin at a glance. *J Cell Sci* 115(Pt 20):3861-3863.
- Patterson GI, Padgett RW. 2000. TGF beta-related pathways. Roles in *Caenorhabditis elegans* development. *Trends Genet* 16(1):27-33.
- Petrie RJ, Doyle AD, Yamada KM. 2009. Random versus directionally persistent cell migration. *Nat Rev Mol Cell Biol* 10(8):538-549.

- Piek E, Moustakas A, Kurisaki A, Heldin CH, ten Dijke P. 1999. TGF-(beta) type I receptor/ALK-5 and Smad proteins mediate epithelial to mesenchymal transdifferentiation in NMuMG breast epithelial cells. *J Cell Sci* 112 ( Pt 24):4557-4568.
- Pierreux CE, Nicolas FJ, Hill CS. 2000. Transforming growth factor beta-independent shuttling of Smad4 between the cytoplasm and nucleus. *Mol Cell Biol* 20(23):9041-9054.
- Pollard TD, Cooper JA. 2009. Actin, a central player in cell shape and movement. *Science* 326(5957):1208-1212.
- Potter CS, Peterson RL, Barth JL, Pruett ND, Jacobs DF, Kern MJ, Argraves WS, Sundberg JP, Awgulewitsch A. 2006. Evidence that the satin hair mutant gene *Foxq1* is among multiple and functionally diverse regulatory targets for *Hoxc13* during hair follicle differentiation. *J Biol Chem* 281(39):29245-29255.
- Prindull G, Zipori D. 2004. Environmental guidance of normal and tumor cell plasticity: epithelial mesenchymal transitions as a paradigm. *Blood* 103(8):2892-2899.
- Rastaldi MP, Ferrario F, Giardino L, Dell'Antonio G, Grillo C, Grillo P, Strutz F, Muller GA, Colasanti G, D'Amico G. 2002. Epithelial-mesenchymal transition of tubular epithelial cells in human renal biopsies. *Kidney Int* 62(1):137-146.
- Remacle JE, Kraft H, Lerchner W, Wuytens G, Collart C, Verschuere K, Smith JC, Huylebroeck D. 1999. New mode of DNA binding of multi-zinc finger transcription factors: deltaEF1 family members bind with two hands to two target sites. *Embo J* 18(18):5073-5084.
- Rodriguez LG, Wu X, Guan JL. 2005. Wound-healing assay. *Methods Mol Biol* 294:23-29.
- Shannon P, Markiel A, Ozier O, Baliga NS, Wang JT, Ramage D, Amin N, Schwikowski B, Ideker T. 2003. Cytoscape: a software environment for integrated models of biomolecular interaction networks. *Genome Res* 13(11):2498-2504.
- Sherr CJ. 1996. Cancer cell cycles. *Science* 274(5293):1672-1677.
- Sherr CJ, Roberts JM. 1999. CDK inhibitors: positive and negative regulators of G1-phase progression. *Genes Dev* 13(12):1501-1512.
- Shi Y, Massague J. 2003. Mechanisms of TGF-beta signaling from cell membrane to the nucleus. *Cell* 113(6):685-700.
- Shirakihara T, Saitoh M, Miyazono K. 2007. Differential regulation of epithelial and mesenchymal markers by deltaEF1 proteins in epithelial mesenchymal transition induced by TGF-beta. *Mol Biol Cell* 18(9):3533-3544.
- Silverman-Gavrila RV, Silverman-Gavrila LB. 2008. Septins: new microtubule interacting partners. *ScientificWorldJournal* 8:611-620.
- Sinha S, Nevett C, Shuttleworth CA, Kielty CM. 1998. Cellular and extracellular biology of the latent transforming growth factor-beta binding proteins. *Matrix Biol* 17(8-9):529-545.
- Song Y, Washington MK, Crawford HC. Loss of FOXA1/2 Is Essential for the Epithelial-to-Mesenchymal Transition in Pancreatic Cancer. *Cancer Res* 70(5):2115-2125.
- Tang Y, Katuri V, Dillner A, Mishra B, Deng CX, Mishra L. 2003. Disruption of transforming growth factor-beta signaling in ELF beta-spectrin-deficient mice. *Science* 299(5606):574-577.
- Tarin D, Thompson EW, Newgreen DF. 2005. The fallacy of epithelial mesenchymal transition in neoplasia. *Cancer Res* 65(14):5996-6000; discussion 6000-5991.
- Ten Dijke P, Goumans MJ, Itoh F, Itoh S. 2002. Regulation of cell proliferation by Smad proteins. *J Cell Physiol* 191(1):1-16.
- ten Dijke P, Hill CS. 2004. New insights into TGF-beta-Smad signalling. *Trends Biochem Sci* 29(5):265-273.

- Thiery JP, Acloque H, Huang RY, Nieto MA. 2009. Epithelial-mesenchymal transitions in development and disease. *Cell* 139(5):871-890.
- Thiery JP, Sleeman JP. 2006. Complex networks orchestrate epithelial-mesenchymal transitions. *Nat Rev Mol Cell Biol* 7(2):131-142.
- Thompson EW, Newgreen DF, Tarin D. 2005. Carcinoma invasion and metastasis: a role for epithelial-mesenchymal transition? *Cancer Res* 65(14):5991-5995; discussion 5995.
- Tsukazaki T, Chiang TA, Davison AF, Attisano L, Wrana JL. 1998. SARA, a FYVE domain protein that recruits Smad2 to the TGFbeta receptor. *Cell* 95(6):779-791.
- Tusher VG, Tibshirani R, Chu G. 2001. Significance analysis of microarrays applied to the ionizing radiation response. *Proc Natl Acad Sci U S A* 98(9):5116-5121.
- van der Flier A, Sonnenberg A. 2001. Function and interactions of integrins. *Cell Tissue Res* 305(3):285-298.
- van der Heul-Nieuwenhuijsen L, Dits NF, Jenster G. 2009. Gene expression of forkhead transcription factors in the normal and diseased human prostate. *BJU Int* 103(11):1574-1580.
- Vandewalle C, Comijn J, De Craene B, Vermassen P, Bruyneel E, Andersen H, Tulchinsky E, Van Roy F, Berx G. 2005. SIP1/ZEB2 induces EMT by repressing genes of different epithelial cell-cell junctions. *Nucleic Acids Res* 33(20):6566-6578.
- Venkov CD, Link AJ, Jennings JL, Plieth D, Inoue T, Nagai K, Xu C, Dimitrova YN, Rauscher FJ, Neilson EG. 2007. A proximal activator of transcription in epithelial-mesenchymal transition. *J Clin Invest* 117(2):482-491.
- Verzi MP, Khan AH, Ito S, Shivdasani RA. 2008. Transcription factor foxq1 controls mucin gene expression and granule content in mouse stomach surface mucous cells. *Gastroenterology* 135(2):591-600.
- Vongwiwatana A, Tasanarong A, Rayner DC, Melk A, Halloran PF. 2005. Epithelial to mesenchymal transition during late deterioration of human kidney transplants: the role of tubular cells in fibrogenesis. *Am J Transplant* 5(6):1367-1374.
- Wang IC, Chen YJ, Hughes D, Petrovic V, Major ML, Park HJ, Tan Y, Ackerson T, Costa RH. 2005. Forkhead box M1 regulates the transcriptional network of genes essential for mitotic progression and genes encoding the SCF (Skp2-Cks1) ubiquitin ligase. *Mol Cell Biol* 25(24):10875-10894.
- Watanabe M, Masuyama N, Fukuda M, Nishida E. 2000. Regulation of intracellular dynamics of Smad4 by its leucine-rich nuclear export signal. *EMBO Rep* 1(2):176-182.
- Weber KL, Fischer RS, Fowler VM. 2007. Tmod3 regulates polarized epithelial cell morphology. *J Cell Sci* 120(Pt 20):3625-3632.
- White ES, Baralle FE, Muro AF. 2008. New insights into form and function of fibronectin splice variants. *J Pathol* 216(1):1-14.
- Willis BC, Borok Z. 2007. TGF-beta-induced EMT: mechanisms and implications for fibrotic lung disease. *Am J Physiol Lung Cell Mol Physiol* 293(3):L525-534.
- Wrana JL, Attisano L, Wieser R, Ventura F, Massague J. 1994. Mechanism of activation of the TGF-beta receptor. *Nature* 370(6488):341-347.
- Xiao Z, Liu X, Henis YI, Lodish HF. 2000a. A distinct nuclear localization signal in the N terminus of Smad 3 determines its ligand-induced nuclear translocation. *Proc Natl Acad Sci U S A* 97(14):7853-7858.
- Xiao Z, Liu X, Lodish HF. 2000b. Importin beta mediates nuclear translocation of Smad 3. *J Biol Chem* 275(31):23425-23428.
- Xie L, Law BK, Chytil AM, Brown KA, Aakre ME, Moses HL. 2004. Activation of the Erk pathway is required for TGF-beta1-induced EMT in vitro. *Neoplasia* 6(5):603-610.
- Xu L, Chen YG, Massague J. 2000. The nuclear import function of Smad2 is masked by SARA and unmasked by TGFbeta-dependent phosphorylation. *Nat Cell Biol* 2(8):559-562.

- Yang J, Weinberg RA. 2008. Epithelial-mesenchymal transition: at the crossroads of development and tumor metastasis. *Dev Cell* 14(6):818-829.
- Yang Z, Zhang X, Gang H, Li X, Li Z, Wang T, Han J, Luo T, Wen F, Wu X. 2007. Up-regulation of gastric cancer cell invasion by Twist is accompanied by N-cadherin and fibronectin expression. *Biochem Biophys Res Commun* 358(3):925-930.
- Zavadil J, Bottinger EP. 2005. TGF-beta and epithelial-to-mesenchymal transitions. *Oncogene* 24(37):5764-5774.
- Zeisberg M, Neilson EG. 2009. Biomarkers for epithelial-mesenchymal transitions. *J Clin Invest* 119(6):1429-1437.

**ABBREVIATIONS**

Amp	Ampicillin
APS	Ammonium persulphate
bp	Base pair
Bmp	Bone morphogenetic protein
BSA	Bovine Serum Albumin
cDNA	complementary DNA
CMV	Cytomegalovirus
DEPC	Diethylpyrocarbonate
DMEM	Dulbecco's Modified Eagles Medium
DMSO	Dimethyl-sulphoxide
DNA	Deoxyribonucleic acid
dNTP	deoxy-nucleoside-triphosphate
ECM	Extracellular matrix
E.coli	Escherichia coli
EDTA	Ethylen diamine tetraacetic acid
e.g.	exempli gratia ('for example')
EMT	Epithelial to mesenchymal transition
FACS	Fluorescence activated cell sorting
FBS	Fetal bovine serum
FDR	False discovery rate
Fig.	Figure
GDF	Growth and differentiation factor
GO	Gene ontology
hrs	hours
HRP	Horseradish peroxidase
IRES	Internal ribosome entry site
Kan	Kanamycin
mA	milli-Ampere
MET	Mesenchymal to epithelial transition
min.	minute
MIS	Muellerian inhibiting substance

ml	milliliter
μM	micromolar
mM	millimolar
mRNA	messenger RNA
NES	Nuclear export signal
NIAC-NTR	Non-invasive application of captured – newly transcribed RNA
NLS	Nuclear localisation signal
nm	nanometer
nM	nanomolar
NP-40	Nonidet-P40
ns-siRNA	non-silencing small interfering RNA
O.D.	Optical density
PBS	Phosphate buffered saline
PCR	Polymerase chain reaction
Pfu	Pyrococcus furiosus
RNA	ribonucleic acid
rpm	rounds per minute
rRNA	ribosomal RNA
RT	Room temperature
S	Svedberg
SAM	Significance analysis of microarrays
SDS	Sodiumdodecylsulphate
siRNA	small interfering RNA
Tab.	Table
TEMED	N,N,N',N'-tatrathylethylenediamin
TFM	Transcription factor matrix
TGF-β	Transforming growth factor-β
TSS	Transcription start site
U	Unit
V	Volt
v/v	Volume per volume
w/v	Weight per volume

## **PUBLICATIONS**

Feuerborn A, Moritz C, Von Bonin F, Dobbelstein M, Trumper L, Sturzenhofecker B, Kube D. 2006. Dysfunctional p53 deletion mutants in cell lines derived from Hodgkin's lymphoma. *Leuk Lymphoma* 47(9):1932-1940.

Feuerborn A, Srivastava P, Küffer S, Grandy W, Sijmonsma T, Brors B, Gretz N, Gröne H.-J. The Forkhead factor FoxQ1 influences epithelial differentiation. – in preparation.

## ACKNOWLEDGEMENTS

I would like to express my sincerest gratitude to Prof. Dr. rer. nat. Peter Angel, my first supervisor, for his continuous and constructive support and the evaluation of this thesis.

I am deeply grateful to Prof. Dr. med. Hermann-Josef Gröne for giving me the opportunity to pursue a PhD-thesis in his department, his constant encouragement throughout the work, and stimulating discussions. I am further very thankful for his helpful critiques and evaluation of this thesis.

I owe a cordially thanks to Prof. Dr. Jonathan Sleeman, member of my TAC, for his valuable suggestions on my work and his time and constant support, also besides the TAC-meetings.

I am very thankful to Maria Saile, Maria Meisner, Mahnaz Bonrouhi, Sylvia Kaden and Tjeerd Sijmonsma for excellent technical support and their contribution to this work.

A special thank-you goes out to William Aaron Grandy, Stefan Küffer and Prashant Kumar Srivastava for 'too many things to list'. A big 'Thank-you!' doesn't do you justice but has to suffice here.

Finally, I thank my family and my fiancée Ann Na Tan for their encouragement and support, for their love and believe, simply for everything. Things wouldn't have been possible without you!